Ship-Induced Waves and Sediment Transport in Göta River, Sweden

LUNDS UNIVERSITET
Lunds Tekniska Högskola

Water Resources Engineering
Department of Building and Environmental Technology
Faculty of Engineering

Master's Thesis:
Jonas Althage

Ship-Induced Waves and Sediment Transport in Göta River, Sweden
Master's Thesis in Water Resources Engineering
Jonas Althage

Water Resources Engineering
Department of Building and Environmental Technology
Faculty of Engineering
Lund University

Abstract

Göta River, in Swedish *Göta älv*, is Sweden's largest river as to flow rate. The surrounding river valley landscape is also among the most prone to landslides in the country, with cohesive sediments, including quick clay, as the dominant soil type. Both natural and anthropogenic erosion and sediment transport are occurring in the river, in the latter case induced by for example ship-generated waves.

The ships that navigate Göta River induce erosion of the river banks and bed by the impact of waves and scouring from propeller jets. During ship passages, large increases in turbidity are detected through measurements in the water, which means that the total load of suspended particulate matter in the river increases due to erosion and sediment transport from ship-induced effects.

By digitizing the variation in the water level when ships pass an observation pier, the ship-generated wave properties have been determined. The waves were found to induce bed shear stresses that frequently exceed the estimated bed sediment critical shear stress. The critical shear stress has been estimated by analysing calculated shear stresses and turbidity readings, linking increases of the latter (which translate into an increase in the mass of suspended particulate matter in the water) to the magnitude of the former. Subsequently, the waves do not only contribute to the sediment transport of the river, but it is also established that they erode the river bed and banks. Through basic assumptions and estimations, ship-generated waves are calculated to erode about 40,000 tonnes of bed sediment annually along the full stretch of the Göta River. Moreover, a predicted increase in the bulk transport by ships could double the erosion by the year 2020. This does not consider the fact that the sediment settles after some time, so the calculated erosion is most likely an over-estimation.

The key factor which determines the magnitude of the wave height is the ship velocity relative to the water flow velocity. Other parameters, such as ship draught, ship size, and water depth, do not show a consistent relationship with the recorded maximum wave height.

Keywords: *Sediment transport, erosion, ship-generated waves, river, channel, turbidity, field measurements, shear stress*

Sammanfattning

Göta älv har den största årliga flödesvolymen av alla vattendrag i Sverige. Det omgivande älvdalslandskapet är också ett av de mest skredbenägna i landet, med kohesiva kornfraktioner, inklusive kvicklera, som den dominerande jordarten. Både naturlig och antropogenisk, till exempel fartygsgenererade vågor, erosion och sedimenttransport sker i älven.

Fartygen som navigerar Göta älv eroderar flodbanken och botten genom vågverkan och påverkan av jetstrålar från propellrar. Under fartygspassager detekteras via mätinstrument stora ökningar i turbiditet, och den totala massan av suspenderat material i älven ökas således på grund av erosion och sedimenttransport från fartygsgenererade effekter.

Genom att digitalisera vattenytans fluktation under fartygspassager vid en observationsbrygga kunde de fartygsgenererade vågornas egenskaper bestämmas. De fartygsgenererade vågorna inducerar tydligt en bottenskjuvspänning som frekvent överskrider den kritiska bottenskjuvspänning. Den kritiska bottenskjuvspänningen har uppskattats genom att analysera beräknade bottenskjuvspänningar och uppmätta ökningar i turbiditet. Genom att relatera turbiditetsökningarna (som betyder att massan suspenderat material i vattnet ökar) till skjuvspänningen kunde den kritiska skjuvspänningen uppskattas. Således är det klart att fartygsvågorna inte bara ger ett bidrag till den redan pågående sedimenttransporten i älven, utan att de även eroderar strandbankarna och botten. Genom uppskattningar och antaganden har erosionen av älvbotten från fartygsvågor beräknats till cirka 40 000 ton sediment årligen. En prognosticerad ökning av maritim godstransport skulle kunna fördubbla den fartygsinducerade erosionen fram till år 2020. Dock tar studien inte hänsyn till det faktum att sedimenten återigen lägger sig på botten efter en viss tid, så den beräknade eroderade massan är med största sannolikhet en överskattning.

Nyckelfaktorn som genomgående kan kopplas till våghöjdernas storlek är fartygets hastighet i relation till vattenhastigheten. Andra parametrar, som fartygens djupgående, deras storlek och vattendjupet, visar inga konsekventa samband med de genererade vågorna.

Nyckelord: *sedimenttransport, erosion, fartygsgenerarade, fartygsinducerade, vågor, flod, älv, kanal, turbiditet*

Foreword

I would like to extend my gratitude to my supervisor and Professor at Lund University, Magnus Larson, for offering me the opportunity to write this thesis and for his guidance, enthusiasm and comments as the work progressed. With equal gratitude I also thank Gunnel Göransson, my supervisor at the Swedish Geotechnical Institute, who always took time to help me with inquiries regarding my work, and helped me during my fieldwork.

I would also like to thank the employees of Vessel Traffic Service in Trollhättan, who were happy to provide me with information about scheduled ship traffic, regardless of the time of day, the people at Gothenburg Water, and especially Åsa Henriksson, for sending and interpreting turbidity data, the Swedish Meteorological and Hydrological Institute, for providing me with data regarding precipitation, run-off etc., and also especially Walter Gyllenram, for notes on hydraulic aspects of the project, and not least the employees at Vattenfall Driftcentralen Bispgården, for helping me with river flow data.

Thank you to the Swedish Geotechnical Institute for providing me with my own office at the very nice facilities in Gothenburg, and access to the institution's database and projects.

Also, last but not least, a sincere thank you to all the people at the Swedish Geotechnical Institute in Gothenburg, who helped me with my work and who really made my time there worth remembering.

Jonas Althage
Gothenburg, November 2010.

Abbreviations and Acronyms

FNU	Formazin Nephelometric Units
SGI	Swedish Geotechnical Institute
SMHI	Swedish Meteorological and Hydrological Institute
SPM	Suspended Particulate Matter
SWRL	Still Water Reference Level
SWL	Still Water Level
TSS	Total Suspended Solids
WPP	Water Power Plant
WTP	Drinking-Water Treatment Plant

List of contents

1 Introduction

Ship-induced erosion is perhaps foremost a problem in harbours, and it has been examined in such areas by many authors. It is however, also a problem in rivers and channels. Due to the demand of transport of goods, the bulk transport by ships is increasing, and so the interference with nature by these vessels increases as well. Ships generate water jets and waves which induce shear-stresses on river banks and beds large enough to erode particulate matter. Apart from accelerating the morphologic process of natural waterways, such as rivers, the interaction also lowers the water quality, making it more difficult to treat water to a desired drinking quality. As many people rely on river water as a source of fresh water, this can create significant problems.

Göta River, in Swedish named *Göta älv*, originates from Lake Vänern in mid Sweden, the nation's largest lake and the third largest lake in Europe after the Russian lakes Ladoga and Onega. The river carries the largest flow rate of all the rivers in Sweden, and also supplies a large population, mainly in Gothenburg, the second largest city in Sweden, with fresh water. The water from Lake Vänern is of very good quality and is almost potable without treatment (Vänerkansliet 2007) and is the prime supplier of water to the river. There is, though, also minor inflow from tributaries as well as from regional precipitation runoff. Although the water is of high quality at the inlet from Lake Vänern, it is continuously degrading along the river stretch due to an increase in for example suspended sediment. The river experiences a high volume of discharged sediment from its surroundings, originating from tributaries and erosion caused by precipitation runoff and from erosion of the river banks and bed. Also, the river bank area of Göta River is among the most liable to landslides of all rivers in Sweden, and the river landscape show clear signs of scarring and landslides of different magnitude (Sundborg and Norrman 1963), see Figure 1.

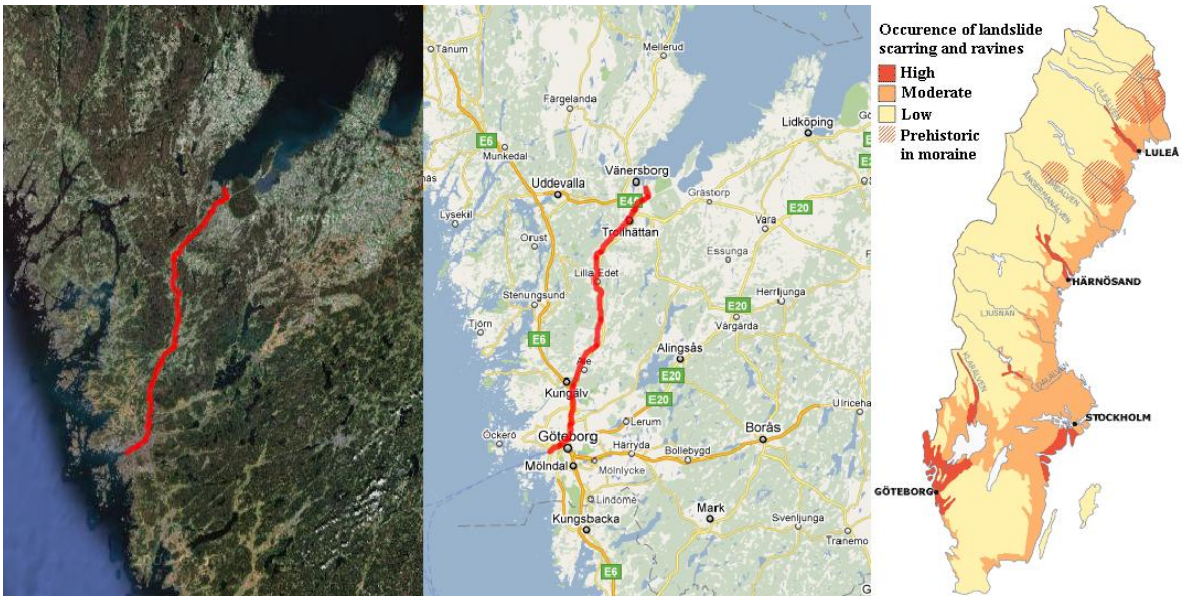

Figure 1- The most downstream stretch of Göta River can be seen in the left and middle figures (©2010 Google, from: www.viss.lst.se). The right picture shows the occurrence level of ravines and landslide scarring in the Swedish landscape (©Geological Survey of Sweden (2010a), translation by Althage (2010)). Note that the landscape in the vicinity of river Göta has an overall high occurrence level of landscape scarring and ravines.

1.1 Project Background

Göta River is utilized as a shipping channel and allows for ship transport of goods both in the upstream (north north-east) and downstream (south south-west) direction. Due to the presence of ship activity, there is an increase in erosion of the river bed and banks. This is partly because the ship propellers induce jets, which have a higher water flow velocity compared to the river flow velocity. Due to an increased shear-stress at the bottom, this may cause sediment to become suspended (or re-suspended) in the water column. Also, the waves generated by the ships erode the river bed and banks. The phenomenon of bed and/or bank erosion due to the above stated reasons is described by Hamill *et al.* (1999 and 2004), Maa *et al.* (1998), and US Army Corps of Engineers (1984), among others.

Due to the sediment transport in the river, the drinking water treatment plants (henceforth also referred to as WTPs) of Gothenburg municipality must, with varying frequency and duration, sometimes close the intake of river water due to its poor quality (Dahlberg 2009). The WTPs have equipment which continuously monitors the water quality by, for example, determining the river water turbidity. The total load of suspended particulate matter (SPM), or load of total suspended solids (TSS), is a good indicator of the water quality and may be correlated to the same (Golterman *et al.* 1983), and the turbidity readings can also be connected to the load of SPM (Minella *et. al.* 2007, Fink 2005, Jiménez 2009 and Packman *et. al.* 1999). One reason for the water quality reduction is because SPM has the ability to adhere contaminants such as heavy metals and chemical substances (Partheniades 2009) to its surface. It is therefore desirable to understand the inducing factors behind SPM in rivers and other water bodies, and also to be able to quantify the total increase in the load of SPM in the water during certain events such as flooding, heavy precipitation, and ship activity, which is studied in this thesis.

1.2 Objective

The aim of this Master's Thesis is to investigate and, to the greatest extent possible, estimate the impact that ship activity has on erosion and sediment transport in the Göta River. The wave-induced erosion of the river bed and banks is the prime concern; the propeller jet induced erosion is briefly discussed but not estimated due to the complexity of determining, for example, the governing parameters.

This thesis is part of a larger project carried out by the Swedish Geotechnical Institute (SGI) called the Göta River project, which aims to, among other things, identify areas in the river valley which may be prone to landslides, and also how the effects of climate change will affect the infrastructure of the area, river ecology, water quality etc.

1.3 Procedure

A thorough study of the existing literature has been carried out, to gain a comprehensive understanding regarding the subject at hand. Many texts regarding hydraulic theory refer to ship interaction with water in harbours or unconfined water bodies of large depth, in contrast to the confined and relatively shallow water body that is a river or channel. The hydraulic theory has, however, been of great help in this work. Studies undertaken regarding the Göta River properties, the surrounding geology etc. have also been examined in order to provide more thorough background knowledge, although the focus was on the former subject.

Existing data, provided by companies and government organizations, have been analyzed and interpreted. The data at hand have primarily been turbidity readings with stored continuous information dating back several years, river flow properties, and specifications of the ship properties. Correlation of turbidity readings and ship activity has been carried out using data from the Swedish Maritime Administration, regarding ship locations etc. SGI has also performed a full survey regarding the river cross section, which has been taken into account The data analyzed in this project is that of the summer of 2010, at which time fieldwork was also undertaken.

Fieldwork has been carried out, to ensure that assumptions regarding the provided data are accurate. All the fieldwork related to ship observations was conducted at Garn, located approximately 45 km north north-east of Gothenburg. The fieldwork includes correlation between turbidity data readings and ship passages and estimation of the ship velocities and notation of ship direction (up- or downstream). Furthermore, the ship passages were recorded using a video camera, capturing the wave motion against a fixed reference pole. By digitizing the videos, the ship-induced wave profiles were determined and used for calculating bed shear-stresses and erosion rate. In addition, the wave characteristics were compared to theoretical calculations regarding the wave heights, using formulations found in the existing literature.

By combining the information gathered from existing data and fieldwork, the bed critical shear-stress was estimated using calculated shear-stresses and measured turbidity.

2 Background

The background to the project involves not only the understanding of the geology and morphology in the study area, but also the theory governing river flows, sediment transport, and ship-induced flows.

2.1 Ship-Induced Flows and Sediment Transport in Rivers

The ship induced flows in the Göta River, *i.e.,* propeller jets and wake and waves, correspond to the extreme cases regarding hydraulic properties, as ships navigate the river at any given time of the year. There are many factors which influence the occurrence, characteristics, and consequences of these phenomena, and they are not easily modelled. The erosion and sediment transport in the Göta River due to ship activity is influenced by the SWL depth, river flow velocity, bed topography etc. Ship-induced waves are also dependent on a number of parameters, such as ship dimensions, displacement, draught, and velocity. Furthermore, propeller jets propagate in different ways depending on, among other things, the number of propeller blades, the blades area and design, and how many revolutions per minute the propeller makes.

2.1.1 Scour of Propeller Jets

The scouring of propeller jets is dependent on many different factors that depend on the design and utilization of the propeller. Using a momentum theory approach, an ideal propeller jet is, according to Hamill *et. al.* (2004), modelled assuming that the jet is created by an ideal, constant diameter actuator disc of negligible thickness in the axial direction, with an infinitive number of blades which rotate at an infinitive velocity. The fluid, which is modelled as ideal, undergoes a uniform pressure increase when passing the disc, and the energy which is transferred to the disc from the engines is supplied to the fluid with zero rotational effects (the flow direction is completely orthogonal to the disc) (Hamill *et al.* 2004).

The rate of scour also depends on how the jet is created and how it develops. The initial jet velocity, the efflux velocity, can be determined from the following equation Hamill *et al.* (2004):

$$V_0 = nD_p\sqrt{\frac{2C_tD_P^2}{A}} \qquad \text{[Eq. 1]}$$

Where
V_0 = Efflux velocity [ms^{-1}]
n = Propeller revolution speed per second [rps]
D_P = Propeller diameter [m]
C_t = Thrust coefficient
A = Projected propeller area [m^2]

The maximum depth of scour is, according to Hamill (1999), a function which depends on several variables, as stated below:

$$\varepsilon_m = f(V_0, D_P, d_{50}, C, \rho, g, \Delta\rho, \upsilon) \quad \text{[Eq. 2]}$$

Where
ε_m = Maximum depth of scour [m]
V_0 = Efflux velocity [ms^{-1}]
D_P = Propeller diameter [m]
d_{50} = Median grain diameter [m]
C = Distance between bed and propeller tip [m]
ρ = Fluid density [kg·m^{-3}]
g = Acceleration due to gravity [ms^{-2}]
$\Delta\rho$ = Sediment density minus fluid density [kg·m^{-3}]
υ = Kinematic viscosity of fluid [kg·m^{-1}s^{-1}]

Hamill (1988) also define an equation which may be used to determine the actual depth of scour from an ideal propeller jet:

$$\varepsilon_m = k\Omega[\ln(t)]^{\Gamma} \quad \text{[Eq. 3]}$$

Where t is the time in seconds and capital omega and capital gamma are defined as:

$$\Omega = 6.9 \cdot 10^{-4} \left(\frac{C}{d_{50}}\right)^{-4.63} \left(\frac{D_P}{d_{50}}\right)^{3.58} F_0^{4.535} \quad \text{[Eq. 4]}$$

$$\Gamma = 4.113 \left(\frac{C}{d_{50}}\right)^{0.742} \left(\frac{D_P}{d_{50}}\right)^{-0.522} F_0^{-0.682} \quad \text{[Eq. 5]}$$

where F_O (=$V_0/(g'h)^{0.5}$) is the densimetric Froude number and the other input variables are as defined in Equation 2. Equation 3 has, according to Hamill *et al.* (1999), demonstrated to provide accurate calculation results for propeller jets which form freely without obstructions, which corresponds to the case in the Göta River. It could, therefore, arguably be applied in the present study.

When studying Equations 1-5 above, it could logically be assumed that any calculations which aim to determine the real scour of propeller jets would be hard to perform in a satisfying manner, as there are several factors which are ship and time specific (for example the propeller revolution velocity and design). Also, the time period during which a specific section of the bed is affected by the jet would be difficult to model as the ship moves with a certain, not constant, velocity. The ship-generated waves formed by a ship are more easily modelled though. Furthermore, Equations 1-5 may, according to Hamill (1988), be applied to soils containing fine to coarse sands, and the applicability to cohesive sediment is not known.

2.1.2 Waves

Wave systems created by ships comprise of a primary and a secondary component, where the primary wave system has its origin in the water pressure and velocity distributions which exist along a moving ship hull. Assuming schematic ship geometry, an ideal variation in both pressure and velocity will occur as the ship moves relative to the water, as shown

in Figure 2. Treating the water as an incompressible fluid, the Bernoulli equation states that, for two arbitrary points 1 and 2 along the ship hull:

$$\left(\frac{U^2}{2} + gz + \frac{p}{\rho}\right)_1 = \left(\frac{U^2}{2} + gz + \frac{p}{\rho}\right)_2 = constant \qquad \text{[Eq. 6]}$$

Where
U = Ship velocity relative to water velocity [ms^{-1}]
g = Acceleration due to gravity [ms^{-2}]
z = Distance from reference level [m]
p = Pressure [Pa]
ρ = Density [$kg \cdot m^{-3}$]

The Bernoulli equation states that should one or several parameters change at one location, so must one or several do for the other point as well.

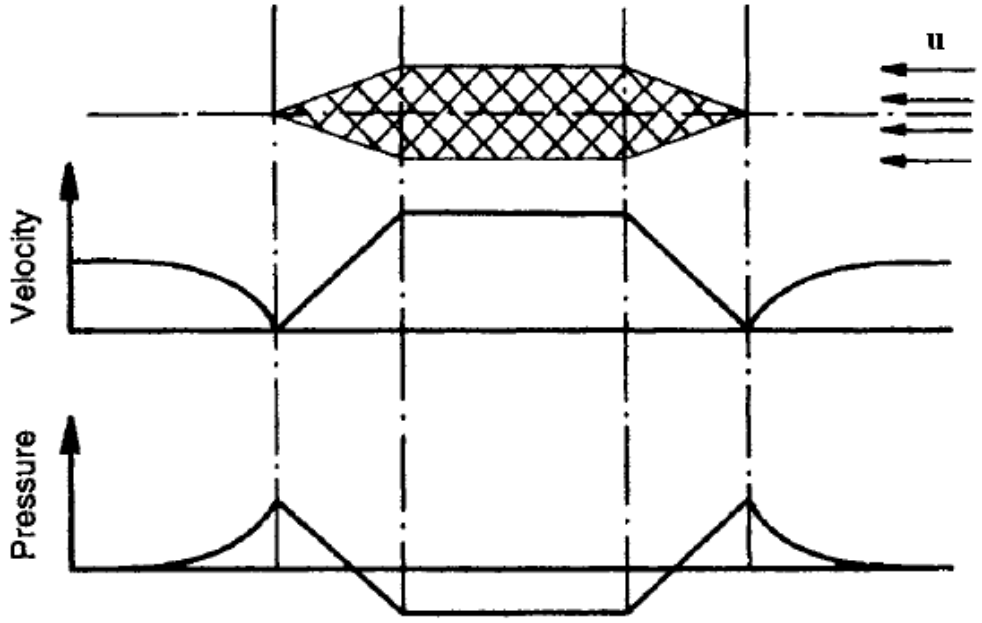

Figure 2 – Water pressure and velocity distribution of an ideal fluid along a ship-like body, inducing the primary wave system of a ship (Bertram 2000).

Ideally, this will create a single wave with a wavelength approximately equivalent to the ship length, with wave crests by the bow and stern and a wave trough mid-ships, which correspond to the primary wave system, visualized in Figure 3. Subsequently, the ship is forcing a finite volume of water in front of its stern. The primary wave system can have a long wave period, and the wave trough, which appears mid-ships, is called drawdown. According to Bertram (2000), the primary wave system amplitude is quadratically dependent on the relative velocity through the water whereas the general wave shape is independent of the velocity (water level zero, maximum and minimum values are at fixed locations).

Enhage and Wisaeus (1975) write that when a ship is travelling in unrestricted water, the primary wave system is rather small, as transport of water to the sides is possible. Should

a ship travel in a channel or river, though, the water is restricted to a small area around the ship due to the no-flow boundaries of the banks. This generates an increase in water volume transported in front of the ship, as well as an increase in velocity of the water transported along the ship, resulting in a primary wave system of greater amplitude (Enhage and Wisaeus 1975).

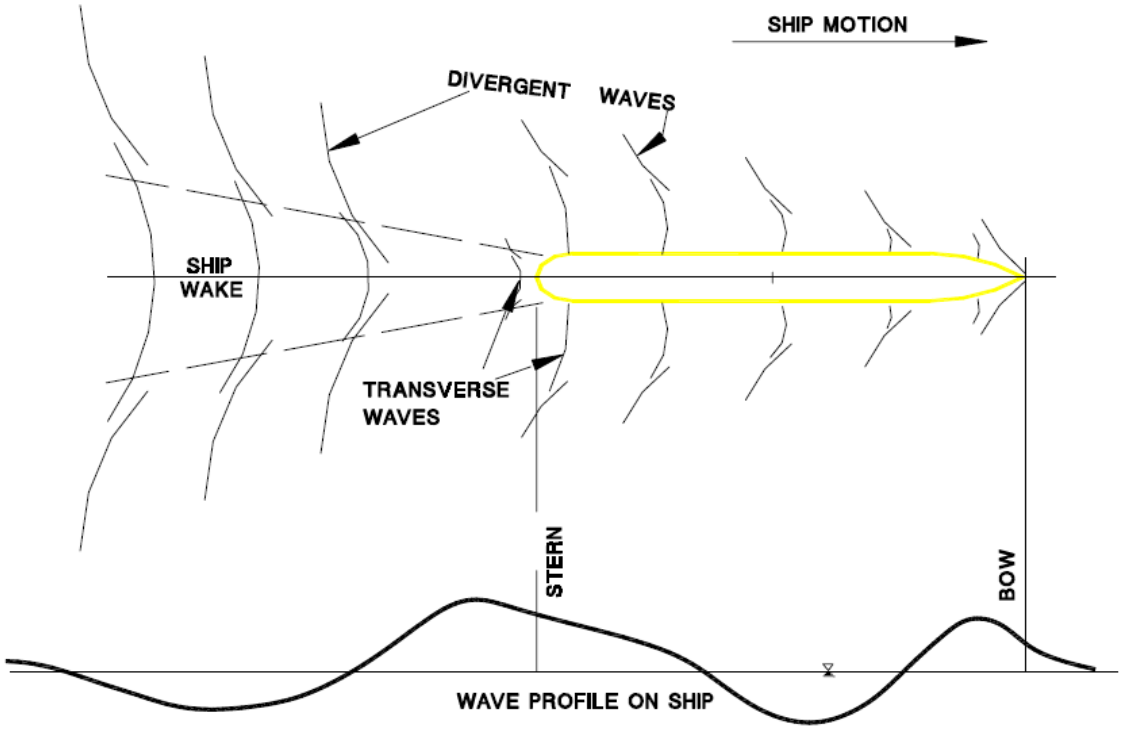

Figure 3 – Primary and secondary wave system induced by ship activity. The primary wave system is here depicted more accurately than the idealized state described earlier, with the crests displaced some distance from the ship bow and stern (US Army Corps of Engineers 2006).

Figure 4 displays the secondary wave system, which consists of a dual system of waves called transverse and divergent waves, also known as Kelvin wake (Lord Kelvin is thought to be the first person to study these waves). The divergent waves propagate with an angle ϑ from the ship centreline of direction. Bertram (2000) writes that for shallow water conditions, this angle varies with depending on the depth Froude number (see Equation 7), reaching a maximum value of 90° as the depth Froude number equals one. During deep water conditions, though, the angle is restricted to 19.5°. The hull design does not affect the angle at which the divergent waves propagate, but it plays a major role in the location of where the main wave pattern originates relative to the ship. Locations with sudden changes in the ship geometry close to the SWL are where the main secondary wave system is formed (for example the bow and stern). The relative ship velocity strongly influences the secondary wave system, as the wavelength has a quadratic dependence on the velocity. The formation of waves is more complex though, as several factors contribute to it (Bertram 2000).

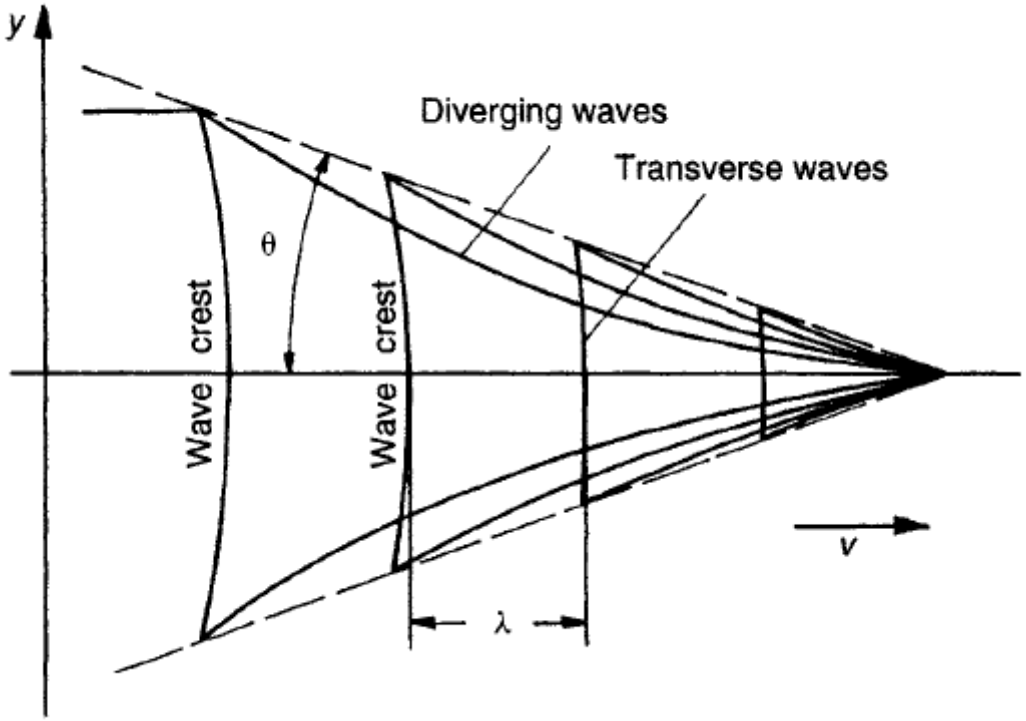

Figure 4 – Secondary wave system induced by a ship. The divergent waves propagate with an angle ϑ, which for deep water conditions is 19.5°. For shallow waters the angle varies with the depth Froude number (Bertram 2000).

The wave system created by a vessel is distinctively different depending on several factors. First, the characteristics of ship-induced waves differ greatly depending on whether they are formed in deep or shallow and unrestricted or restricted waters (the Göta River naturally corresponds to a restricted water body). Other factors which affect the wave system are:

- Ship dimensions and hull design (Kriebel and Seelig 2005).
  This includes the overall ship length, width, and the slenderness of the ship.

- Ship draught (Kriebel and Seelig 2005).
  The draught of a ship is approximately linearly dependent on the total displacement of water, which affects the Bernoulli wave formation.

- Ship velocity relative to water velocity (Bertram 2000).
  The ship velocity is one parameter included in the Froude number. As stated earlier, the ship velocity relative to the water velocity affects the amplitude and period of the waves to a great extent.

- SWL depth (Kriebel and Seelig 2005).
  The water depth influences whether ships navigate in shallow, transitional, or deep water. These conditions influence the waves.

- Location of the sailing line.
  Henn *et.al.* (2001) state that depending on where in the river profile ships navigate, the wave heights change on either side of the ship. If a ship sails

closer to, say, the port bank, the waves on that side will be higher compared to on the other side (Henn *et.al.* 2001).

- Bed topography (Torsvik *et. al.* 2006).
  Depending on the river profile, water flows have different transport patterns, regarding for example the mean flow rate etc.

Furthermore, Torsvik *et al.* (2006) argue that a change in depth Froude number affects the ship-generated wave system in shallow water for ships which travel at super- or subcritical speed close to the transcritical speed. The depth Froude number is written as shown in Equation 7:

$$F_D = \frac{U}{\sqrt{gh}} \qquad \text{[Eq. 7]}$$

Where
F_D = Depth Froude number
U = Ship velocity relative to water velocity [ms^{-1}]
g = Acceleration due to gravity [ms^{-2}]
h = SWL depth [m]

The depth Froude number can change because of two reasons, namely if the SWL depth or the ship velocity relative to water velocity changes. A decrease in Froude number means that either the ship velocity has decreased or that the SWL height has increased, *i.e.,* the bed is declining (naturally both parameters can change at the same time). An increase in Froude number then has the opposite parametric change.

Torsvik *et. al.* (2006) found, through computational experiments, that a ship travelling in a narrow channel, which either cruises at constant velocity over a changing bed topography or changes velocity through constant acceleration or retardation over a constant depth, induces solitary waves of various heights and periods. The experiments were conducted for transitions from super- to subcritical speeds and *vice versa*. The authors concluded that when ships move from sub- to supercritical speeds, the time period of the transition is the governing factor as to wave height. For the inverse case, though, the solitary wave was always generated with a notable height. In both cases is that the solitary wave period and height increases the longer the transition takes. This is argued to be because the wave is allowed to fully develop over a longer time when travelling in the transcritical region Torsvik *et. al.* (2006).

A general schematic summary of how the flow and wave patterns behave around a ship which navigates a restricted channel is presented in Figure 5.

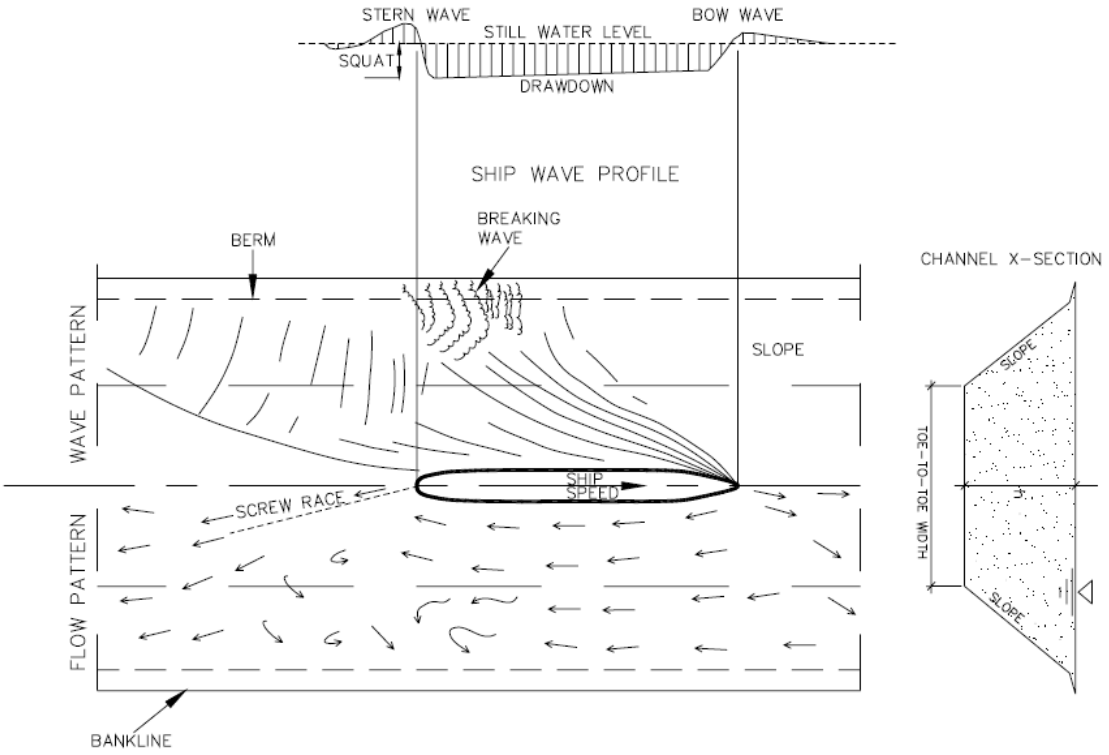

Figure 5 – Typical ship-induced wave and flow pattern in a narrow channel of trapezoidal design. The drawdown by the ship is illustrated at the top of the figure (US Army Corps of Engineers 2006).

2.2 Calculating Wave Height, Drawdown, and Shear Stress

There are a number of authors whom have conducted studies in an attempt to derive formulations which adequately describe both the drawdown and wave heights generated by ships in channels, canals, or rivers. After evaluating several papers by various authors, it was concluded that the formulations best applicable in the present study were those derived by Kriebel and Seelig (2005). The study was favourable as it takes into account, among other factors, depth-to-draught ratio, and ship velocity and hull design, whilst also being consistent with regard to physical assumptions. Furthermore, the study suggested a superior prediction model for ship-generated drawdown and maximum wave height when compared to other existing equations. Additionally, the distance from the sailing line was normalized using:

$$\frac{y}{L_s} \qquad \text{[Eq. 8]}$$

where y = Distance from sailing line [m]
L_s = Ship length [m]

and tests performed by Kriebel and Seelig (2005) showed the best correlation between measured and calculated maximum wave height occurred for y/L_s = 1. Fortunately, this corresponds fairly well with the position of the turbidity reader water intake, as well as the location of the measuring point that is used when observing waves generated by passing ships, in the present field work. The ratio naturally differs to some extent depending on the location of the sailing line and ship length, but it is considered to lie within a fairly close interval of $0.90 < y/L_s < 1.10$ in general during field observations.

When attempting to calculate ship-generated drawdown and maximum wave height, there are several factors which must be either known or estimated within a reasonable frame of error. Failing to do so will undoubtedly result in faulty calculations and conclusions.

2.2.1 Calculating Ship-Induced Maximum Wave Height

Kriebel and Seelig (2005) state that conventionally, when attempting to determine the properties of waves generated by ship activity, the Froude number used depend on whether the water is deep or shallow. When deep-water conditions are present, the ship length-based Froude number has been favoured. For shallow water, on the other hand, the depth-based Froude number has been preferable. Kriebel and Seelig (2005) have, though, derived a modified Froude number which is applicable regardless of water depth and is included in Equation 9 below. Applying the equations, maximum ship-induced wave height in a restricted water body is determined from:

$$\frac{gH}{U^2} = \beta(F_* - 0.1)^2 \left(\frac{y}{L_s}\right)^{-1/3} \qquad \text{[Eq. 9]}$$

Where H = Maximum wave height [m]
g = Acceleration due to gravity [ms^{-2}]
F_* = Modified Froude number
U = Ship velocity relative to water velocity [ms^{-1}]

β = Dimensionless coefficient dependent on ship entrance length
y = Distance from sailing line [m]
L_s = Ship overall length [m]

Kriebel and Seelig (2005) derived the modified Froude number as:

$$F_* = F_L exp\left(\alpha \frac{T}{h}\right) \quad \text{[Eq. 10]}$$

Where
F_* = Modified Froude number
F_L = Length based Froude number
α = Dimensionless coefficient varying with hull form
T = Ship draught [m]
h = Still water depth [m]

Kriebel and Seelig (2005) argue that the dimensionless coefficient α is mainly dependent on the ship block coefficient, C_B, through the relationship:

$$\alpha = 2.5(1 - C_B) \quad \text{[Eq. 11]}$$

The block coefficient C_B in Equation 11 is in turn defined as:

$$C_B = \frac{\nabla_s}{L_s B T} \quad \text{[Eq. 12]}$$

Where
C_B = Ship block coefficient
∇_s = Displaced water volume [m^3]
L_s = Ship length [m]
B = Maximum ship width [m]
T = Ship draught [m]

Kriebel and Seelig (2005) write that, depending on the hull design of the ship, the block coefficient varies. For commercial merchant ship, like tankers and bulk carriers, the block coefficient most often lies within the interval 0.6 – 0.8. Returning again to Equation 10, the length based Froude number is defined as:

$$F_L = \frac{U}{\sqrt{g L_s}} \quad \text{[Eq. 13]}$$

Where
F_L = Length-based Froude number
U = Ship velocity relative to water velocity [ms^{-1}]
L_s = Ship length [m]
T = Ship draught [m]
g = Acceleration due to gravity [ms^{-2}]

Finally, before theoretical calculations of the maximum wave height induced by a ship can be performed, the dimensionless coefficient β from Equation 9 must also be determined as:

$$\beta = 1 + 8 \cdot tanh^3 \left[0.45 \left(\frac{L_s}{L_e} - 2 \right) \right] \quad \text{[Eq. 14]}$$

Where
β = Dimensionless coefficient dependent on ship entrance length
L_s = Ship length [m]
L_e = Ship hull entrance length [m]

The ship hull entrance length, L_e, is defined as the distance between the ship bow and the point of maximum ship hull width (see bottom right of Figure 6). Now, quickly rearranging Equation 9, the maximum wave height created by a ship can theoretically be estimated as:

$$H = \frac{U^2}{g} \beta (F_* - 0.1)^2 \left(\frac{y}{L_s} \right)^{-1/3} \quad \text{[Eq. 15]}$$

Where
H = Wave height [m]
U = Ship velocity relative to water velocity [ms^{-1}]
g = Acceleration due to gravity [ms^{-2}]
β = Dimensionless coefficient dependent on ship entrance length
y = Distance from sailing line [m]
L_s = Ship overall length [m]

The dimensionless ratio between overall ship length and hull entry length depends on the hull design. Slender ships which are designed to perform well at high speeds have a longer ship hull entry length than vessels which are optimized for transport of goods (for example warships and tankers, respectively). The ships which operate the Göta River have, in general, a short entry length, which is illustrated in Figure 6.

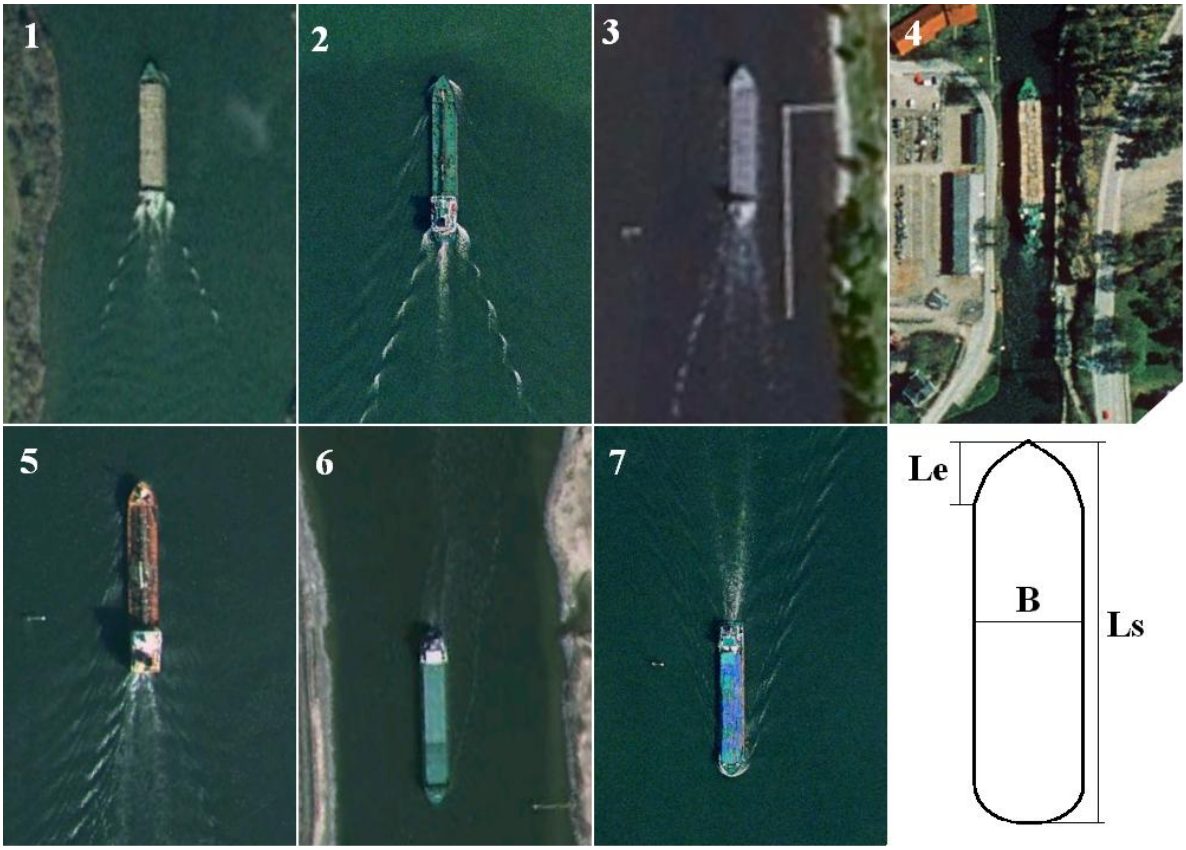

Figure 6 - Satellite photos of ships navigating the Göta River, as well as a general ship geometry figure (down right). All ships chosen were located above the Gothenburg harbour areas, so that ships which do not navigate the river up to Garn station are not analyzed. The photos suggest a short ship hull entrance length (photos 1, 5 and 6 © Google 2009, photos 2, 3, 4 and 7 © Lantmäteriet/Metria 2010).

2.2.2 Calculating Ship-Induced Drawdown

A technique to calculate the initial long-period fluctuation of the SWL created by ships, *i.e.,* the drawdown, has also been developed by Kriebel and Seelig (2005). The drawdown, which is normalized through division by the ship draught, is calculated as:

$$\frac{\Delta H}{T} = \mathrm{C}_1 \exp\left(\mathrm{C}_2 \mathrm{F}_*\right) \qquad \text{[Eq. 16]}$$

Where

ΔH = SWL drawdown [m]
T = Ship draught [m]
C_1 = Dimensionless coefficient
C_2 = Dimensionless coefficient
F_* = Modified Froude number

The modified Froude number has the same properties as when calculating the ship-induced maximum wave height:

$$F_* = F_L exp\left(\alpha \frac{T}{h}\right) \qquad \text{[Eq. 17]}$$

Where

F_* = Modified Froude number
F_L = Length based Froude number
α = Dimensionless coefficient varying with hull form

T = Ship draught [m]
h = Still water depth [m]

Also in the same way as when calculating the maximum wave height, the dimensionless coefficient α in Equation 17 is once more determined by using the ship block coefficient C_B:

$$\alpha = 2.5(1 - C_B) \quad \text{[Eq. 18]}$$

Where the ship block coefficient is in turn determined as:

$$C_B = \frac{\nabla_s}{L_s B T} \quad \text{[Eq. 19]}$$

Where
C_B = Ship block coefficient
∇_s = Displaced water volume [m^3]
L_s = Ship length [m]
B = Maximum ship width [m]
T = Ship draught [m]

The length-based Froude number in Equation 17 is defined as:

$$F_L = \frac{U}{\sqrt{g L_s}} \quad \text{[Eq. 20]}$$

Where
F_L = Length based Froude number
U = Ship velocity relative to water velocity [ms^{-1}]
L_s = Ship length [m]
T = Ship draught [m]
g = Acceleration due to gravity [ms^{-2}]

Returning again to Equation 16, it also contains two dimensionless coefficients C_1 and C_2, which Kriebel and Seelig (2005) define as:

$$C_1 = 0.0026 C_B - 0.001 \quad \text{[Eq. 21]}$$

$$C_2 = -215.8 \frac{T}{L_s} + 26.4 \quad \text{[Eq. 22]}$$

Where
C_1 = Dimensionless coefficient
C_2 = Dimensionless coefficient
C_B = Block coefficient
L_s = Ship length [m]
T = Ship draught [m]

All parameters in Equation 16 are now defined and so the ship-induced drawdown may be calculated as:

$$\Delta H = \mathrm{TC}_1 \exp\left(\mathrm{C}_2 \mathrm{F}_*\right) \quad \text{[Eq. 23]}$$

Where
ΔH = SWL drawdown [m]
T = Ship draught [m]
C_1 = Dimensionless coefficient
C_2 = Dimensionless coefficient
F_* = Modified Froude number

Kriebel and Seelig (2005) say that equations 9 - 23 described above have certain limitations restricting their range of applicability. This is because it is a recently developed set of equations and hence the amount of data which has been incorporated does not cover all parameter ranges. The model should therefore only be used if the following requirements are met:

- The modified Froude number should have a value of 0.1 – 0.5.
- The value of $\beta(F_* - 0.1)^2$ is lower than 0.4.

2.2.3 Determining Wave Properties and Bed Shear Stress

There are a number of ways to calculate the shear stress, which is induced by the flow on the river bed. Depending on the characteristics of the flow regime, the final calculations differ to some extent. For example, uni-directional flows generate shear stresses in a different way compared to oscillatory flows, and a combination of the two requires a third approach. The ship-generated waves studied in this thesis correspond to a solely oscillatory flow regime. The equation describing the average bed shear stress from oscillatory flow alone is defined by, among others, Voulgaris *et.al.* (1995):

$$\tau_w = \frac{1}{2} \rho f_w U_{orb}^2 \quad \text{[Eq. 24]}$$

Where
τ_w = Wave-averaged bed shear stress [Nm^{-2}]
ρ = Density of water [$kg \cdot m^{-3}$]
f_w = Wave friction factor
U_{orb} = Wave orbital velocity near the bed [ms^{-1}]

In accordance with linear wave theory, Soulsby (1997) define the wave orbital velocity as:

$$U_{orb} = \frac{\pi H}{T \cdot sinh\left(2\pi h / L\right)} \quad \text{[Eq. 25]}$$

Where
U_{orb} = Wave orbital velocity near the bed [ms^{-1}]
H = Wave height [m]
T = Wave period [s]
L = Wave length [m^{-1}]
h = SWL depth [m]

Furthermore, again returning to Equation 24, the wave friction factor is defined by Soulsby (1997) as:

$$f_w = 1.39\left(\frac{A}{z_0}\right)^{-0.52} \quad \text{[Eq. 26]}$$

Where f_w = Friction factor
A = Length scale [m]
z_0 = Roughness length [m]

The roughness length for cohesive sediment is approximated by Soulsby (1997) as 0.2 mm. Finally, the length scale *A* is defined as:

$$A = \frac{U_{orb}T}{2\pi} \quad \text{[Eq. 27]}$$

Where A = Length scale [m]
T = Wave period [s]
U_{orb} = Wave orbital velocity near the bed [ms^{-1}]

It is important to emphasize that the equations of this section describe the shear stress applied exclusively from oscillatory flows, which in this case equals the ship-generated wave systems in the Göta River (wind-generated waves are not of concern due to their low amplitude). Jepsen *et al.* (2004) have studied the effect on erosion rates of linear, oscillatory, and combined linear and oscillatory flow regimes on, for example, material from the Canaveral Ocean Dredged Material Disposal Site. The study concluded that, at the same flow rates, undeveloped oscillatory flows deliver a far larger shear stress compared to a uni-directional flow which is fully developed (Jepsen *et.al.* 2004).

When the process of digitizing the wave systems which are created during ship passages is complete, certain properties such as the wave height and wave period can be extracted graphically. The digitizing does not, however, provide information regarding, for example, the wavelength and celerity, so these properties must instead be calculated. Assuming that linear, or Airy, wave theory may be applied, the first thing that must be determined is whether the water in which the waves are observed, *i.e.,* where the wave height is determined, is considered to be deep, shallow, or transitional. Depending on the outcome, different formulas are applied in order to determine the wavelength and celerity. The US Army Corps of Engineers (1984) summarizes the typical classification of the water depth when describing waves in Table 1.

Table 1 - Classification of water conditions for describing waves using the SWL depth, *h*, and the wavelength, *L* (US Army Corps of Engineers 1984).

	Shallow water	**Transitional water**	**Deep water**
Relative depth	$(h/L) < (1/25)$	$(1/25) < (h/L) < (1/2)$	$(h/L) > (1/2)$

Furthermore, the US Army Corps of Engineers (1984) states that once the water conditions are known, the wave celerity and wavelength may be calculated as displayed in Table 2.

Table 2 – Summary of formulations which may be applied to determine wavelength and celerity for linear wave theory (US Army Corps of Engineers 1984).

	Wave length, *L* [m]	**Wave celerity, *C* [ms^{-1}]**
Shallow water	$L = T\sqrt{gh}$	$C = \frac{L}{T} = \sqrt{gh}$
Transitional water	$L = \frac{gT^2}{2\pi}\tanh(\frac{2\pi h}{L})$	$C = \frac{L}{T} = \frac{gT}{2\pi}\tanh(\frac{2\pi h}{L})$
Deep water	$L = L_0 = \frac{gT^2}{2\pi}$	$C = C_0 = \frac{L}{T} = \frac{gT}{2\pi}$

2.2.4 Applicability to the Current Project

There are certain aspects regarding the applicability of Equations 9 - 23 to this project which raise some concerns. The prime reason is the fact that there are no parameters defining the grade of restriction, neither of the water body, nor for the relationship between the projected area of the ship profile and the river profile. As stated in the earlier chapters of this report, especially the drawdown is heavily influenced by the existence or absence of no-flow boundaries. Exclusion of such parameters from the equations presumably has influence on the reliability of the calculations.

Given the concerns stated above, it can be argued that the use of another formula would be preferable when attempting to define foremost the drawdown. But the fact that the two sets of equations which provide ways for determining the sought after parameters (maximum wave height and drawdown) have been developed by the same authors, Kriebel and Seelig (2005), weighs heavily in favour of the use of both. The consistent approach used in deriving the equations also speaks in favour of them. Therefore, it was decided to apply Equation 9 - 23 when attempting to theoretically calculate the ship-induced maximum wave height and drawdown for this project.

There is an additional factor that could influence the estimation of the river bed erosion though, and that is, the shoaling and refraction which occur due to the inclination of the bed. As the ships navigate in depths around 7.7-8.4 metres and the reference point where the wave heights are observed is located at depth around 4-4.8 metres, there could be a transformation in wave properties. This aspect has not been investigated in this work however. This does not matter for the analysis at the measuring point though, as the wave properties are determined through observations here.

Furthermore, with reference to Equations 24 – 27, which describe how to calculate the shear stress for oscillatory flows, it might be argued that the linear wave theory is not fully applicable since waves are limited in number and travels as a package. Also, when the waves enter shallow water, some of the basic assumptions in linear wave theory are not

valid any more, for example, small ratios between wave height and water depth and between wave height and wavelength. Normally, the wave height increases up to a point where the wave breaks, simultaneously as the wavelength decreases. Theoretically, the wave period stays constant, but in reality the wave period, or at least the mean wave period, decreases when deep water waves enter shallow water (Gyllenram, 2010). Overall, the use of linear wave theory will probably lead to an overestimation of the shear stresses, as a wave package would not provide a sufficient number of waves to develop the steady-state conditions that the linear wave theory describes. For the sake of simplicity, though, linear wave theory is applied in this study. In support of this assumption, the water conditions at the reference point, where the wave heights were recorded, were either deep or transitional, but never shallow.

In short, the methods of calculating the aforementioned parameters are considered fully appropriate to apply, especially as the shear stress and rate of erosion incorporate empirical parameters which will be determined through field studies, and not theoretical considerations.

2.3 Göta River Case-Study Area

The Göta River has, according to *Göta Älvs Vattenvårdsförbund* (2008), an annual mean flow rate of approximately 550 m^3/s and it supplies just short of 800 000 people with fresh water.

2.3.1 River Catchment Area

The river's catchment area is approximately 50 000 km^2 and is the largest in all of Sweden by far, accounting for close to 10 percent of the country's land area (about 23 and 116 percent of Great Britain's and Denmark's land area, respectively). *Göta Älvs Vattenvårdsförbund* (2008) state that approximately 15 percent of the river's catchment area is located in Norway. The downstream river stretch itself is 93 kilometres long, running from Lake Vänern to the Kattegat Sea on the Swedish west coast, but the catchment mainly encompasses areas situated north of Lake Vänern. At Kungälv, just north-east of Gothenburg, the river splits into two parts, named Nordre River (*Nordre älv* in Swedish) and Göta River, where the latter is commonly called the Gothenburg Branch. The annual flow volume is divided in a 3:1 ratio in favour of Nordre River (*Göta Älvs Vattenvårdsförbund* 2008). A typical section of Göta River is about 6 – 9 metres deep and around 150 – 200 metres wide.

The catchment area in the river vicinity experiences a somewhat uniform mean annual, and also monthly, precipitation volume. A study of available data from SMHI (Swedish Meteorological and Hydrological Institute) (2010a and 2010b) shows a clear correlation between data from measuring stations in the river vicinity; see Figure 7 and Figure 8. Due to the sizable catchment area, though, different precipitation patterns are most likely present if one compares for example northern and southern areas.

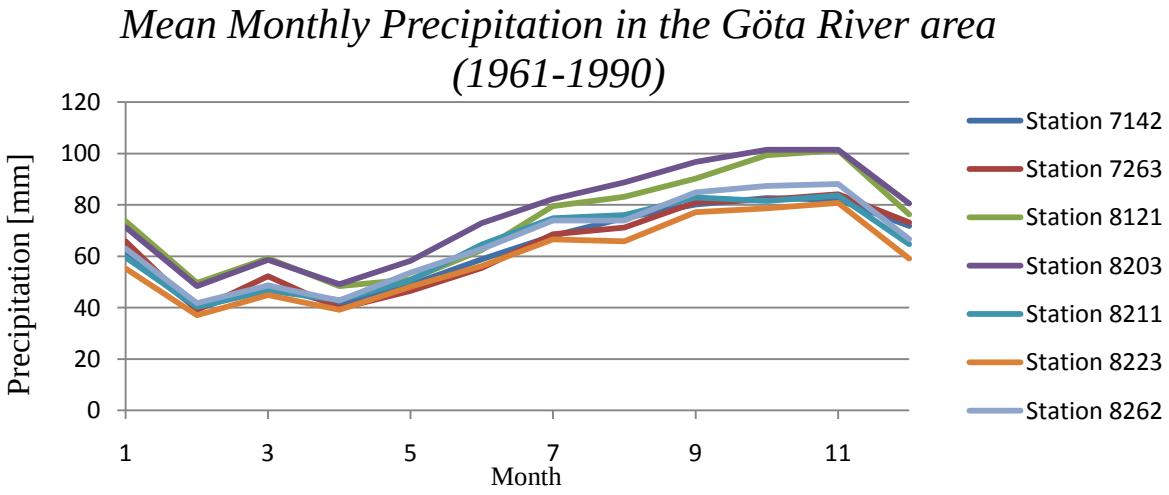

Figure 7 - Mean monthly precipitation data during 1961-1990 from seven measuring stations in the Göta River region. Data is taken from SMHI (2010a and 2010b) and compiled by Althage (2010).

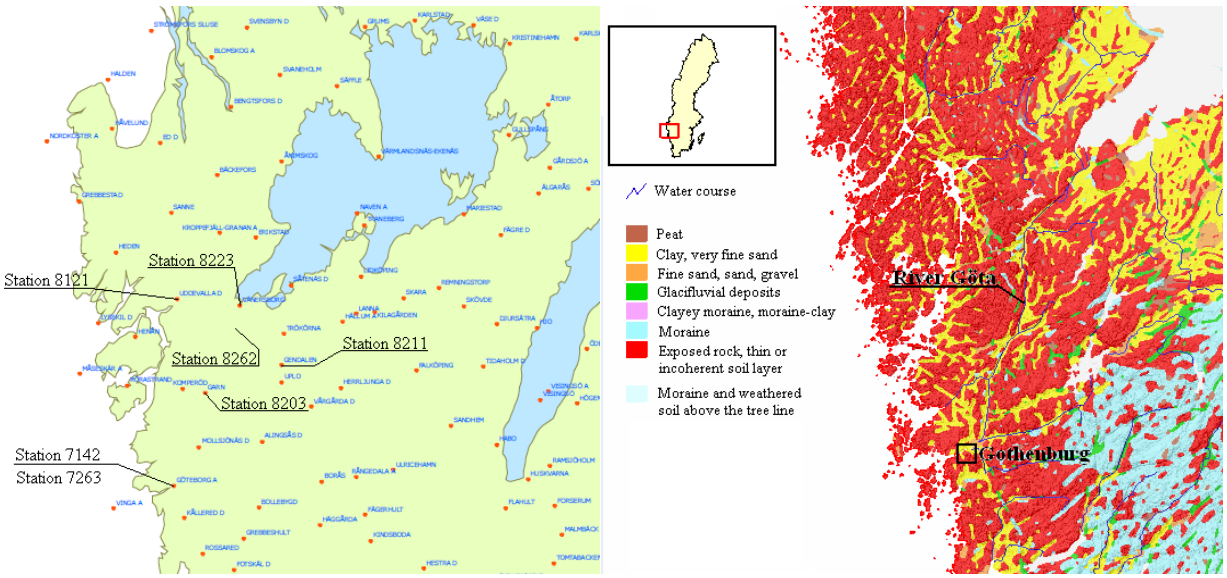

Figure 8 – Left: Approximate location of selected stations for precipitation data (SMHI 2010c). Right: Overview of the geology in the Göta River vicinity (©Geological Survey of Sweden (2010b), translation by Althage (2010)).

The monthly discharge from a number of local catchment areas in the Göta River vicinity also reveals a clear pattern. Although the precipitation is abundant during May-August, the monthly discharge is low due to less runoff and more evapotranspiration, see Figure 9.

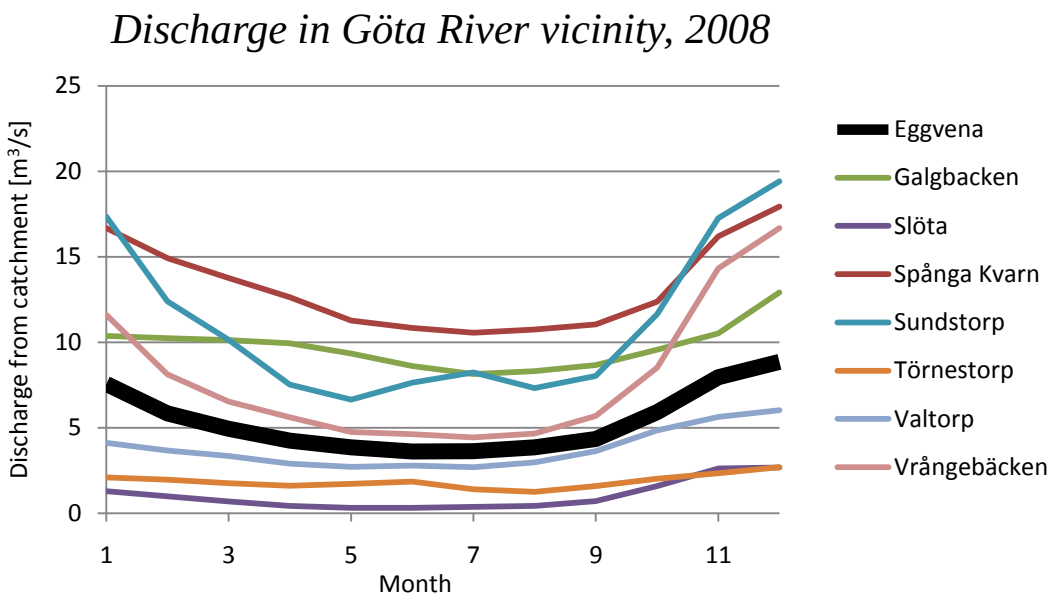

Figure 9 – Total monthly discharge from eight sub-catchments in the Göta River catchment area. The areas are located in such a way so that they contribute to the Göta River flow through tributaries, *i.e.* the water does not pass through Lake Vänern. Note the thicker black line, visualizing data from Eggvena station. All data was provided by SMHI (2010d) and compiled by Althage (2010).

The discharge of the regional catchments is important to consider, as it may provides information regarding the volume of precipitation runoff. The runoff can in turn be linked to soil erosion and, consequently, also to the contribution of particulate matter to the river system during different periods of the year. When aiming to investigate ship-generated erosion and sediment transport, it is preferable to do so when there is as little influence from other sources as possible. Hence, the discharge from the local catchment

areas should be low. The areas listed in Figure 9 are located so that the discharge primarily contributes to Göta River directly, without running through Lake Vänern.

In order to determine if the graph in Figure 9 can be said to represent the average annual discharge, a closer study has been performed for Eggvena catchment. The result is shown in Figure 10.

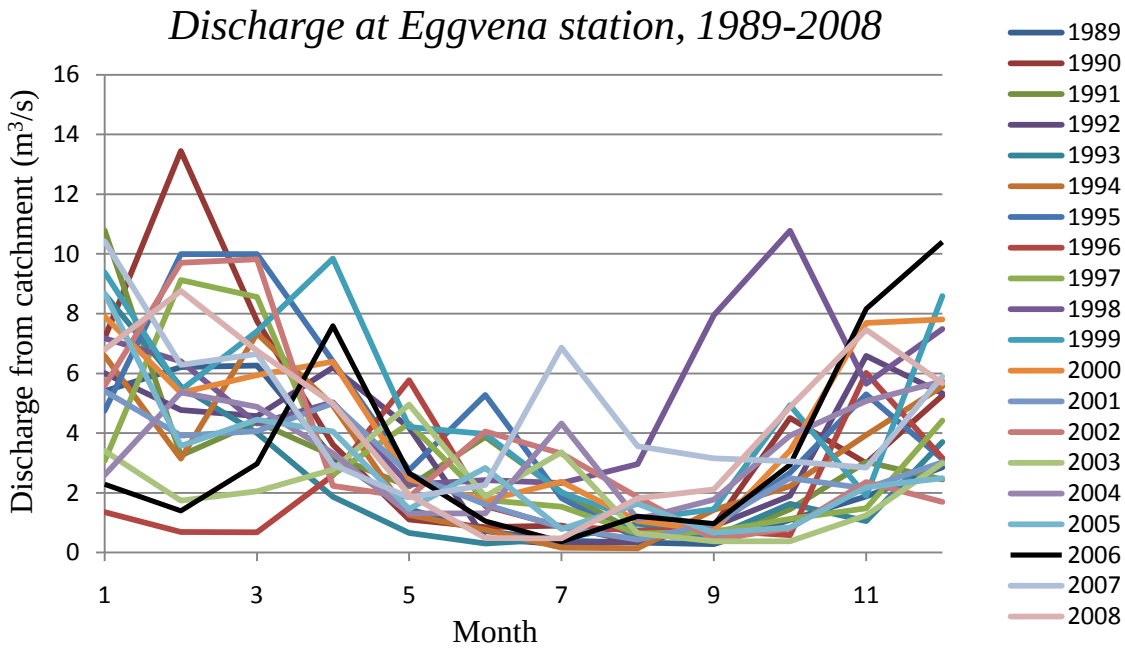

Figure 10 – Annual discharge distribution from Eggvena during 1989 – 2008. All data taken from SMHI (2010d) and compiled by Althage (2010).

It is assumed that the discharge of other sub-catchments in the area behave in a similar way. It can be seen that there is a clear trend indicating that monthly discharge is relatively low during June to August. When examining Figure 10, one can see that the months June, July, August, and September are especially suitable for the present study, which involve turbidity data, as the influence of SPM transported with precipitation runoff would presumably be low.

2.3.2 Geology and Morphology

Sundborg and Norrman (1963) state that the Göta valley geology is characterized by large areas of exposed mountainous Precambrian rock (mainly gneiss, but also diabase) and late Quaternary marine and glaciomarine clays (cohesive sediment) in the low landscape. The dominating marine clays of the river landscape have alternating layers of more rugged soil fractions, and also quick clay. The river itself flows through a valley landscape with large soil depths of up to 130 meters in the Gothenburg area and generally around 50-60 meters in the northern parts of the valley area (Sundborg and Norrman 1963). Therefore, the wetted perimeter of the river is greatly dominated by erodible soil fractions. An overview and a close-up plan view of the Göta River area is provided in Figure 8 and Figure 11 respectively, where the latter is a good representation of the river valley area as a whole.

As previously stated, quick clay is present in the Göta River area. Quick clay consist of clays deposited in a marine environment, which have the ability to change from relatively stiff

conditions to a sort of liquid mass if disturbed. Depending on the volume of quick clay, this could induce large landslides if the soil is influenced by external factors such as waves which erode river banks and transport the sediment on a large scale (Bogen and Bønsnes 2001). It is not known, however, how large the wave-generated river bed and bank erosion is in the Göta River. Therefore, despite several estimations, determining the risk of landslides due to a change in quick clay properties is not fully possible. Moreover, the location and volume of quick clay in the area is unknown. The quick clay has, though, been the cause of scarring in the Göta River vicinity.

According to Hultén *et. al.* (2006), five landslides of various sizes have occurred in the Göta River valley during the second half of the 20th century. The landslides varied in magnitude, but the two largest ones affected 24 and 32 hectares of land respectively (Hultén *et. al*. 2006). It is possible that these landslides could have been induced by erosion and sediment transport in the river and adjacent areas, making the soil unstable.

2.3.3 Sediment Transport

Sundborg and Norrman (1963) provide an estimation regarding the annual total mass of transported sediment in the Göta River. The mass is estimated to be in the range of 130 000 – 200 000 tonnes annually, and the assumed distribution of the erosion from different sources is shown in Table 3.

Table 3 – Estimated total annual mass transport and distribution from various sources of sediment in River Göta (Sundborg and Norrman 1963).

Contribution of inorganic material	Primary location	Percentage of total mass transport	Mass (tonnes/year)
SPM from Lake Vänern	River inlet	30	39 000 – 60 000
SPM from tributaries	Various locations along the river	10	13 000 – 20 000
River bank erosion	Upstream of Lilla Edet	20	26 000 – 40 000
River bed erosion	Downstream of Lilla Edet	40	52 000 – 80 000

The TSS in the water contains not only eroded material, but also organic matter, and the latter constitutes about 2-10 % of the TSS (Göransson 2010).

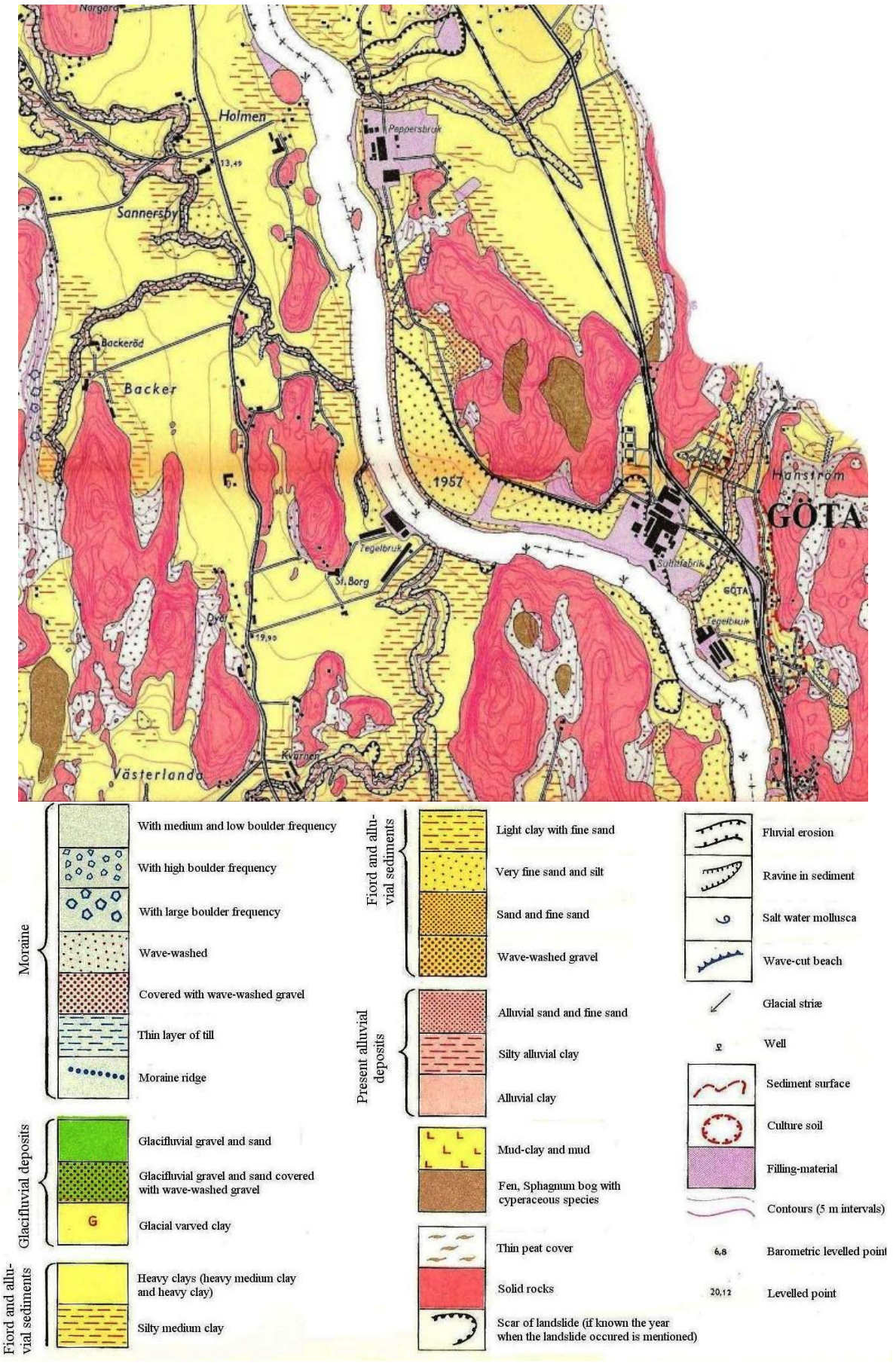

Figure 11 – Close-up plan view of a typical section of the Göta valley geology with descriptive information regarding the different soil types (Geological Survey of Sweden 1959).

2.3.4 River Flows and Water Levels

Between 1807-1934, the Göta River was not regulated, and the flow was determined mainly by the water level of Lake Vänern (the difference in height between the river inlet at Lake Vänern and outlet at Kattegat is approximately 44 m). Hultén *et.al.* (2006) write that, prior to the regulation of the Göta River, Lake Vänern had natural annual water level fluctuations of up to 2.50 metres (43.18-45.68 metres above sea level). The river was regulated in order to better manage a number of water power plants (WPPs) situated along the river stretch at Vargön, Trollhättan, and Lilla Edet. The river had, preceding regulation, a minimum and maximum flow rate of 200 and 850 m^3/s, respectively. Even though there was a large variation between the smallest and the largest flow rate, the daily variations were small. This was due to the fact that Lake Vänern served as an equalising storage basin (Hultén *et.al.* 2006).

Larson and Hanson (2006) state that the mean flow rate between 1807-1934 was 543 m^3/s, and that it decreased to 516 m^3/s between 1935-1990. Further information regarding the river's historic flow properties can be seen in Table 4.

Table 4 – Flow properties of the Göta River prior to and after the regulation of the inflow from Lake Vänern (Larson and Hanson 2006).

Flow Rate [m^3s^{-1}]	1807-1934	1935-1990
Mean	543	516
Maximum	850	1033
Mean maximum	635	836

Today, the water flow regulations include restrictions regarding the maximum and minimum flow allowed in the river. It was determined in the Swedish Court (Ruling 1937-06-19, including addition 1955-03-25), that the flow rate restrictions were to be determined by the still water level (SWL) of Lake Vänern. The restrictions are set in order to protect, for example, infrastructure and private property from flooding. The still water reference level (SWRL) is not fixed, but differs depending on date, ranging from +44.85 metres above mean sea level during 1 June - 31 December, to +44.55 metres above mean sea level at 9 March. A summary of the restrictions is shown in Table 5, and are valid for the WPP at Vargön, which is closest to Lake Vänern.

Table 5 – Regulation of the Göta River flow rate at Vargön water power plant (Ruling 1937-06-19, including addition 1955-03-25).

Water level of Lake Vänern	Minimum flow rate [m^3s^{-1}]	Maximum flow rate [m^{3-1}]
Below SWRL	*)	900 + 30
Maximum 30 cm above SWRL	900 - 30	900 + 30
More than 30 cm above SWRL	1 000 - 30	1 000 + 30

*) Plaintiff possess right to regulate flow rate, but may not jeopardize the supply of fresh water in Göta River. A minimum reference level of Lake Vänern must also not be reached.

The WPP facilities in the Göta River are the property of Vattenfall, a state-owned energy company. A short summary of the company power plants along Göta River is shown in Table 6.The restrictions in Table 5 are valid for Vargön WPP. For Lilla Edet power plant, the rules are somewhat different and are also based on the water level downstream of its location. The restrictions are enforced by Vattenfall and monitored by government authorities. There have, though, been scenarios when the maximum allowed flow rate of 1 030 m^3/s was exceeded. One such time was, according to Larsson (2005), during the autumn and winter of the year 2000, when heavy precipitation occurred during a longer period of time in the catchment area of the Göta River. This resulted in a mean weekly contribution of water to Lake Vänern of 2 600 m^3/s, which forced the county administrative board of Västra Götaland to assume control of the regulation during the winter of 2000/2001. Supported by Swedish legislation, the flow rate of the Göta River was increased to around 1 200 m^3/s for a considerable amount of time (see Figure 12) (Larsson 2005).

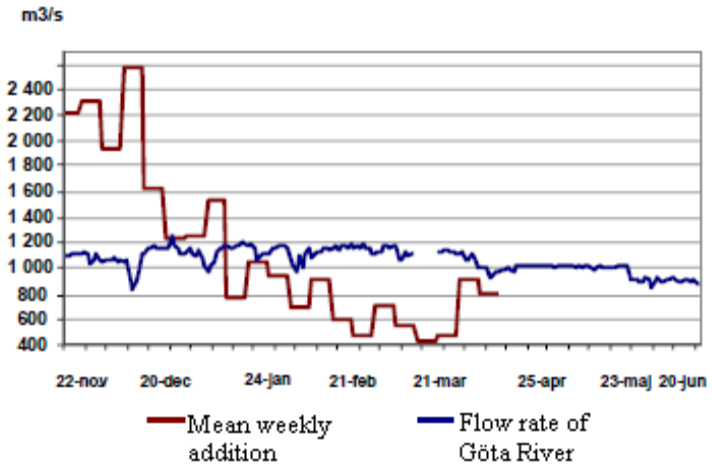

Figure 12 – Values for addition from precipitation to Lake Vänern and also the flow rate of Göta River for the period 22nd of November 2000 to 21st June 2001 (Larsson 2005).

Several sluices and power dams are located along the Göta River, with the most downstream dam situated at Lilla Edet. After this point, the water flows without anthropogenic interference to its outlet into the Gothenburg harbour area (Hultén *et. al.* 2006). The river stretch immediately downstream of Lilla Edet has an annual water level fluctuation of approximately 2.16 metres (Vattenfall 2006a), chiefly due to the regulation of the flow rate at the water power plant of Lilla Edet. The fluctuations in flow rate and SWL height for the year 2006 can be seen in Figure 13.

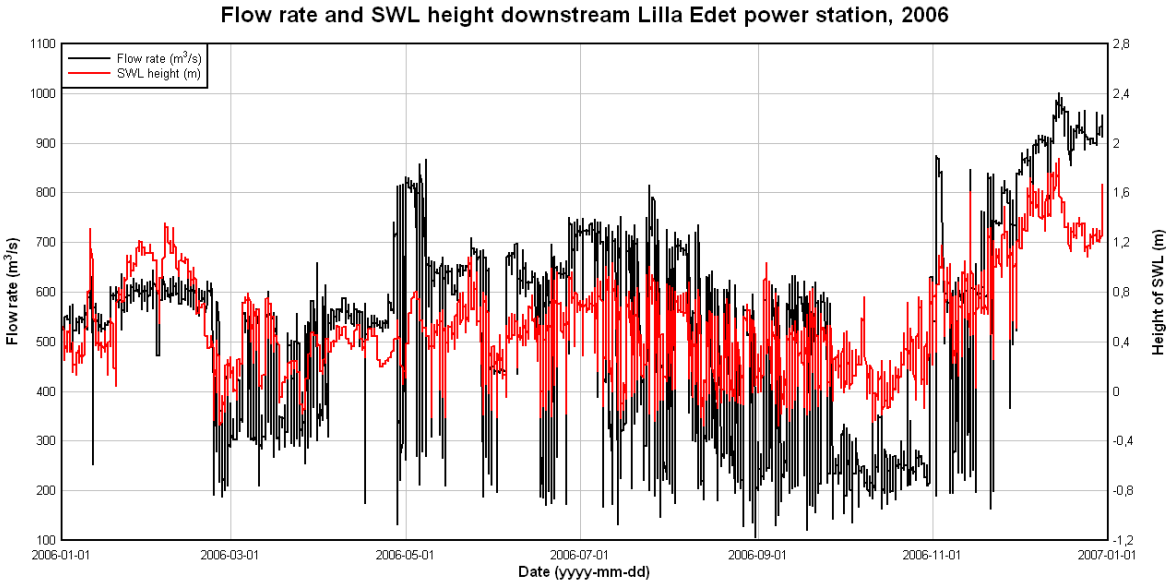

Figure 13 – Plot showing the variation in flow rate and SWL height for 2006. The values are valid immediately downstream of Lilla Edet WPP. The height of the SWL refers to a fixed point set by the operator of the power station, Vattenfall. Data provided by Vattenfall (2006a) and compiled by Althage (2010).

The variation of the Kattegat Sea water level is a factor which influences the hydraulic conditions of the river stretch downstream of Lilla Edet. Depending on the sea water level, the river flow velocity changes, as the energy slope of the river is reduced at times of a high sea water level, and increased at times of low sea water level. This is illustrated by the Manning equation, which is described by, among others, French (1994) as:

$$Q = \frac{1}{n} A R^{2/3} \sqrt{S} \qquad \text{[Eq. 28]}$$

Where

Q = Flow rate [$m^3 s^{-1}$]
n = Manning resistance coefficient [$s m^{-1/3}$]
A = Wetted perimeter of the cross sectional area [m^2]
R = Hydraulic radius [m]
S = Energy slope

The bed topography of the Göta River has been mapped by SGI during 2010, and at Garn station (see Figure 16) it has the transversal depth profile as shown in Figure 14. By knowing what the river profile looks together with the water level, the hydraulic radius and the wetted perimeter of the cross sectional area can be determined.

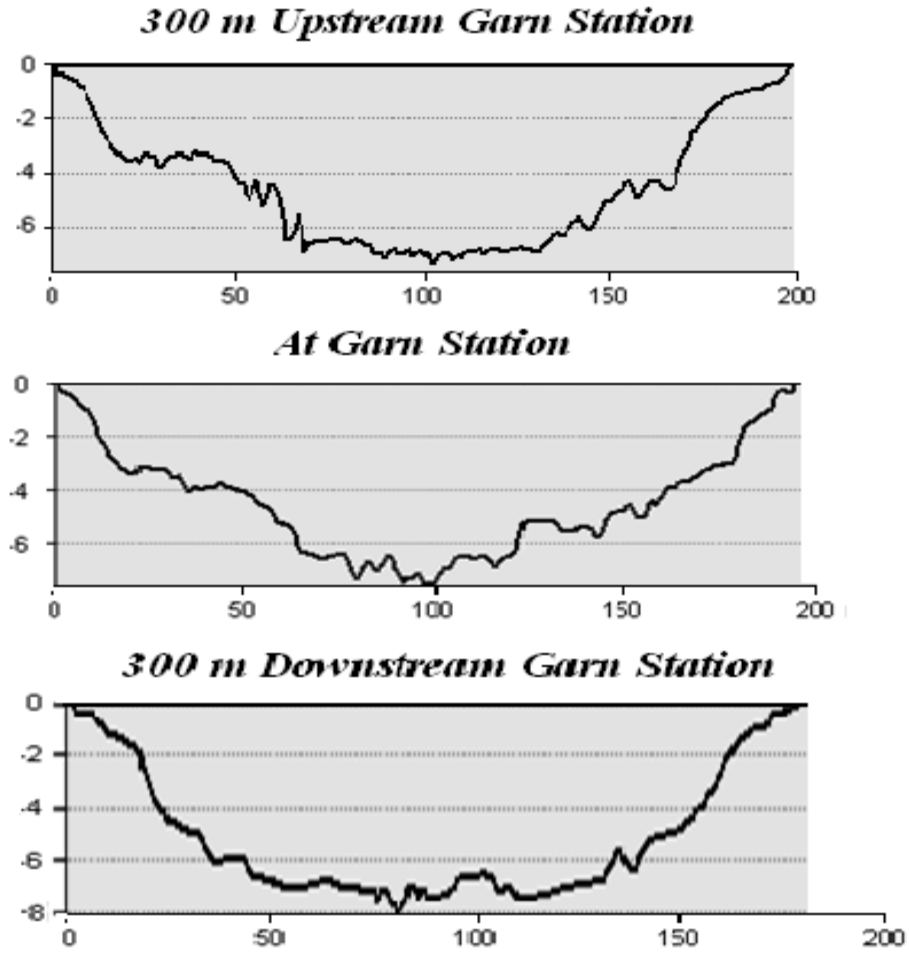

Figure 14 – Depth profile of the Göta River 300 metres upstream of Garn station (top), at Garn station (middle) and 300 metres downstream of Garn station (bottom) (Öberg 2010).

As can be seen from the figure above, the bed topography changes slightly from section to section, but correlates rather well regarding maximum depth. The bottom profile (300 metres downstream Garn station) is clearly more parabolic though.

Table 6 – Vattenfall's four water power plant facilities that are operational along the Göta River (Vattenfall, no date).

Facility	Operational from	Annual power production [GWh]	Maximum effect [MW]
Vargön	1934	165	34
Hujum & Olidan	1941 & 1920	1 260 (combined)	172 & 77
Lilla Edet	1926	210	43

The Kattegat sea level is influenced by, among other things, astronomical tides, oceanic winds, and regional air pressure variation. From Kattegat, ships enter or exit Gothenburg harbour.

2.3.5 Ship Activity

According to the Swedish Maritime Administration (2010a), the general maximum allowed velocity for vessels navigating the Göta River is set to ten knots, with some sections restricted to five or seven knots (see Table 7). Additionally, the ship size is restricted to

89.0 · 13.2 · 5.4 m (overall length · width · draught), but some exceptions can be made if ships are granted special admission. This is applicable for ships which frequently traffic the river (Swedish Maritime Administration 2010a).

Table 7 – Velocity restrictions in areas where the general 10-knot speed limit does not apply (Swedish Maritime Administration 2010a).

From	To	Velocity restriction [knots]
Lärje	Kolumbo Västra	5
S:a Tjurholmen	Svenstorp norra lt	5
Tunge	Röda Sten	7
Holmen fyr	Smörkullen	5
Lunden	Konvaljön	5
Bommen	Grop bridge	5
Board 114/109	Dalbo bridge	5

Annually, approximately 1 600 cargo and tanker ships operate in the river. The velocity restriction at Garn station, where field observations, measurements, and historical data were collected, is 10 knots. This relatively high restriction on the velocity causes more severe hydraulic impact from the ship activity.

2.3.6 Erosion through Hydraulic Impact

The erosion in rivers can derive from a number of factors. It can be caused by both natural causes, such as precipitation and natural river flows, and anthropogenic disturbances such as regulation of water flows, dredging of rivers, and ship traffic. The hydraulic impact caused by navigating ships is induced by the creation of wave systems, which generates an increased shear stress that acts on the river bed and the banks, and propeller jets, scouring the river beds. The increased erosion which might follow can be detected by for example observations in changes in water turbidity, if the mobilized material is assumed to be transported away by the flowing water and not to settle in the studied area.

Numerous studies argue that the load of TSS in a river may correlate to turbidity values (Minella *et. al.* 2007, Fink 2005, Jiménez 2009 and Packman *et. al.* 1999), but also that such relationships are site specific and varies depending on the equipment used, location of turbidity readers, and so on. Furthermore, Campbell *et al.* (2004) write that the load of TSS may differ with turbidity values depending on particle size, geometry, and colour. Clay particles have, for example, a disc-like geometry, whereas fine sand is more spherical, which means that the two grain fractions scatter light in different waves in relation to their mass, and the way light is scattered is actually how turbidity is measured.

2.4 Future Scenarios

The Göta River landscape, and also the river itself, have undergone extensive change in a relative short period of time, essentially due to the regulation of the river and re-occurring landslides throughout the region. Even though great efforts to control the river and the landscape have been made, it is probable that future events, both natural and anthropogenic, will occur which alter the present state of the region.

2.4.1 Ship Traffic

The Institute of Shipping Analysis (2006) state that the expected increase in marine cargo transport which is handled in Gothenburg Harbour is 1.4 million TEU (Twenty-foot Equivalent Unit) between 2006 and 2020. This accounts for an annual increase of 7 % from 2006. It is a logical conclusion to reach, that the transport on Göta River will take on part of this increase, and so the ship activity will intensify in the future. If so, the Göta River will experience a heavier strain on its banks and bed, and erosion and sediment transport created by passing ships will increase, unless measures are taken in order to decrease the hydraulic impact of the ships. If the annual percentage increase in ship traffic becomes reality, the estimated annual eroded bed material from ship-induced waves could be doubled.

2.4.2 Climate Change with Focus on Net Precipitation

In the future, Sweden will, according to model predictions, experience an increase in precipitation and temperature due to climate change (Swedish Commission on Climate and Vulnerability 2007). Depending on how the net precipitation is affected, increases in precipitation within the Göta River catchment area will likely result in a greater discharge and therefore also a greater flow rate compared with today. Greater flow rate means that an increase in mean water flow velocity is likely to occur as well, thus enhancing the sheer stress acting on the river bed and banks. This would in turn affect how the hydraulic impact of vessels navigating the Göta River interacts with the river bed and banks, as the ship velocity relative to the water is a factor which affects the ship-generated waves.

3 Methodology

3.1 Interpreting Available Data

There are several corporations and government institutions which monitor and record data from the Göta River on a continuous basis. First, Gothenburg Water receives and stores minute data regarding the river water temperature, conductivity and turbidity, as well as several other properties, from measuring stations at various sites along the Göta River. Second, the state-owned energy corporation Vattenfall keeps records regarding the flow rate and SWL height at several positions in the river. Third, SMHI gathers, compiles, and stores data regarding precipitation, evaporation etc. Finally, the Swedish Maritime Administration has historical data of ship activity in the Göta River.

3.1.1 Turbidity Data

The turbidity data is of special interest, because it can be linked to the total load of SPM in the river (see section 2.3.6). The measuring stations of Gothenburg Water undergo weekly inspections and are calibrated and serviced at the same time, according to Andersson (2010), in order to provide accurate readings. After maintenance it is not unusual for turbidity levels to decrease to some extent, as particles accumulate by the sensors during the week are flushed away (Andersson 2010).

Turbidity data acquired from Gothenburg Water show a great number of re-occurring peaks in turbidity values. These peaks are characterized by an initial very steep gradient, promptly reaching high values of turbidity, followed by an exponential-like decrease back to values as they were before the rapid increase. Considering the external appearance of the peaks, suggesting a point source spill pattern at the measuring station, they could logically derive from one of two reasons, namely local landslides or ship activity. Considering the fact that the Göta River vicinity has a high occurrence level of landslides, the former reason could at first glance seem rational. But the sheer number of peaks rules this out as the origin of the irregularities, leaving ship activity as the most likely inducing factor.

3.1.2 Ship Activity

Ship activity can in theory be observed in retrospect using turbidity data, since the characteristic patterns of the graphs associated with ship passage are easily distinguished. In order to confirm the ship activity, though, additional data is required. This is provided by the Swedish Maritime Administration (2010b), which records and stores information regarding the time when pilots are deployed on ships, assisting in navigating the Göta River. The stored data only contains information regarding the time and location when the pilot boards and disembarks the ships, and stating if the ship navigates up- or downstream the river. Simply adding or subtracting the estimated time for transportation to the measuring stations of Gothenburg Water provides dates and times for ship activity, which can be correlated with the turbidity readings. Regrettably, it is not possible to obtain any specific information regarding the ships themselves, such as dimensions, draught, velocity etc., when working with large volumes of historical data. It is possible to obtain such information if each vessel is studied specifically, but this requires access to the facilities and databases of the Swedish Maritime Administration.

3.1.3 Water Level and Flows

As described earlier, the water level and flow rate are monitored by Vattenfall at several locations along the Göta River. The only information which is of interest in this project is that collected from downstream of the Lilla Edet power plant, as there is no anthropogenic interference to the water after this point. The data include measurement values every hour and is given in metres (water level) and cubic metres per second (flow rate). The flow rate can be assumed to differ to a negligible degree at Garn compared to downstream Lilla Edet, due to the close distance between the two locations. The SWL, though, is not so easily transformed to Garn.

The water level measurements provided by Vattenfall are given related to the mean sea level, but it is unknown which coordinate system is employed. It is necessary to determine the absolute depth at Garn station, as it is a prominent factor when attempting to theoretically define the hydraulic impact of passing ships. Extensive measurements have been completed under contract by SGI to determine the river topography using depth-finding devices, such as sonar equipment. The gathered information has been compiled to provide detailed topographical maps of the bulk of the stretch in the elevation system RH 2000 (the Swedish National Height System 2000). The maps incorporate the SWL, and this information may be used to estimate the depth of the river, but it is not fully accurate. This is because there is no information stating what SWL is used, *i.e.,* if it is the annual mean SWL or the local SWL at the time of the measurement. Due to the variation of the SWL, it is therefore not possible to determine the exact reference depth using this information.

3.1.4 Reliability and Correlation of Available Data

The available data used in this project is considered to be of high quality. Discrepancies rarely occur and those that do can be explained through communication with the employees of the various institutes and companies which provided the data. One such case is shown in Figure 15, which shows values of turbidity, temperature, and conductivity from Garn station. Through communication with Gothenburg Water, it was explained that the event was caused by an unscheduled pump stop.

Furthermore, the estimated time for ship passage at Garn may naturally be more or less accurate depending on for example the ship velocity, how fast the pilot may assume control of the ship and start the navigation process and other such factors. If large time discrepancies exist between the peak turbidity values and the estimated time of ship passage, especially if several ships passed within a short time interval, it may simply be excluded from the evaluation as it may impair the quality of the analysis. This is of course if *in situ* observations cannot confirm the data. In doing so, the data reliability is further assured.

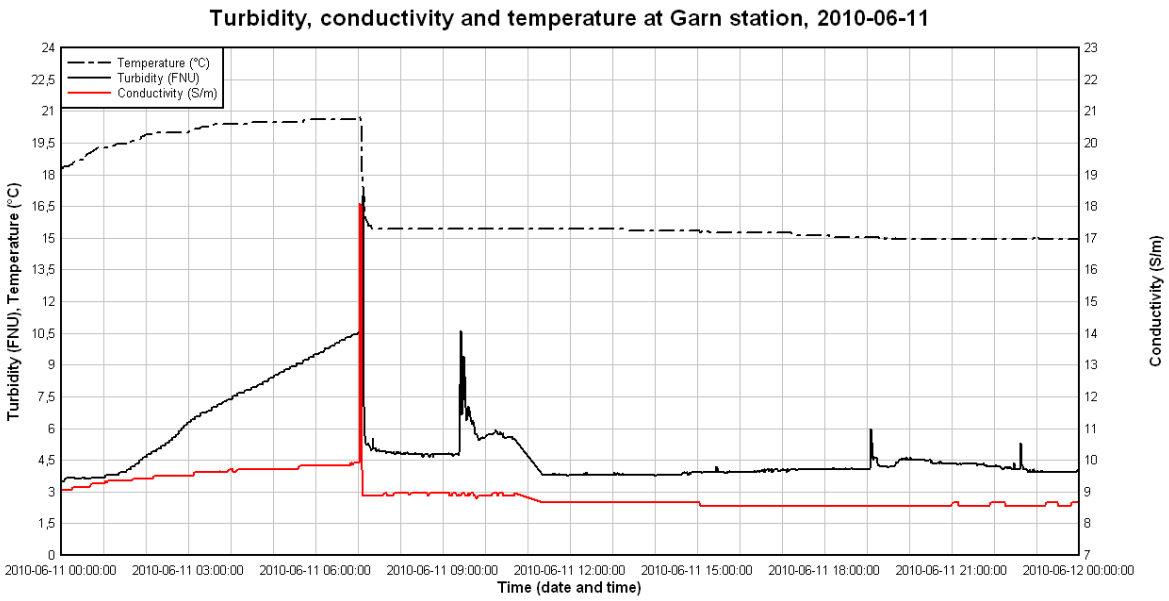

Figure 15 - Plot of water turbidity, temperature and conductivity from Garn station. There was a malfunctioning of the pumping equipment, and thus the water in the pipes could not flow, causing a rise in temperature. At around 07:00 the pump started working again (Gothenburg Water 2010).

As discussed earlier, there is no detailed information available stating at what specific time the topography of the river bed was determined or if the mean SWL was used for example, and hence it is not possible to acquire a reference point to which the observations made can be correlated. In order to determine the absolute depth at Garn station, field observations must be performed and correlated first to the Vattenfall data, and then to the topographical maps.

3.2 Field Observations and Measurements

The measuring stations which analyse the properties of the water in Göta River are utilized and maintained by Gothenburg Water. Early fieldwork during the winter of 2009–2010 was carried out in order to determine where the observations should be made the following summer. It was concluded that field observations and measurements regarding ship passages should be conducted at Garn station (see Figure 16), located approximately 44 kilometres north-north-east of Gothenburg. This location was chosen for several reasons:

- The salt wedge which is present some distance into the Göta River due to the saline water of the Kattegat Sea does not reach Garn station. This gives a more uniform and constant distribution of the density and conductivity through the water column. Also, the rate of erosion is not affected by saline water, as an increased salinity increases risk of erosion (Bradbury 2005). Thus, the erosion at Garn station should better represent erosion along the bulk of the river stretch, as the salt wedge is only present in the lower river section, even if the difference is small.
- The river stretch is fairly straight, meaning hydraulic modelling will presumably be easier compared to a meandering section. Waves are also assumed to be fully formed due to the long and straight section, which is approximately four kilometres.
- The equipment which monitors the turbidity is located some distance from the river bank and bed. The water intake is also situated about 2 metres above the river bed. This will provide data which better represent the river water as a whole compared to if the equipment was located immediately off the river bank or at the bottom.
- Maximum allowed vessel velocity is ten knots. This corresponds to the highest allowed velocity in the river. A higher vessel velocity increases the hydraulic forcing imposed by the ships.
- Access to the location is unlimited. Several other stations are located on industrial ground within fenced areas. Access to such stations for others than industrial employees is limited to employees of Gothenburg Water.

Minor disadvantages with the selected location exist as well, though. The station is, for example, located far from Gothenburg, making it time consuming to travel there. Also, the stretch is lined with anthropogenic erosion protection, so erosion of the river banks, and hence maximum turbidity, will most likely not occur. These factors did not hinder the study markedly though, as they are of negligible influence to the outcome of this work, and the river bed erosion may actually be estimated more accurately if there is less erosion of the banks.

Figure 16 – Left map; the location of Garn and Lilla Edet (© Lantmäteriet/Metria). Middle map; an overview of the location of Garn station (© Lantmäteriet/Metria). To the right are pictures from the point where observations were conducted. The top right picture is facing the upstream direction and the pipe which supplies the measuring equipment with water is extracted from the left side of the pier here, whereas the bottom right picture is facing the downstream direction (© Althage 2010).

3.2.1 Water Depth and Variation

As the data provided by Vattenfall (see section 3) are extracted from Lilla Edet WPP, it is of interest to determine whether the same fluctuations are valid where the field work was conducted. Using marked reference poles, which were fastened into the river bed close to the river bank, the SWL was noted during field studies. This information was later used in order to estimate the water depth at the Garn station.

After some time, one of the initial reference poles was washed away and could not be recovered. In order to have two separate reference options, another pole was hammered into the bed some 40 metres downstream of the first one. This pole was used as a backup reference should the remaining original pole also be damaged or washed away. After some more time, the second original pole broke just over the river bed and had to be replaced by yet another one. Because of the backup reference pole, the last pole could be secured to the river bed in such a fashion so it could be referred to the original reference pole with ease, thus securing the quality of the observations.

3.2.2 Ship Activity and Associated Hydraulic Impact

The presumed effects from ship-generated hydraulic impact were both over- and underestimated prior to observations. The drawdown was, for example, not thought to be able to produce such strong effects as it sometimes indeed proved to do, and the wave crest which sometimes swept onto the river bank following the drawdown trough was especially underestimated prior to the observations. But also the effects were sometimes overestimated, especially when large ships with deep draught produced small wave heights and drawdown, when greater effects were expected based on earlier observations. Also, some ships produced waves which were barely noticeable, while small recreational craft could muster waves of much larger amplitude (although not as long wave periods).

As the number of observations of ship passages grew larger, it became increasingly clear that ship draught, for example, which was originally considered to be one of the prime governing factors with regard to the magnitude of wave height and drawdown, did not consistently provide high values for these quantities. The same reasoning approximately

applies to ship size and SWL depth. In fact, the one factor which seemed to provide values for maximum wave height and drawdown in direct relation to its magnitude was the ship velocity relative to the water velocity.

Most often, the drawdown did not produce a hydraulic impact which endangered the slope stability of the bank, *i.e.,* the wave did not break upon the bank itself. On some occasions, though, the wave trough following the drawdown exceeded the SWL prior to ship passage, and could cause waves to break as far up on the bank as the vegetation line at Garn station (see Figure 17). These waves directly impacted areas of the river bank that the secondary wave systems were never recorded to do during the fieldwork.

Figure 17 – Wave troughs following the drawdown after two ship passages. The top picture is taken on 2010-06-04 when the ship Patria was navigating the river. The bottom picture is from 2010-08-02 during a passage by Birthe Bres. Note how high up on the bank the waves break, reaching as far as the vegetation line (© Althage 2010).

Immediately following such an event, a prominent rise in turbidity close to the bank could be observed, suggesting the erosion of bed material at the bank. When wave breaking occurred on the river bank and mobilized material, the SPM was transported towards the river centre, experiencing excessive mixing due to the following secondary wave system produced by the ships. The turbidity plots for the passages which generated the waves shown in Figure 17 can be seen in Figure 18 and Figure 19.

It is worth adding that only a few observations were made when the ship velocities reached the restriction of 10 knots. But also, a few times when ships were heading in the downstream direction, the velocities exceeded the restriction by up to 10 % (the velocity was thus 11 knots).

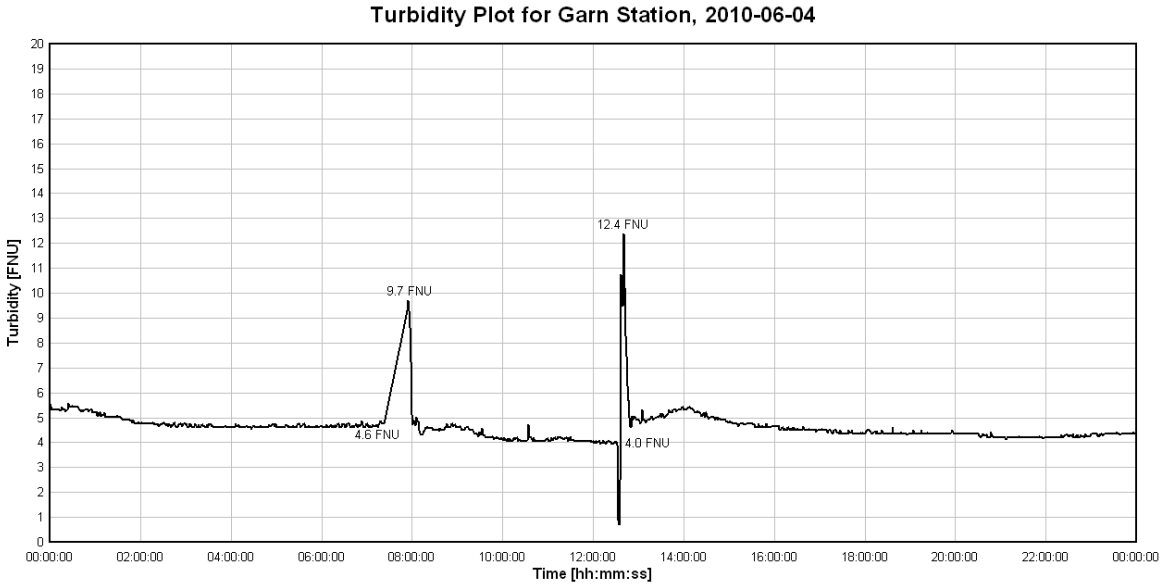

Figure 18 – Turbidity plot for 2010-06-04. The left peak was caused by the ship Patria, and the right peak by the ship Fostraum. Both passages induced a long-period wave with the drawdown causing a wave that broke high on the river bank. No photos of the breaking wave during the second passage could be taken. There is some data missing from the turbidity log just prior to the first passage, so the real turbidity peak might be higher than what the graph shows. The sudden drop in turbidity at the second passage is thought to be caused by the drawdown being so large that the water level dropped under the water intake that supplies the measuring station with water.

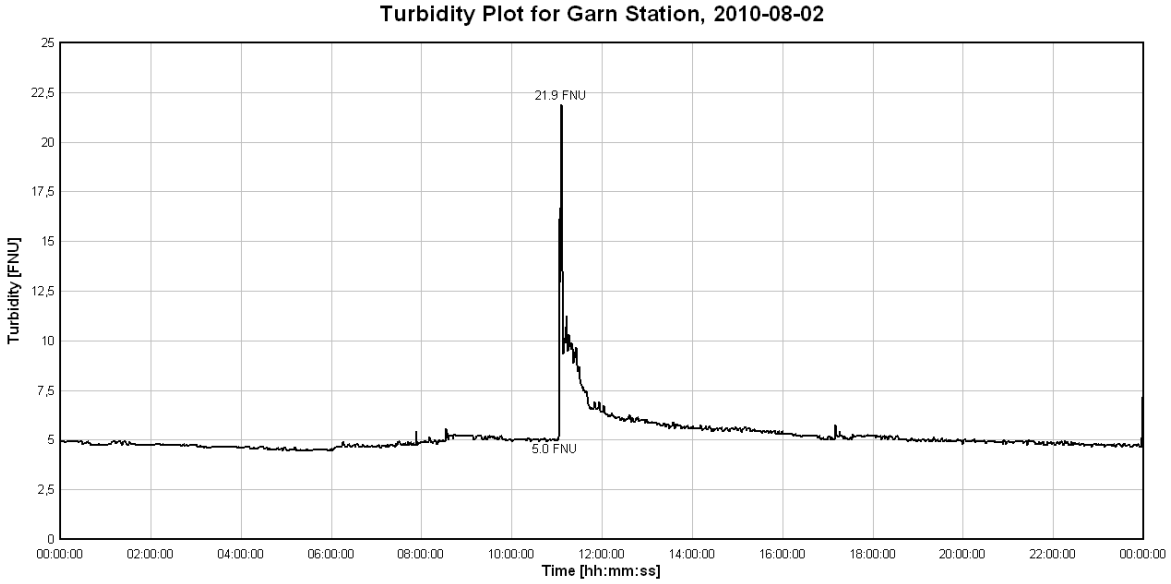

Figure 19 – Turbidity plot for 2010-08-02. Turbidity peak was caused by the ship Birthe Bres.

A summary of all ship passages, including photos, ship specifications, flow data etc. is compiled in Appendix I (there is a total of 17 passages, numbered in chronological order).

As for the secondary wave pattern of transverse and divergent waves, the latter produced the largest waves, immediately following the ship passages. The transverse waves were estimated to be present in the river for a longer time, though. During some passages, waves traveling almost completely parallel to the main flow direction of the river were observed as long as 18 minutes after ship passage. It could not be ascertained whether these were reflected waves or transverse waves traveling after the ship.

3.2.3 Turbidity

Observations during ship passages confirmed the theory suggesting that ship-induced hydraulic impact suspends and erodes particulate matter, causing the observed peaks in turbidity. During days with good weather conditions, when SPM could easily be observed, it was obvious that the detected increase in turbidity was primarily due to erosion from wave motion. An area near the eastern river bank, where Garn station is located, was greatly affected by the wave systems (see Figure 20). During the period when waves swelled upon the river bank, the water often became increasingly turbid, and stayed so for a considerable period of time after the wave system had dissipated. The visually observed width of high load of SPM, shown in Figure 20, sometimes reached approximately 20 metres from the bank, and seemed to decrease in mass per unit volume of water with distance from the bank. It could not be determined, though, how the total load of SPM per unit width changes with distance from the river bank.

Figure 20 – Observed increase in SPM at Garn station. Pictures are taken after the wave systems of the ship Patria, passing in the downstream direction, had dissipated. The intake of water to Garn station is located at the beam in the left photo, some 10-11 metres off the bank, and is clearly affected by the increased load of TSS. Note the apparent decrease in SPM mass per unit volume of water with distance from the river bank (© Althage 2010).

There were, though, times when no increase in turbidity could be observed visually. This corresponded to passages which had little hydraulic impact on the river bed and bank, generating waves of small amplitude.

3.2.4 Equipment Setup

During the field work, some equipment was prepared in order to document the river conditions and to make sure that the wave pattern could be recorded properly. All field equipment was used at Garn station where the ship passages were observed.

Reference poles were secured to the bed bottom as shown in Figure 21, and used to note the local SWL variation. The poles were marked with blue lines every ten centimetres to more clearly provide a good reference during, for example, wave action. The poles were not used for the detailed recording of the waves, though, as they were placed too close to the banks, where wave reflection is a disturbing factor.

Figure 21 - Poles secured in the bottom at Garn station. The blue markers are evenly spaced 10 cm apart. The left picture was taken just before the passage of the ship Patria. The right picture was taken about five minutes after the ship had passed Garn station. Notice the large increase in turbidity (© Althage 2010).

The video camera, used to document the wave motion, and the length-scale reference unit were set up as shown in Figure 22. The camera was able to capture both the passing ship and the wave systems, as it was placed a bit off the pier, facing in the downstream direction.

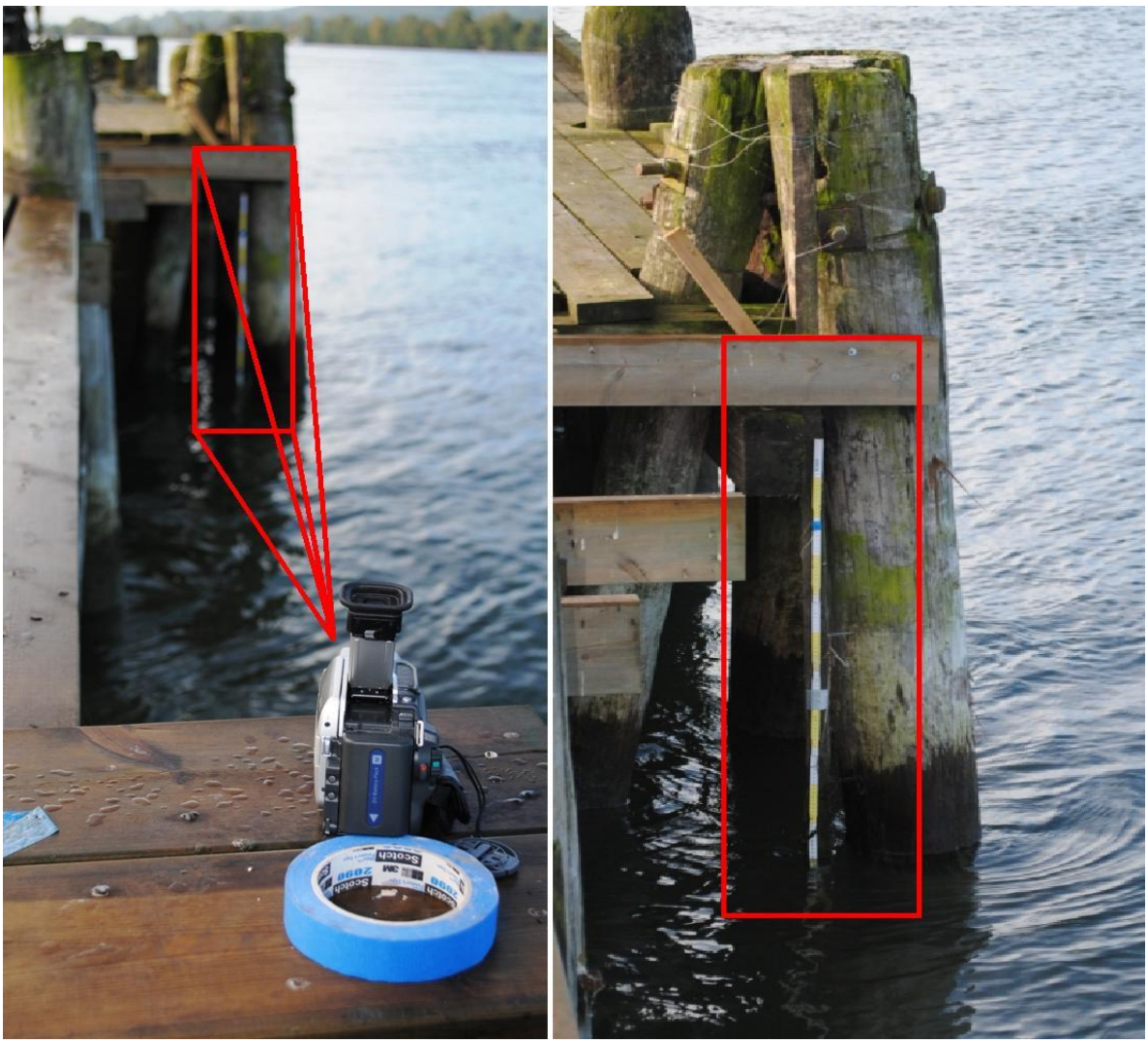

Figure 22 – Setup of the video camera and the reference pole, facing in the downstream direction of the Göta River. By digitizing video images, wave profiles were determined at a distance of approximately 84 metres from the sailing line (© Althage 2010).

The instruments operated by Gothenburg Water are shown in Figure 23. The water intake and the pumping equipment are located close to the location of the video camera, whereas the automated laboratory equipment, measuring for example the water turbidity, conductivity, and temperature, is situated just off the river. The water which runs through this station may be used in order to establish a correlation between turbidity and mass of TSS in the water, as it may be sampled immediately after the turbidity has been determined.

Figure 23 – Left; Equipment operated by Gothenburg water for continuously monitor the river water quality (© Althage 2010). Right; Location of the pump which supplies water to the monitoring equipment (© Göransson 2010).

3.3 Determining Wave Profiles

One of the main objectives of this thesis is to determine the wave profiles created by the ships and to estimate the related acting forces from the waves on the river bed. It is possible to do this using more than one technique. A common way is to install a wave gauge and connect it to a computer, which registers the motions of a buoyant object travelling up and down a rod as waves passes. This option was not suitable for this project as the water is quite deep at Garn station, and there was no easy way of safely securing the wave gauge to the bottom or to the pier. Instead, a video camera was mounted and directed towards the pier, where a measuring stick was fastened. By filming the water surface moving vertically on the reference pole, which is of known length and has proper markers, the wave profile is, although quite time consuming, easily extracted and digitized using computer software. Because of the extensive period of time needed for each digitizing, the focus has been mainly to determine the ship-induced drawdown and maximum wave height, although the whole main wave system was digitized, until the waves had almost dissipated. The digitizing took about three or four hours per passage to carry out. The process is simple and does not require access to any special equipment, and is completed in a few steps.

First of all, the videos are decompiled into separate frames so that one can choose a frame for any specific time. In order to get a good resolution of the wave profile, the videos are decompiled into 30 frames per second of video. Then, the video itself is studied in order to select the time intervals when extra fine resolution must be chosen in order to properly determine the locations of the wave crests and troughs, which are used to determine the wave heights and periods. Using the program *digitize07* (written by Todd Pataky) for MatLab, the frames corresponding to the selected times are uploaded and analysed. Applying simple "click-and-extract" techniques built into the program, pixel-coordinate data is extracted and then manually transformed into real world coordinates by using the known reference points of the video, *i.e.,* the measuring stick. All the coordinate data was stored together with the associated time and was used to create graphs such as Figure 24.

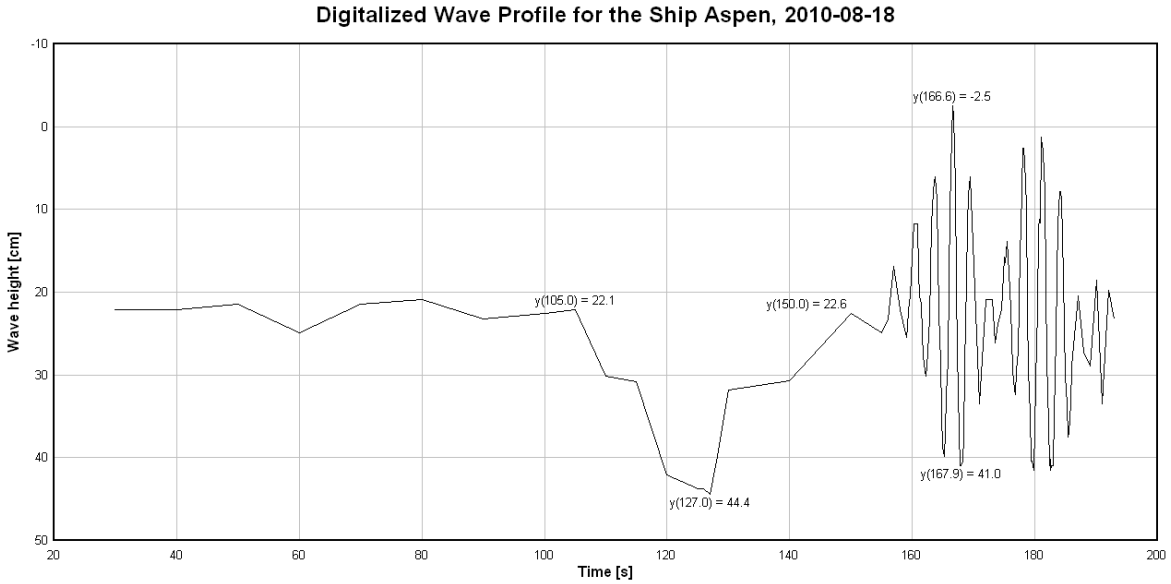

Figure 24 - The digitized wave profile for the ship Aspen, navigating the Göta River 2010-08-18. The real world coordinates were determined using the program digitize07 for MatLab.

Precautions were taken in order to guarantee high-quality data, and so the first five or six frames were always double checked in order to confirm that the technique provided adequate results. Any suspicious transformed coordinates were also checked a second time in order to eliminate errors. Furthermore, the time interval used when determining maximum wave height was as narrow as every second frame, that is, 15 elevation points per second. Due to a limited resolution of the video camera used, high accuracy cannot be claimed in all cases, but the error margin is considered to be quite small.

Afterwards, the wave profiles were compared to each other and plotted against other parameters, for example, the ship draught and ship velocity relative to water velocity. In doing so, any major errors which could have been made during the digitizing process, the transformation to graphical format and so forth, could be identified and promptly corrected.

It is important when carrying out this type of field work that the diameter of the reference pole, towards which the video camera is directed, is considerably less than the wave length. Should this not be the case, there is risk of interference with the waves created by the pole. Furthermore, the reference pole should be placed well off the bank so that waves which are reflected off the banks do not disturb the incoming wave profile. During some ship passages, the reflected waves would influence the incoming waves, affecting the recorded wave profiles. Luckily, though, the maximum wave heights were found in the early stages of the incoming wave package, so there were rarely any problems with regard to reflected waves. The wavelengths were also long enough not to cause interference from the pier poles.

4 Results

In order to arrive at firm conclusions regarding the ship waves and their effects, a thorough analysis involving existing data, field measurements, and theoretical calculations must be conducted. Throughout the project, the many factors which influence the wave formation were studied in relation to each other, and in relation to the pre-existing data and observations made by the author. Before any calculations could be made, though, certain parameters, such as the depth at Garn station, would have to be determined.

4.1 Water Depth and Variation

The SWL variation at Garn station was initially assumed to coincide with the fluctuations immediately downstream of Lilla Edet rather well. Although, certain factors were considered to more or less affect the relationship:

- Changes in flow rate at Lilla Edet bring with it a change in SWL. This is not detected as swiftly further downstream. Hence, a delay in SWL variation is to be expected in the response at Garn compared to Lilla Edet.
- The state of the Kattegat Sea SWL. An increase in sea SWL could make the SWL of the Göta River rise.

The SWL variation at Garn station was compared to that of Lilla Edet WPP, where information is stored continuously once every hour. Because of this time resolution, two values were extracted from the WPP for every observation value. One value was taken about 0-60 minutes before the observation at Garn was made, and one about 60-120 min before. This allowed for some transport time of the water, if large changes in flow rate took place. The result can be seen in Figure 25, together with the estimated total water depth at Garn station for 21 observations. The real depth at Garn station could not be determined exactly, only approximately estimated. Even though there are detailed scans of the river, which include the SWL, it has not been possible to determine at what exact time these scans were made, hence the local fluctuation of the SWL precludes the possibility to determine the depth from these scans more than approximately. The scans also have a zero elevation related to the sea level in the coordinate system RH 2000 (Öberg 2010). The best estimation of the actual depth at Garn has been carried out and it includes some easy calculations and assumptions.

First, it is assumed that the SWL decreases linearly from Lilla Edet WPP to the Kattegat Sea and that at the outlet, the SWL height is zero. By comparing the data at the WPP, which refers the SWL to the sea level as well (Vattenfall 2010), and the observed SWL at Garn station, a similar variation is noted. It is only logical that the variation is more pronounced the farther upstream the river you look giving the assumption made regarding a linear decrease in SWL. By simple map measuring, it was estimated that Garn lies about 6.45 km from the WPP, whereas the river outlet lies 58.0 km away. This means the distance from the WPP to Garn equals about 11.3 percent of the total downstream stretch from Lilla Edet. Therefore, simply by linearizing the WPP values the estimated total depth at Garn station is given by:

$$h = \frac{h_{wpp}}{2} + 7.5 + \Delta h \qquad \text{[Eq. 29]}$$

Where

h = SWL depth at Garn station [m]
Δh = Correction factor [m]
h_{wpp} = Sum of two consecutive SWL readings from Lilla Edet WPP [m]

The correction factor Δh was necessary to use in order to obtain the best fit when comparing the simple model to the observed fluctuations in SWL from Garn station. The number 7.5 is the approximate average depth in metres under the zero reference level along the ship sailing line at Garn station. By applying this equation, allowing for a correction to better fit the observed SWL variation, the total depth at Garn station was determined for all the ship passages which were observed (see Figure 25).

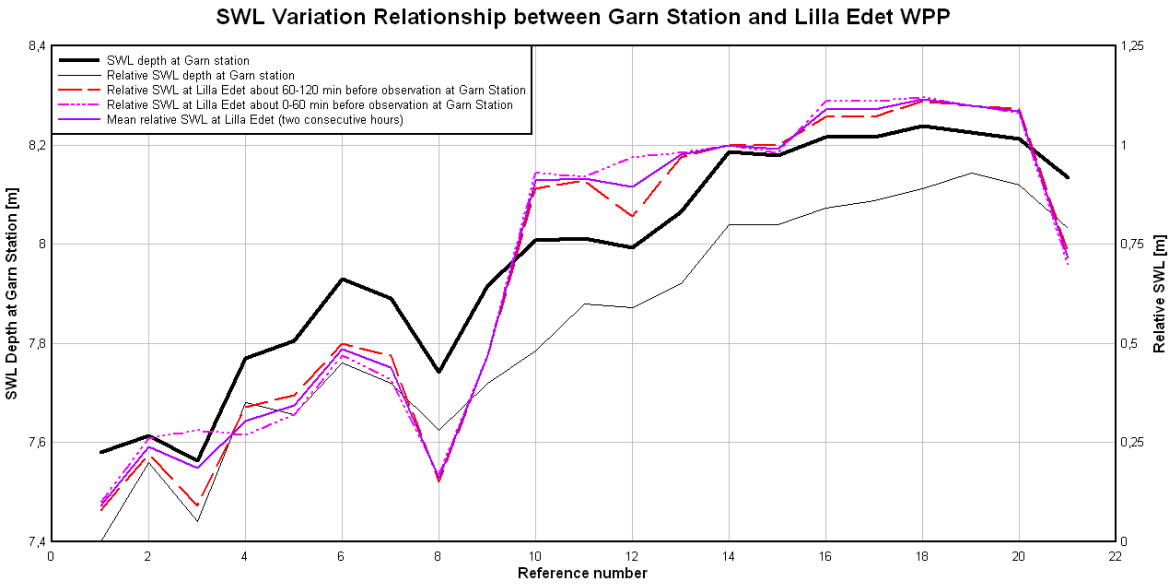

Figure 25 - Graph of the variation in SWL at Garn station and Lilla Edet WPP for 21 observations. Also, the estimated total water depth at Garn station is included. It is important to point out that the reference numbers are in chronological order, but not of relevance to each other. The water depth at Garn station is shown prior to the introduction of the correction factor Δh (Althage 2010).

It can be concluded that, using this approach, no clear pattern can be distinguished regarding how to fully determine the SWL at Garn station simply by looking at the data from Lilla Edet WPP which has been used. The variation is too large to permit any simple method to obtain a depth of high quality, although estimations have to be made. This may be due to several reasons:

- The outlet SWL is not always zero due to tidal influence, oscillations from wind setup generated by shear stresses etc.
- The SWL at the WPP occasionally falls below zero, which in all probability means that the outlet SWL is below zero as well (this was never the case for the observations above, though).
- A high SWL gives a steeper gradient per unit river length compared to a low SWL.
- The SWL decrease is most likely not fully linear due to the non-uniform river bed topography.

- Different time intervals should have been used for the data from the WPP.

An opportunity for determining the absolute depth at Garn station did not occur during the project, but this is considered to be of minor importance for the analysis results. This is because other factors such as the location of the sailing line is very hard to determine exactly as well, and because of the changing bottom topography the absolute depth is not easily defined. The depth precisely orthogonal to the equipment set up is not, for example, a depth well chosen, as the wave characteristics are influenced by the river properties either up- or downstream the station where the waves are generated in the first place. The estimated SWL depth presented in Figure 25 is therefore considered to be a good estimation for use in the modelling. The SWL was, however, further adjusted to provide the same fluctuation in height as was recorded using the reference poles in the project. This gives a relative SWL depth, which is of sufficient quality to be used in the calculations.

4.2 Ship Activity, Turbidity, and SPM

The data provided by Gothenburg Water from Garn station gives detailed information on the water turbidity. When comparing the raw data to actual official graphs from the institution, though, a time difference was noted. The discrepancy was about one hour, where the raw data was ahead of the official graphs. This did not prove problematic as both sources of information were used in order to properly correlate the time of ship passage to the turbidity readings. In fact, the raw data was only used as it enabled the presentation of self-made graphs which better visualized the data. It could sometimes be hard, though, to exactly distinguish when a ship passed Garn station just by looking at the turbidity graphs due to little or no influence on the turbidity. This is not a problem, though, as the conclusion then is simply that the ship did not induce a rise in turbidity.

Most of the ship passages generated a clear rise in turbidity, but some had little or no influence. The maximum net increase in turbidity (over base level) was 16.9 FNU (Formazin Nephelometric Units), and the minimum was not clearly distinguishable.

The turbidity patterns show interesting features when two ships navigate the channel close to each other (passing the same point within a one-hour interval, for example). During three different days when field work was carried out, the same occurrence was noted. Even if the ships had similar properties and the SWL depth was the same, the ship which passed first generated the highest rise in turbidity of the two, which is illustrated in Figure 26, Figure 27, and Figure 28 below.

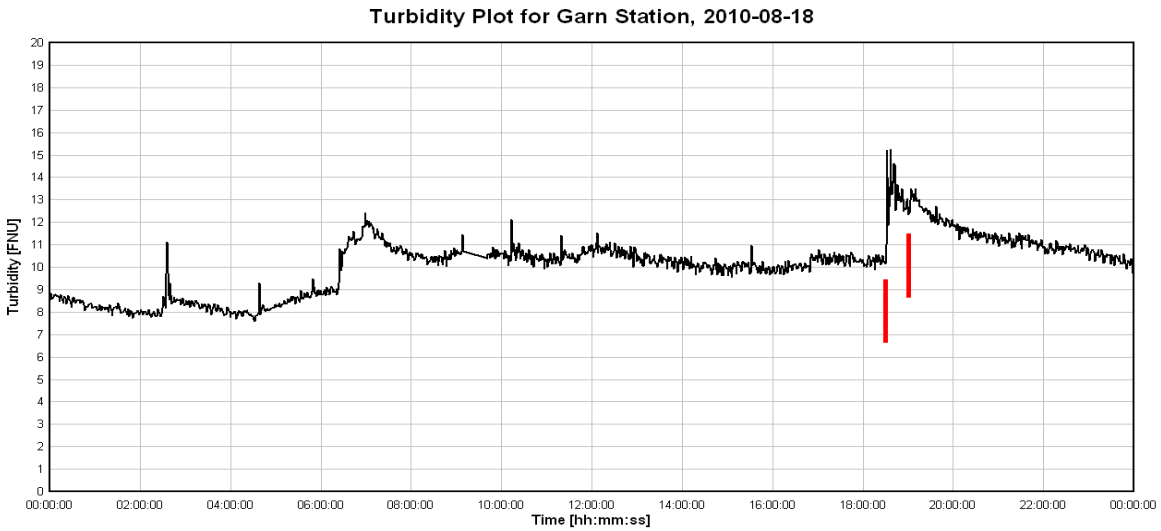

Figure 26 – Turbidity plot showing two ships passing Garn station within a short interval. The first passage produced the greatest increase in turbidity. The red vertical lines mark the ship passages.

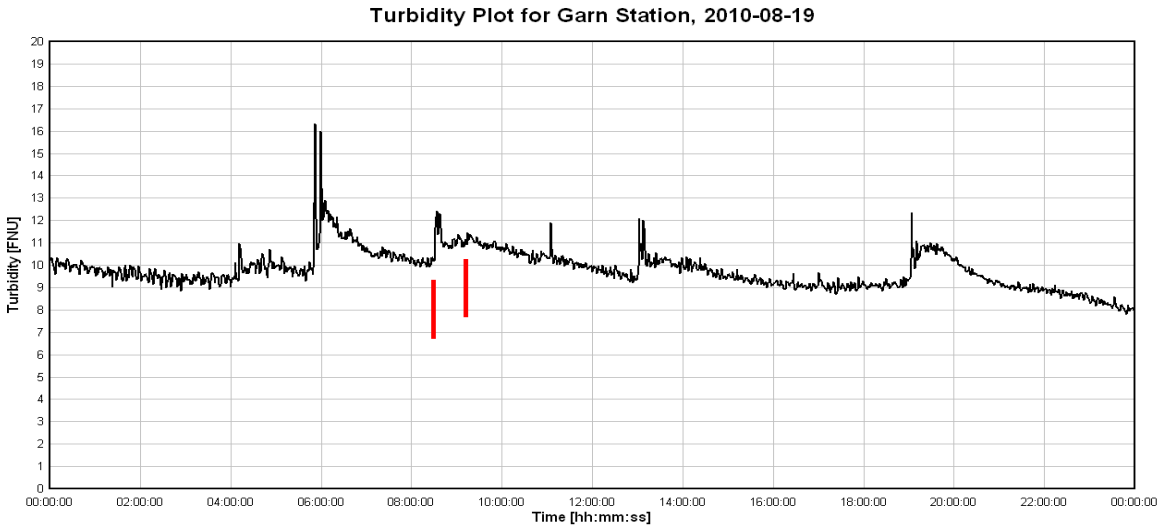

Figure 27 - Turbidity plot showing two ships passing Garn station within a short interval. The first passage produced the greatest increase in turbidity. The red vertical lines mark the ship passages.

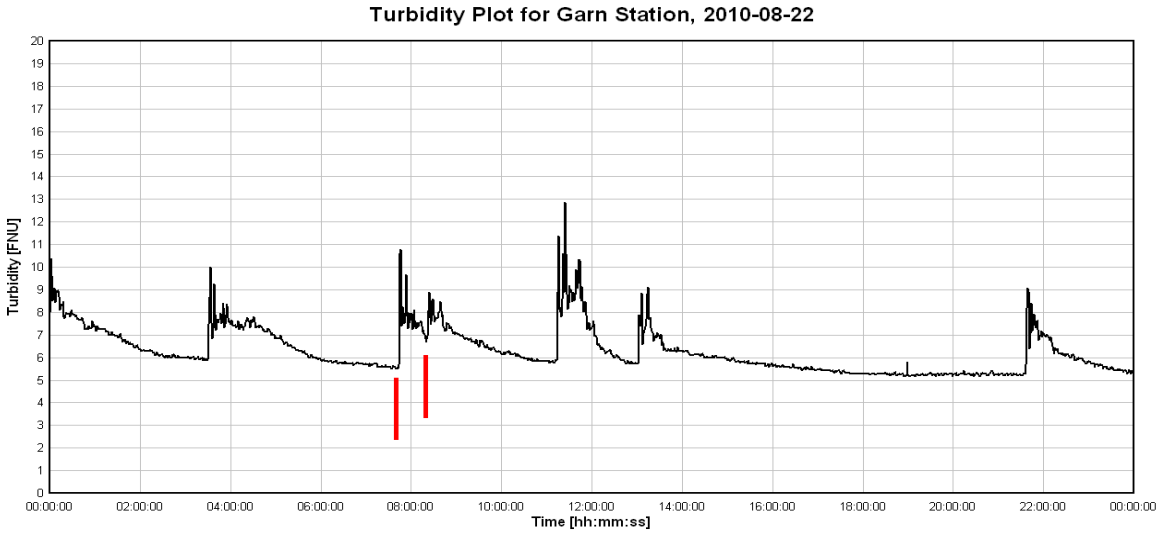

Figure 28 - Turbidity plot showing two ships passing Garn station within a short interval. The first passage produced the greatest increase in turbidity. The red vertical lines mark the ship passages.

One possible explanation, which is considered to be the likely cause of the pattern, is the existence of a bed surface layer of sediment which is easily induced into suspension. The top layer would thus have a critical shear stress notably lower than the underlying bed material. The theory is that when the first ship passes, the drawdown and the following wave system suspends, or perhaps more correctly re-suspends, this top layer and possibly some particulate matter with higher critical shear stress from underneath. Part of this SPM does not settle before the passage of the next ship, which then to a greater extent affects the aforementioned particles with a higher critical shear stress. This would logically mean that the second ship would not cause as large an increase in turbidity as the first ship. If one would argue that the second ship should produce an even bigger turbidity increase compared to the first ship due to the fact that some material is already suspended, it is important to remember that the turbidity is a measurement which is not volume dependent. It is indeed most likely that the total mass of SPM in the water is larger after the second ship passage, but the concentration per unit volume of water is less due to the advection and dispersion of the SPM suspended by the first passage. Therefore, it is possible that the second ship passage better describes the erosion of the river bed as it theoretically may suspend bed material that has not been mobilized before.

4.3 Turbidity and Precipitation

As discussed earlier, precipitation is thought to cause disturbances to the levels of turbidity in the Göta River through transport of particulate matter in connection with surface and tributary runoff. This type of contribution was observed at Garn station 14th of July 2010, when heavy precipitation occurred in the Göta River area. In Figure 29, this external contribution to SPM from runoff is shown as a slow increase in mean turbidity.

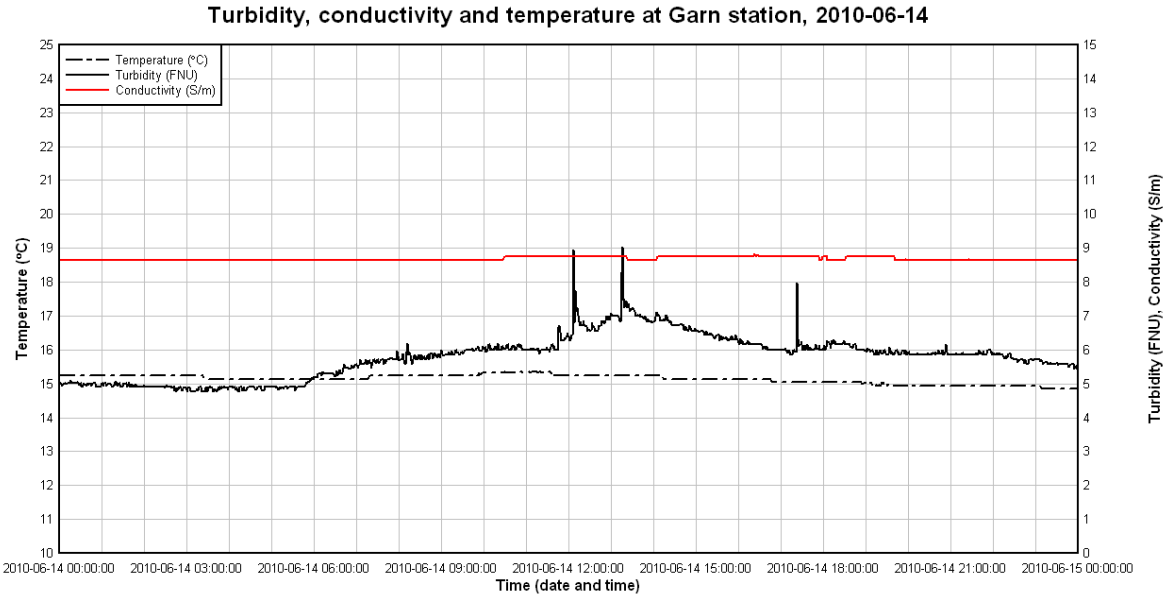

Figure 29 – Turbidity, conductivity, and temperature plotted against time for 2010-06-14. During this date, heavy precipitation occurred, starting a few hours into the day. The increase in mean turbidity, starting at around 05:40, is thought to be influenced by increased contribution of particulate matter transported with runoff. The two peaks at around 12:00 and 13:15 are due to ship activity. Observations were conducted on site. Data provided by Gothenburg Water (2010) and compiled by Althage (2010).

The increase could, though, also partly be explained by a rapid contribution of particulate matter from the river banks. During fieldwork, it was noted that the stones, blocks and boulders, constituting the anthropogenic erosion protection, had a more or less extensive

cover of clay which was easily scraped off (see Figure 30). It is possible that the material loosens and is added to the river water when exposed to precipitation.

Figure 30 – Anthropogenic erosion protection at Garn station. The blocks and boulders are partly covered by fine cohesive sediment at times of low SWL, which is easily scraped off. This layer is thought to be easily eroded and consequently, to varying extent, also added as SPM to the river during times of precipitation. This could partly explain the prompt increase in mean turbidity in times of precipitation (© Althage 2010).

4.4 Theoretical and Observed Maximum Wave Height and Drawdown

Some of the parameters needed, in order to perform proper calculations regarding the maximum induced wave height and drawdown during ship passages, have been determined using data from field observations and various other sources, so that the end result is not corrupted by erroneous input data. There are three parameters which could be possible sources of errors, though, which were not possible to determine with great accuracy.

The first parameter is the water velocity, which was difficult to determine properly along the navigation line. Using data from Vattenfall (2010), though, the mean river flow rate could be obtained and, by approximating the river profile area, the mean flow velocity for the whole profile could be estimated. The second parameter is the distance from the sailing line to the observation point. This distance was plainly estimated to 84 metres for all calculations. The third factor is the ship block coefficient, which could not be determined due to a lack of data regarding the ship hull design. For ships which were unloaded, though, the block coefficient could be determined using data for ship draught, length, width, and dead weight, giving the displaced water volume and the ship box volume (see Equation 13). One ship with 3.2 metres draught, which was considered unloaded, had a block coefficient of 0.759. Another ship with draught 3.5 metres would, if unloaded at the time, have a block coefficient of 0.712 (it is likely that the ship had some cargo on-board at the time of passage, though). Due to this uncertainty, the calculations were performed for three different cases, namely with a block coefficient of 0.6, 0.7 and 0.8.

It was noted, that when all passages were included, the result differed compared to that produced if only the upstream passages were considered (the usptream passages constituted 13 out of the total 17 passages). For the correlation of H_{max} against different governing parameters, the calculated result provided a better fit when the downstream passages were excluded (see Figure 31 and Figure 32).

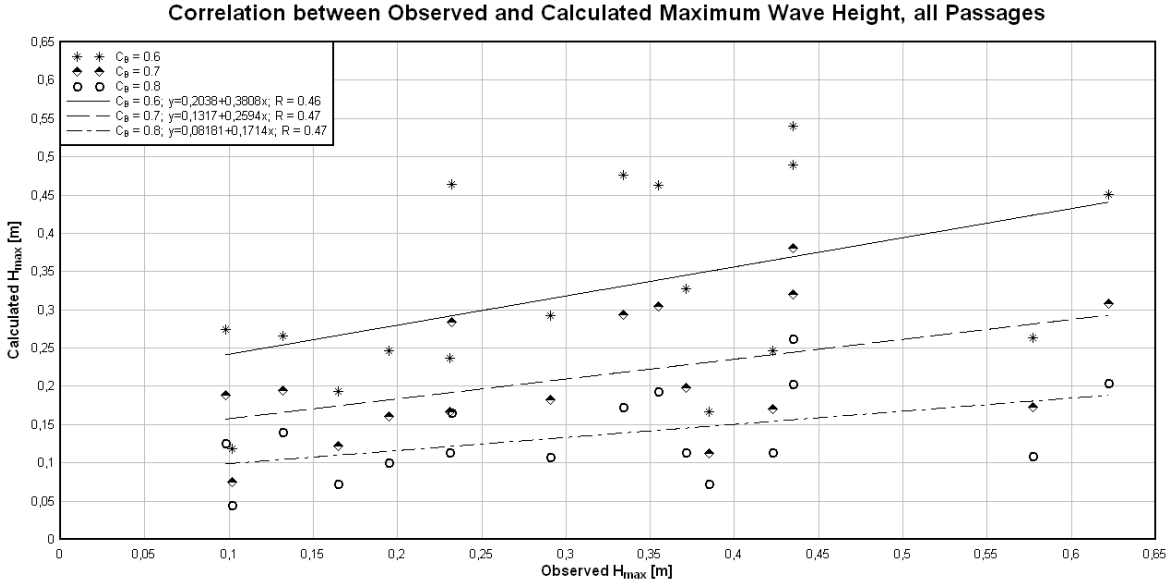

Figure 31 - Observed maximum wave height plotted against calculated maximum wave height for all ship passages. Three sets of calculations were performed, using the values 0.6, 0.7 and 0.8 for the block coefficient, with *R*-values of 0.46, 0.47 and 0.47, respectively. Note the relatively low variation along the line which corresponds to C_B = 0.8.

It can be seen that there is a clear correlation between the observed and calculated wave heights, regardless of choice of block coefficient. Furthermore, it can be seen that the lower the value of the block coefficient, the larger the calculated wave height is (as can be derived from Equations 10 - 16). But, the graph above clearly shows that, when all ship passages are considered, the smaller observed wave heights are better predicted when a larger block coefficient is used. As the observed wave heights increase, though, to values around 0.2 metres, the predictions agree less well with the measurements. The data set which uses C_B = 0.6 also displays a larger gradient increase compared to the other two sets (C_B = 0.7 and C_B = 0.8). This choice of block coefficient is considered too low to be appropriate, however, especially considering that the vessel which was unloaded had a block coefficient of 0.759. Thus, a more appropriate value is thought to lie closer to 0.75. Around this value, 0.75, the variation around the fitted line is relatively low as well.

The correlation increases when the downstream ship passages are excluded from the analysis. Again, the higher block coefficient values predict lower wave heights better and there is also a low variation along the line which incorporates C_B = 0.8. As the real block coefficient is estimated to around 0.75, it would seem that the Kriebel and Seelig (2005) equations consistently underestimate the effect that ships have on the wave formation though, except for lower values. But there is a clear trend indicating that the model is built on proper physical assumptions. It is interesting to see the relatively low variation for the set with C_B = 0.8, though, which could indicate a well-founded equation, which perhaps only needs the addition of a coefficient in order to increase the calculated gradient.

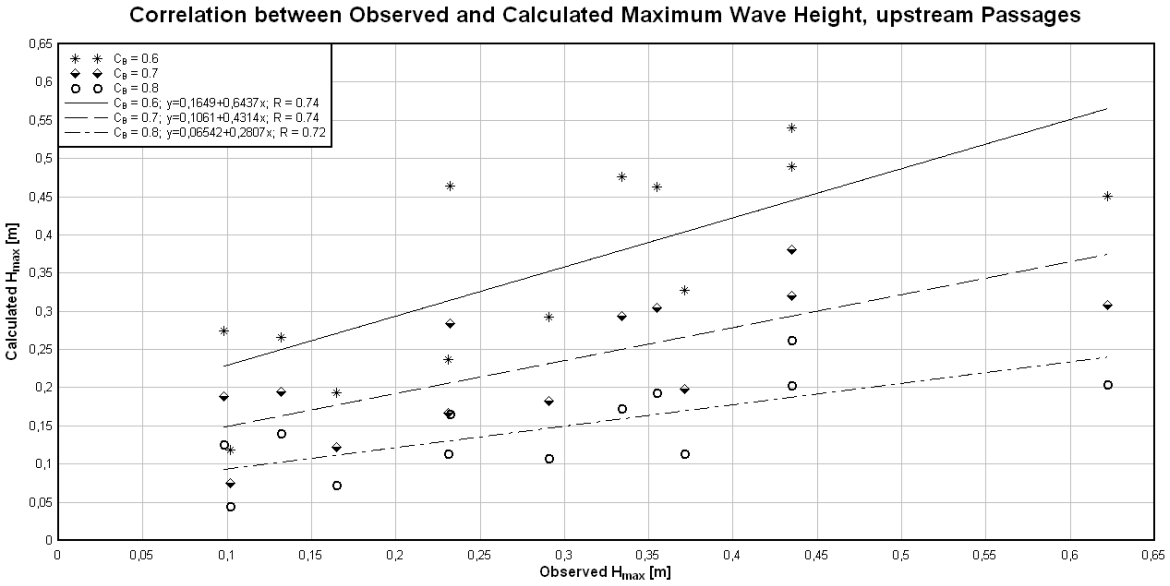

Figure 32 - Observed maximum wave height plotted against calculated maximum wave height for ships travelling in the upstream direction only. Three sets of calculations were performed, using the values 0.6, 0.7 and 0.8 on the block coefficient, with *R*-values of 0.74, 0.74 and 0.72, respectively. It can be seen that the lower observed wave heights are better predicted when a larger block coefficient is used. But, as the observed wave height increases, to values around 0.3 metres, the quality of the result is reduced. The exclusion of the downstream observed ship passages provides a better correlation between calculated and observed H_{max}. Note the relatively low variation along the line which corresponds to C_B = 0.8.

The fact that there is such a prominent difference in the quality of the correlation between the inclusion and exclusion of the downstream passages could be due to several reasons. The bed topography is not identical, for example. This could induce wave patterns with different characteristics. Moreover, perhaps the assumption to use the mean flow velocity of the river when determining the ship velocity relative to the water is too crude. But it should also be pointed out, that there are only a few downstream passages, so the statistical certainty may be argued as well.

The relationship between observed and calculated drawdown has been treated using the same approach as H_{max}, using three sets of block coefficients and isolating the upstream passages in a separate comparison as well. In the same manner as for H_{max}, there is a gradient which describes an increase in calculated drawdown as the real drawdown increases. But the relationship between theory and observations is much less pronounced for the drawdown, which can be seen in Figure 33 and Figure 34.

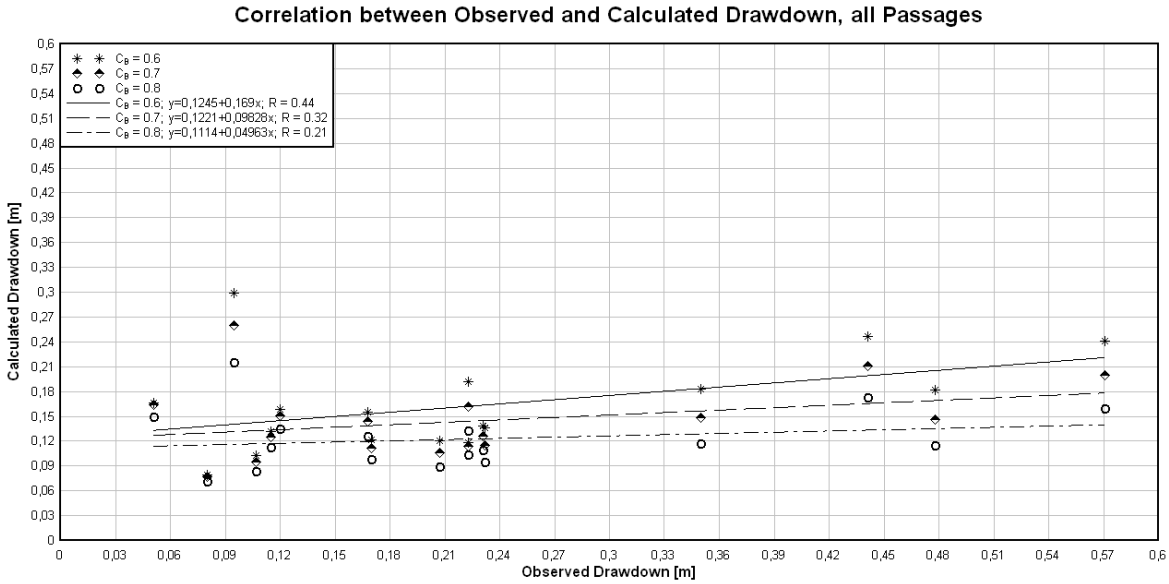

Figure 33 - Observed drawdown plotted against calculated drawdown for all ship passages. Three sets of calculations were performed, using the values 0.6, 0.7 and 0.8 on the block coefficient, with *R*-values of 0.44, 0.32 and 0.21, respectively. The data shows limited correlation between the calculated and the observed drawdown.

In fact, it can be argued that there is little correlation with the actual drawdown, especially if one considers that the block coefficient in reality is approximately 0.75. It can be concluded, however, that there is an almost negligible variation between the inclusion and exclusion of the downstream ship passages in the graphs.

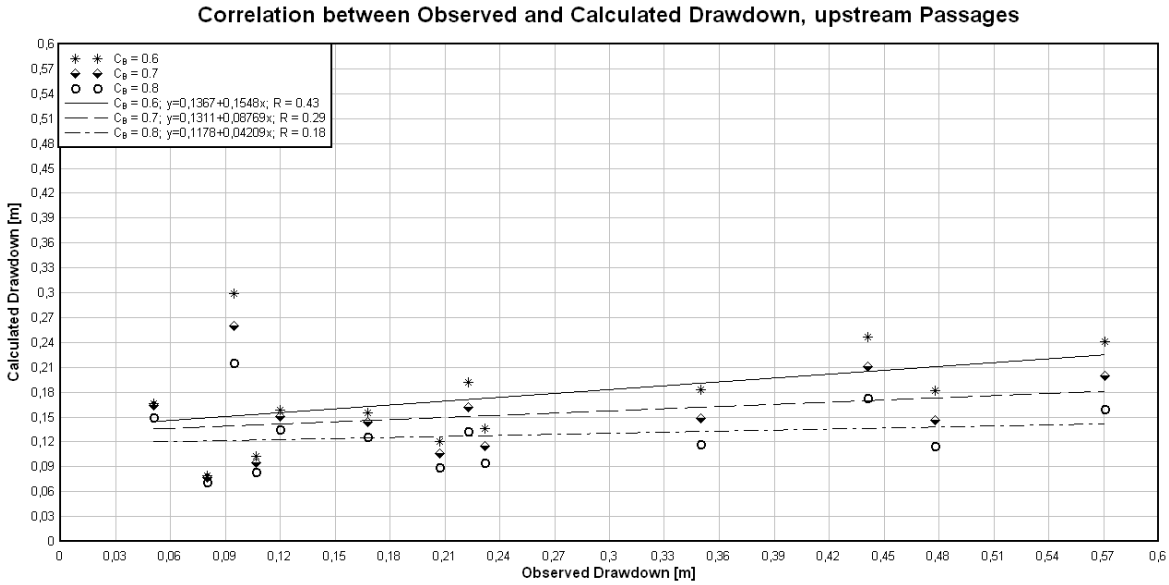

Figure 34 - Observed drawdown plotted against calculated drawdown for all ship passages. Three sets of calculations were performed, using the values 0.6, 0.7 and 0.8 on the block coefficient, with *R*-values of 0.43, 0.29 and 0.18, respectively. The data shows a poor correlation result between the calculated and the real drawdown.

It is also noteworthy to add that there is a relatively low variation in drawdown for different values of the block coefficient, compared to the large variation noticed in the calculations of the maximum wave height.

4.5 Derived Equation for Maximum Wave Height and Drawdown

After the measured maximum ship-generated wave heights and drawdown were determined and compared to the calculations with a general formula, it was interesting to investigate if a site-specific equation could be developed as well that produces improved agreement. Naturally, it is much easier to develop an equation that describes a limited data set from a single site compared to one that has general applicability. However, depending on the variables selected to include in the empirical analysis, the quality of the result varied greatly. After trial and error, using a wide range of parameters to form dimensionless groups, the final result that is considered to best fit the observed maximum wave height is given in Equation 30 below:

$$\frac{gH_{max}}{U^2} = 0.09893 - 0.8796\frac{Q}{UL_sB} - 0.03968\frac{h}{T} + 1.246F_L \qquad \text{[Eq. 30]}$$

Where

g= Acceleration due to gravity [ms^{-2}]
H_{max}= Maximum ship-induced wave height [m]
U = Ship velocity relative to water [ms^{-1}]
Q = River flow rate [m^{3}s^{-1}]
L_S = Ship length [m]
B = Ship width [m]
h = River depth [m]
T = Ship draught [m]
F_L = Ship length Froude number

The equation above was derived using multiple linear regression analysis in a program called Analyse-it. During the attempts to find an equation which could properly describe the ship-induced wave heights, it was noted that a significant variation in accuaracy was obtained depending on whether or not the data for ships travelling in the downstream direction was included. Whenever these data was included, the regression analysis produced equations which fitted the observed values less well than when they were excluded. This behavior re-occured for most choices of variables and dimensionless groups. Thus, the equation above is developed only based on observations for ships traveling in the upstream direction, *i.e.,* 13 passages (there were only four ships observed that traveled in the downstream direction; see Appendix I – Summary of Ship Passages). The final result of the multiple linear regression analysis is shown in Figure 35. The predictive capability of the equations were determined simply by comparing the coefficient of determination, R^2, and the Pearson product-moment correlation coefficient (also simply called the correlation coefficient), R (the final result for H_{max} and upstream passages were 0.70 and 0.84, respectively). The closer the coefficient of determination comes to one, the better the equation predicts the outcome.

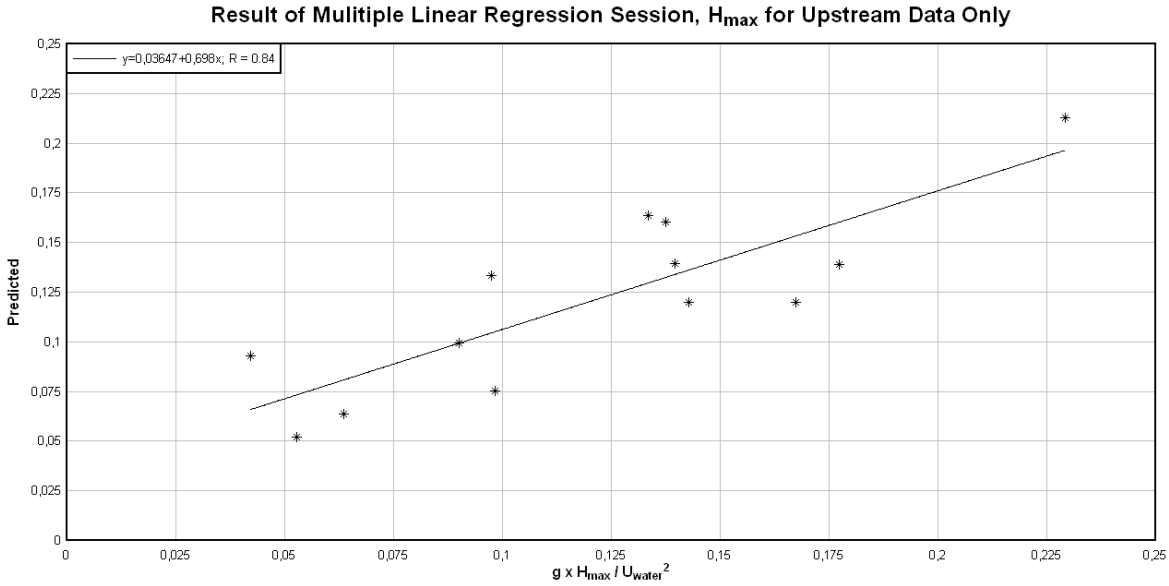

Figure 35 - Result of multiple linear regression calculations for H_{max}. The data only include cases with ships traveling in the upstream direction, which accounts for 13 out of 17 passages. The values of R and R^2 for the result are 0.84 and 0.70, respectively.

As can be seen in Equation 30, there are many parameters included, such as the river flow rate. This variable is introduced in the trial and error session in order to partly counteract a possible source of error when using the mean velocity, namely the flow rate divided by an estimated river profile area, instead of the actual velocity along the sailing line. It is thought that this could be a reason why the downstream direction data differed in the analysis. But after introducing this parameter, the difference between including and excluding the downstream data was still present in the analysis. Perhaps the river topography can be a possible parameter that causes different behavior along the up- and downstream stretch of the river at Garn station, influencing the generated wave heights.

In the same manner, the ship-generated drawdown was analyzed using multiple linear regression, and the result was once again optimal when the same parameters were used. Furthermore, the coefficient of determination was highest when the calculations only used data from the upstream ship passages. The equation which provided the most accurate result (R^2 = 0.62) is shown below:

$$\frac{g \cdot Drawdown}{U^2} = 0.2196 - 0.6935\frac{Q}{UL_sB} - 0.09693\frac{h}{T} + 0.8956F_L \qquad \text{[Eq. 31]}$$

Where

g= Acceleration due to gravity [ms^{-2}]
Drawdown = Water drawdown [m]
U = Ship velocity relative to water [ms^{-1}]
Q = River flow rate [m^3s^{-1}]
L_S = Ship length [m]
B = Ship width [m]
h = River depth [m]
T = Ship draught [m]
F_L = Ship length Froude number

The equation result is also illustrated in Figure 36.

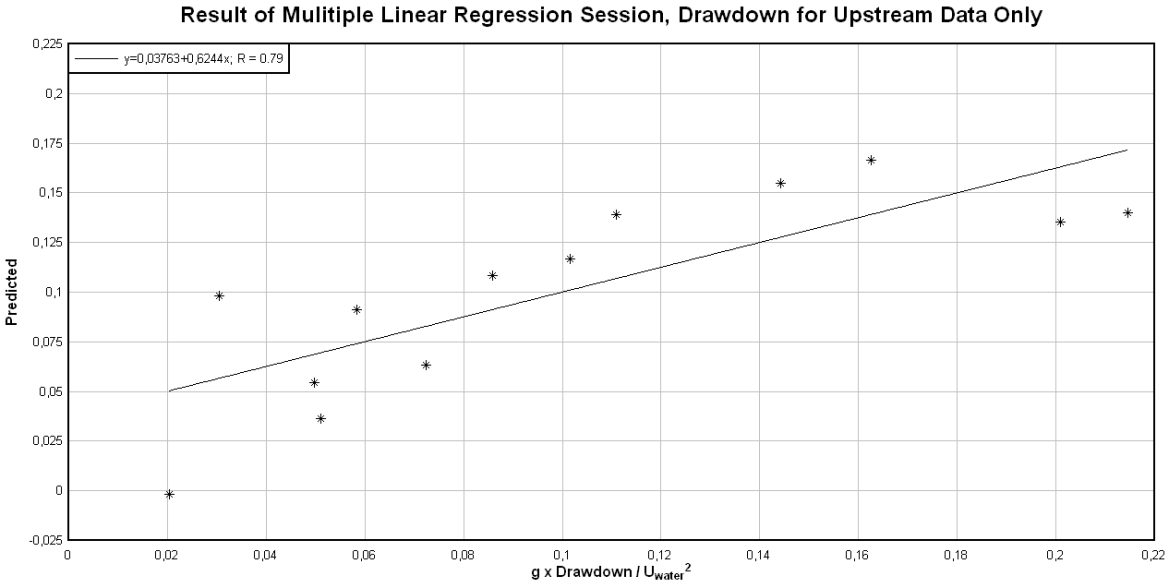

Figure 36 - Result of multiple linear regression calculations for ship drawdown. The data only include cases with ships traveling in the upstream direction, which accounts for 13 out of 17 passages. The values of *R* and R^2 for the result are 0.79 and 0.62, respectively.

In comparison, when all passages were included, the best results for H_{max} and the drawdown, when the same dimensionless groups were used, were determined as given by Equation 32 and Equation 33:

$$\frac{g \cdot Drawdown}{U^2} = 0.258 - 0.4926\frac{Q}{UL_sB} - 0.008601\frac{h}{T} + 0.4315F_L \qquad \text{[Eq. 32]}$$

$$\frac{g \cdot H_{max}}{U^2} = 0.08838 - 0.1139\frac{Q}{UL_sB} - 0.04463\frac{h}{T} + 0.8988F_L \qquad \text{[Eq. 33]}$$

Where

g= Acceleration due to gravity [ms^{-2}]
Drawdown = Water drawdown [m]
H_{max} = Maximum ship-induced wave height [m]
U = Ship velocity relative to water [ms^{-1}]
Q = River flow rate [m^3s^{-1}]
L_S = Ship length [m]
B = Ship width [m]
h = River depth [m]
T = Ship draught [m]
F_L = Ship length Froude number

The results are graphically displayed in Figure 37 and Figure 38, respectively.

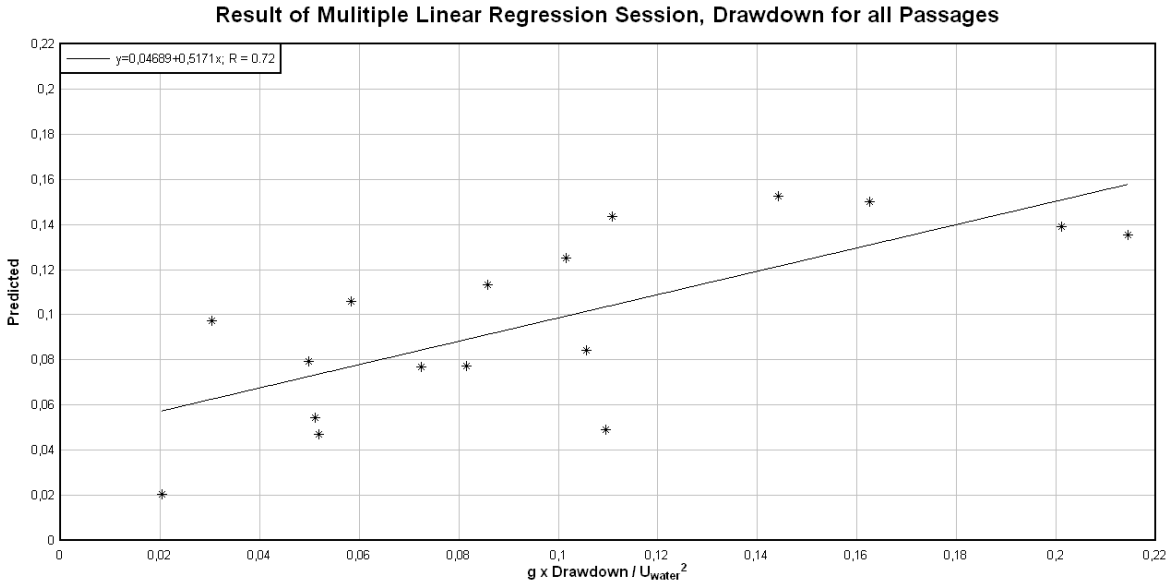

Figure 37 - Result of multiple linear regression calculations for ship drawdown. The data include all passages. The values of *R* and R^2 are for the result 0.72 and 0.52, respectively.

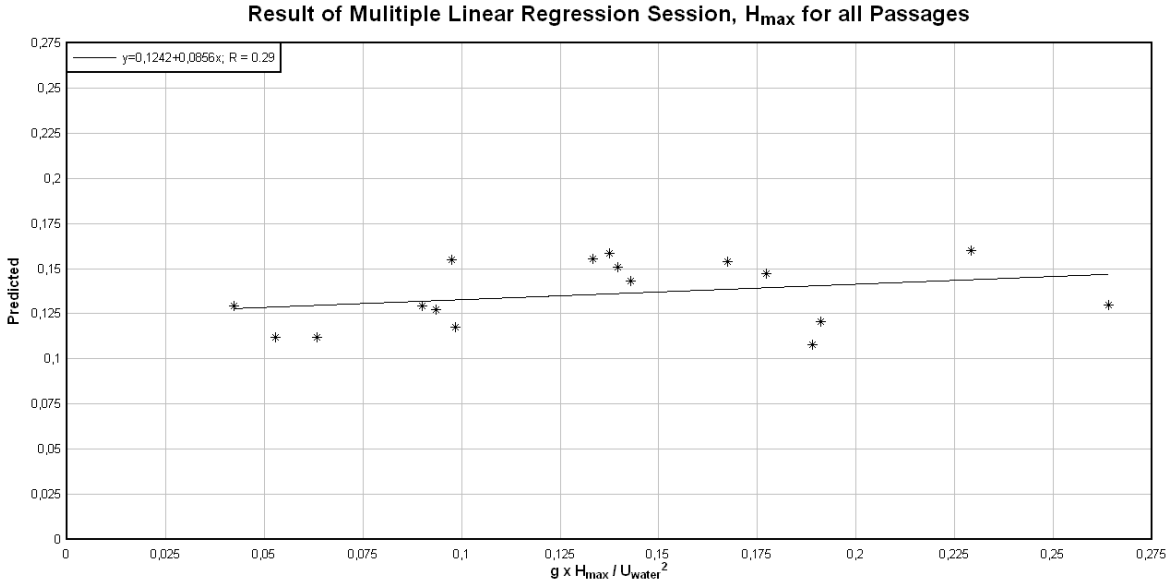

Figure 38 - Result of multiple linear regression calculations for ship-generated H_{max}. The data include all passages. The values of *R* and R^2 for the result are 0.29 and 0.09, respectively.

Thus, when all passages are included for the maximum wave height, the result yields poorer correlation compared to when only upstream passages are used. A summary of how well Equations 30 – 33 fitted the data is shown in Table 8.

Table 8 - Coefficient of determination and the correlation coefficient for Equations 30 – 33.

	R^2	*R*
H_{max}, all passages	0.09	0.29
H_{max}, upstream passages	0.70	0.84
Drawdown, all passages	0.52	0.72
Drawdown, upstream passages	0.62	0.79

4.6 Digitized Wave Profiles and Calculated Shear Stresses

By using the digitized wave profiles, a number of wave properties such as the height, length and period may be established. These parameters are in turn needed in order to determine the shear stress acting on the river bed.

The shear stress and the duration it acts on the bed during the passage of a wave package, which is used in the erosion calculations, may be derived using at least two alternative wave heights: either the root-mean-square wave height ($H_{rms} \sim H_s/1.4$), which would have a time of action equivalent to the duration of the whole secondary wave system, or the maximum wave height (H_{max}) with an associated duration of various length, depending on the properties of the secondary wave system. In short, this means that if choosing H_{rms}, the shear stress acts during a longer period of time compared to if H_{max} is chosen, but the wave height is smaller. It is not possible beforehand to estimate which wave height gives the greatest shear stress during the period of action, due to differences in wave periods and wavelengths. Therefore, both shear stresses due to the root-mean-square and maximum wave heights, taking into account the different wavelengths and duration, have been determined. The result is illustrated in Table 9 and Table 10.

Table 9 – Summary of root-mean-square wave properties. The data is valid for the point where observations were made, *i.e.,* about 11 metres off the river bank. Water conditions are determined according to Table 2. The time of action for H_{rms} equals the full duration of the secondary wave system. The mean period for H_{rms} is the duration divided by the number of waves.

Passage number	Water condition	Water depth [m]	Wave length [m]	H_{rms} [m]	Mean period [s]	Duration [s]	Orbital velocity [ms^{-1}]
1	Transitional	4.24	9.90	0.093	2.53	47.0	0.0199
2	Transitional	4.05	28.85	0.358	5.11	52.0	0.5618
3	Transitional	4.23	34.34	0.255	5.82	29.0	0.4693
4	Deep	4.32	7.90	0.134	2.25	27.0	0.0136
5	Transitional	4.30	9.17	0.068	2.43	17.0	0.0113
6	Transitional	4.38	11.45	0.170	2.73	30.0	0.0487
7	Transitional	4.53	13.63	0.297	3.00	36.0	0.1174
8	Transitional	4.53	9.70	0.071	2.50	40.0	0.0119
9	Transitional	4.57	17.37	0.375	3.46	45.0	0.2341
10	Transitional	4.53	12.74	0.186	2.89	55.0	0.0633
11	Transitional	4.62	12.77	0.122	2.89	52.0	0.0399
12	Transitional	4.66	10.24	0.257	3.25	34.0	0.0464
13	Transitional	4.63	13.34	0.268	2.96	38.5	0.0963
14	Transitional	4.44	20.97	0.182	3.93	55.0	0.1625
15	Deep	4.44	7.42	0.234	2.18	24.0	0.0171
16	Transitional	4.33	21.36	0.159	4.00	52.0	0.1516
17	Transitional	4.43	10.76	0.095	2.64	37.0	0.0226

The time period for when H_{max} is acting is somewhat arbitrarily chosen as one seventh of the total wave system duration, although there are arguments for this. For example, most often, there are two or three waves which are of far greater height than the remaining

waves. The total of number of waves in a wave package is typically around 10-15. Furthermore, the first wave often has a period much longer than any other wave. Hence, one seventh is thought to be a value which is applicable for the calculations of the duration.

Table 10– Summary of maximum wave height properties. The data is valid at the point where observations were made, *i.e.,* about 11 metres off the river bank. Water conditions are determined according to Table 2. The duration time for H_{max} is set to one seventh of the time during which the secondary wave system is acting.

Passage number	Water condition	Water depth [m]	Wave length [m]	H_{max} [m]	Period [s]	Duration [s]	Orbital velocity [ms^{-1}]
1	Deep	4.24	6.25	0.165	2.00	5.2	0.0073
2	Transitional	4.05	8.93	0.622	2.40	7.4	0.0786
3	Transitional	4.23	13.51	0.355	3.00	4.1	0.1060
4	Transitional	4.32	8.95	0.231	2.40	3.9	0.0292
5	Deep	4.30	6.25	0.102	2.00	2.4	0.0043
6	Transitional	4.38	8.95	0.291	2.40	4.3	0.0353
7	Transitional	4.53	12.02	0.435	2.80	5.1	0.0922
8	Transitional	4.53	8.96	0.132	2.50	5.7	0.0139
9	Deep	4.57	4.78	0.577	1.75	6.4	0.0051
10	Deep	4.53	5.06	0.385	1.80	7.9	0.0048
11	Deep	4.62	2.97	0.195	1.38	7.4	0.0001
12	Transitional	4.66	12.84	0.435	2.90	4.9	0.0974
13	Deep	4.63	4.78	0.423	1.75	5.5	0.0035
14	Transitional	4.44	10.45	0.334	2.60	7.9	0.0562
15	Deep	4.44	4.51	0.371	1.70	3.4	0.0028
16	Transitional	4.33	11.59	0.232	2.75	7.4	0.0512
17	Transitional	4.43	9.70	0.168	2.50	5.3	0.0240

Table 9 and Table 10 show that there are no observations where the water depth may be regarded as shallow at the measuring point. Consequently, the concern, noted in paragraph 2.2.4, that the wave properties may be calculated incorrectly because the waves are nonlinear, might be unfounded.

The generated shear stresses are calculated in accordance with the equations in Section 2.2.3, and may be correlated with the increase in mass of SPM in the water. This increase may be estimated using the turbidity readings and relationship between SPM and turbidity developed by Göransson (2010).

Göransson (2010) observed strong correlation between the mass of SPM and the turbidity readings. Water samples collected during ship passages at Garn station have been analysed in a laboratory, in order to find a regression relationship between the two quantities. The result is shown in Figure 39.

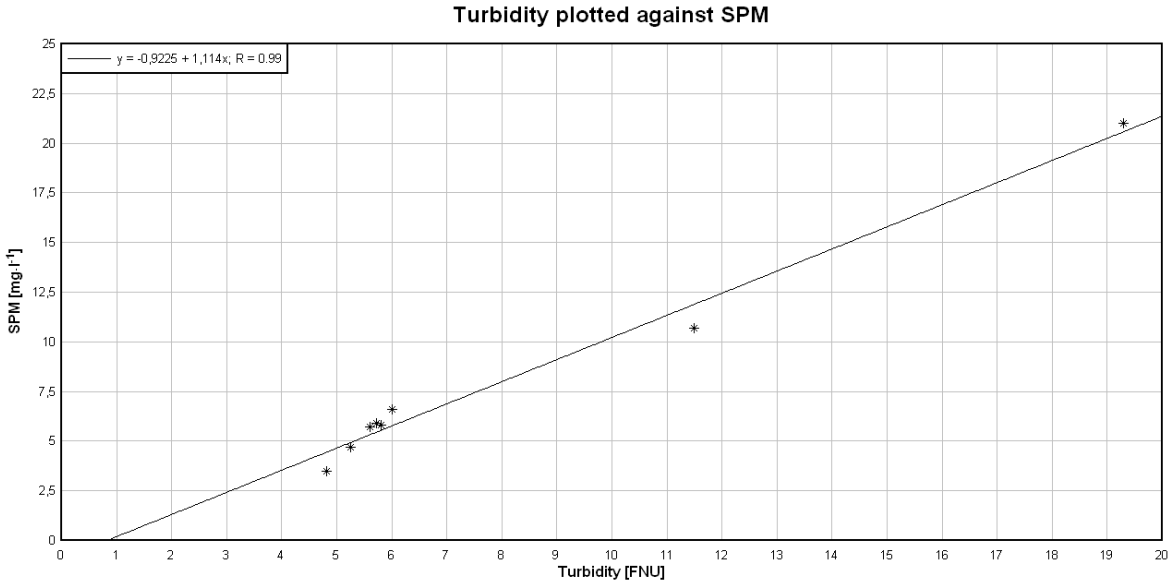

Figure 39 - Turbidity plotted against mass of SPM for eight water samples. Samples were taken during ship passages at Garn station by Göransson (2010). The linear curve shown could fit the data points well, with a correlation coefficient of 0.99. Due to the low number of samples, the statistical significance can be argued though, especially for higher values in turbidity (data from Göransson 2010, graph by Althage, 2010).

A linear curve is fitted to the data, showing the expected behaviour that higher turbidity values give higher mass of SPM, with a correlation coefficient of 0.99. The statistical significance of the fit can be argued, though, as the number of data points is low, especially for higher turbidity values. The fit, however, provide a basis for estimations. In fact, the linear curve is used as a reference in order to estimate the calculated erosion. The mass increase of SPM is thus calculated as:

$$Mass\ of\ SPM\ [mg/l] = -0.9225 + 1.114 \cdot Turbidity\ value[FNU] \qquad \text{[Eq. 34]}$$

The final result of calculated shear stresses, created by ship-generated waves, and the increase in turbidity and mass of SPM per unit volume is presented in Table 11.

Table 11 – Summary of calculated shear stresses created by ship-generated waves and increases in turbidity and mass of SPM due to ship activity. The shear stresses in bold font display the highest calculated value per passage.

Passage number	Shear-stress (H_{max}) [Nm^{-2}]	Shear-stress (H_{rms}) [Nm^{-2}]	Turbidity increase [FNU]	Mass increase of SPM (related to turbidity) [$mg \cdot l^{-1}$]
1	0.0103	**0.0403**	1.5	0.75
2	0.3165	**3.9246**	6.2	5.98
3	0.4387	**2.8105**	19.6	20.91
4	**0.0731**	0.0244	No clear increase	-
5	0.0047	**0.0178**	No clear increase	-
6	0.0968	**0.1457**	3.5	2.98
7	0.3699	**0.4930**	5.0	4.65
8	**0.0239**	0.0190	1.1	0.30
9	0.0065	**1.3158**	2.3	1.64
10	0.0059	**0.2085**	No clear increase	-

11	$2.1880 \cdot 10^{-5}$	**0.1053**	No clear increase	-
12	**0.3939**	0.1239	2.1	1.42
13	0.0037	**0.3833**	~0.5	<0.3
14	0.1848	**0.7174**	5.3	4.98
15	0.0027	**0.0348**	2.2	1.53
16	0.1536	**0.6414**	7.2	7.10
17	**0.0535**	0.0476	No clear increase	-

It is clear that the root-mean-square wave height provides maximum shear-stresses far greater than the maximum wave height does in some cases. This is because the mean wave length is far greater due to the choice of dividing the duration time of the secondary wave system with the number of waves, thus assigning a mean wave period to H_{rms} which often greatly exceeds the wave period for H_{max}. Given these findings, the root-mean-square values would in general erode the river bed quicker than the values for the maximum wave height.

4.7 Induced Shear Stress and Erosion

Sanford and Maa (2001) define the rate of erosion as shown in Equation 35 below, stating that the formulation is widely used to describe Type II erosion, which means that the erosion is not depth limited (the sediment critical shear-stress does not change with depth).

$$E = M(\tau_b - \tau_c) \qquad \text{[Eq. 35]}$$

Where
E = Rate of erosion [$kg \cdot s^{-1}m^{-2}$]
M = Empirical constant [sm^{-1}]
τ_b = Shear stress at bed bottom [Nm^{-2}]
τ_c = Bed critical shear stress [Nm^{-2}]

Given this definition, the use of a Type II erosion formulation might then partly contradict the theory presented in section 4.2, where it was argued that a thin layer of top sediment might have a lower critical shear-stress than the underlying sediments. At present, though, there is no data available suggesting a proper estimation of parameters which may be used to perform calculations using a Type I erosion. Therefore, Type II erosion is assumed to prevail in the present study.

The empirical constant M in Equation 35 has been estimated by Larson and Hansson (2006) for three sections of the Göta River. Fortunately, Garn station is situated between two of these sections, and so the mean value of the two estimations ($M = 0.255 \cdot 10^{-6}$ sm^{-1}) may be used in order to calculate the erosion rate from ship-generated waves in this area. However, this value for the constant M has been developed with the river flow rate as eroding mechanism. Moreover, the estimation does not consider the force applied by ship waves, which should have more erosive power than the river flow. Therefore, the value might underestimate the erosion from ship-generated waves, and another method of calculating the erosion should be employed. As stated in the previous section, both the method with the root-mean-square wave height and the maximum wave height were used to determine the erosion.

The critical shear stress for the bed sediment is hard to estimate, as there are no investigations which have provided useful results regarding this quantity yet. Furthermore, the critical shear stress is site specific, and may exhibit large variations from one section to another section in the river. One possible method to determine the critical shear stress, though, may be through correlation between calculated shear stresses and the relationship between SPM and turbidity, see Figure 40.

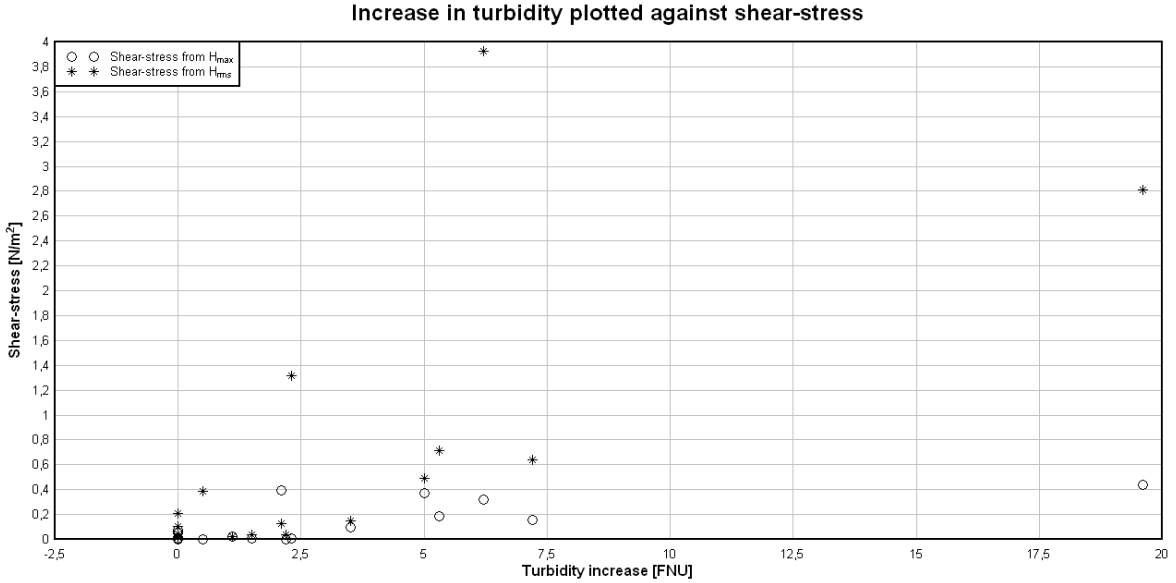

Figure 40 – The increase in turbidity induced by passing ships plotted against the shear stress created by the ship waves. The graph provides a possibility to estimate the magnitude of the critical shear stress.

The figure above suggests that a shear stress around 0.2-0.4 N/m^2 corresponds to the critical shear stress, as a rise in turbidity, and hence also mass of SPM, is visible around these values. Even though it is apparent that shear stresses below 0.1 N/m^2 may be used as a good value as well, the increase in turbidity can be explained by other factors. For example, the SPM is likely transported from areas closer to the bank, where the water depth is smaller compared to at the reference point, and thus the shear stress is greater. Considering this argument, the reference critical shear stress is chosen as 0.3 N/m^2, in order to enable estimates of ship wave-generated erosion. This assumption is somewhat strengthened by unpublished and preliminary investigations performed on the Göta River bed sediments, suggesting a critical shear stress around 0.2-0.4 N/m^2.

In order to use the turbidity data, the SPM concentration derived from the turbidity-SPM relationship provided by Göransson (2010) is first transformed from mg/l into kg/m^2 using the water depth, giving the total estimated mass of SPM in the water column per unit bed surface area:

$$kg/m^2 = \frac{Water\ depth\ in\ metres}{1000} \cdot mg/l \qquad \text{[Eq. 36]}$$

Now, all parameters necessary to calculate the sediment transport, rate of erosion, and the total eroded mass for the ship passages are either known or estimated. Thus, the result of Equation 35 can now be viewed in Table 12.

Table 12 – Summary of the estimated rate of erosion and eroded mass of sediment per square metre at Garn station during ship passages. The estimates are valid for a reference point located approximately 11 metres off the bank, where the water depth was around 4-4.8 metres (depending on the SWL depth). The passage number refers to the observed ship passage, and is given in chronological order.

Passage number	Rate of erosion (H_{max}) [kg·s^{-1}m^{-2}]	Eroded mass (H_{max}) [kg·m^{-2}]	Rate of erosion (H_{rms}) [kg·s^{-1}m^{-2}]	Eroded mass (H_{rms}) [kg·m^{-2}]	Eroded mass from SPM correlation [kg·m^{-2}]
1	-	-	-	-	0.0032
2	$4.2075 \cdot 10^{-9}$	$3.1136 \cdot 10^{-8}$	**$9.2427 \cdot 10^{-7}$**	**$4.8062 \cdot 10^{-5}$**	0.0242
3	**$3.5369 \cdot 10^{-8}$**	**$1.4501 \cdot 10^{-7}$**	$6.4018 \cdot 10^{-7}$	$1.8565 \cdot 10^{-5}$	**0.0903**
4	-	-	-	-	-
5	-	-	-	-	-
6	-	-	-	-	0.0131
7	$1.7825 \cdot 10^{-8}$	$9.0905 \cdot 10^{-8}$	$4.9215 \cdot 10^{-8}$	$1.7717 \cdot 10^{-6}$	0.0211
8	-	-	-	-	0.0014
9	-	-	$2.5903 \cdot 10^{-7}$	$1.1656 \cdot 10^{-5}$	0.0075
10	-	-	-	-	-
11	-	-	-	-	-
12	$2.3945 \cdot 10^{-8}$	$1.1733 \cdot 10^{-7}$	-	-	0.0066
13	-	-	$2.1242 \cdot 10^{-8}$	$8.1780 \cdot 10^{-7}$	<0.0014
14	-	-	$1.0644 \cdot 10^{-7}$	$5.8540 \cdot 10^{-6}$	0.0221
15	-	-	-	-	0.0068
16	-	-	$8.7057 \cdot 10^{-8}$	$4.5270 \cdot 10^{-6}$	0.0307
17	-	-	-	-	-
MEAN PER PASSAGE	**$4.7852 \cdot 10^{-9}$**	**$2.1340 \cdot 10^{-8}$**	**$1.2279 \cdot 10^{-7}$**	**$5.3679 \cdot 10^{-6}$**	**0.0134**

As mentioned previously, the erosion which is calculated using the derived wave shear stresses provides values which are too low. Thus, in order to calculate the total annual erosion due to ship passage, it is considered appropriate to use the eroded mass obtained from the relationship between SPM and turbidity (*i.e.,* the right-most column). If the mean for all ship passages is used, an estimate of the total annually eroded mass of sediment from the Göta River caused by ship-induced waves is given by:

$$TAEM = \frac{MEM_{SPM} \cdot L_{RIVER} \cdot 2 \cdot S_{NO.} \cdot A_{RW}}{1000} \qquad \text{[Eq. 37]}$$

Where

$TAEM$ = Total Annual Eroded Mass [tonnes]
MEM_{SPM} = Mean Eroded Mass per ship passage [kg·m^{-2}]
L_{RIVER} = Length of river ≈ 93 km
$S_{NO.}$ = Annual number of ships ≈ 1 600
A_{RW} = Affected river width [m]

The multiplication by two in Equation 37 accounts for the fact that the waves affect two sides of the river (only the bottom areas close to the banks are included in the calculations). If the mean eroded mass derived from the SPM-turbidity relationship is used, the result is:

$$TAEM = \frac{0.0134 \cdot 93\,000 \cdot 2 \cdot 1\,600 \cdot 11}{1000} = 43\,866\ tonnes \qquad \text{[Eq. 38]}$$

This includes organic material, however, and the eroded mass should be about 90-98 % of the above stated value, *i.e.,* about 40 000 tonnes. If the predicted increase in ship bulk transport occurs in the Gothenburg region, and the Göta River experiences a similar increase, the total erosion from ship traffic could by the year 2020 double in mass.

However, the result from the calculation above is based on four major simplifications. First, the width affected by erosion is modelled as a constant and equals a representative width where the observations were made, *i.e.,* about 11 metres. Second, the erosion is considered constant along the entire river length and unaffected by the river width. Third, the SPM-turbidity relationship is assumed to be valid and also to be applicable to the whole river. Finally, the maximum registered increase in turbidity is due to erosion of the river bed and all material mobilized during ship passage is transported out from the river without being re-deposited. The final assumption, especially, yields an overestimation of the sediment transport since the measurements indicate that all material mobilized by the ships is re-deposited and the net transporting velocity thus becomes much lower.

The increase in turbidity to the initial maximum peak takes just about one minute. This means that there should not be enough time for dispersion and diffusion to take effect, transporting sediment from areas closer to the bank, but the peak value would represent the local mobilization of material. This observation would in turn to some extent validate the second assumption stated above, as the erosion most likely increases the closer the waves gets to the banks. It could even mean that assumption two may underestimate the erosion. To balance this, the first assumption is most likely incorrect, and that the erosion is considerably lower at some other sections of the river, due to the high velocities allowed at Garn, rendering the first assumption an over-estimation. Furthermore, the man-made erosion protection, which is present at for example Garn, does not cover the whole river stretch. Upstream of Lilla Edet WPP, there is less erosion protection, and the same applies for the Gothenburg Branch (the southern of the two separated river stretches) where ships navigate. This would seemingly underestimate total river bank erosion. In conclusion, the assumption that all material mobilized is directly transported with the river and not re-deposited implies that the calculation of the erosion from ship-induced waves most likely represents a significant overestimation.

5 Discussion

After observing the potential impact from ship-generated waves on sediment transport and erosion in the Göta River, it might be reasonable to recommend that actions should be taken in order to reduce these effects. Considering how great a role the ship velocity in relation to the water flow velocity plays in terms of forming waves of high amplitude, it feels logical to recommend that the restriction of ten knots is lowered to perhaps eight knots, at least along the stretch where observations were conducted during this investigation. Such a measure would seemingly have little influence on the ship traffic on the river, especially as many ships do not travel at the maximum allowed velocity. New restrictions should only be considered at sections where they do not pose any threat to ship navigation, as ships sometimes need to increase velocity in order to turn properly etc.

If future changes in climate, especially increased precipitation, occur in Scandinavia, which is likely, the erosion in the Göta River from ships may also increase as the river flow rate, flow velocity, and SWL depth could increase. If the SWL of the river rises, ship-generated waves may perhaps to a greater extent reach the vegetation line, and expose never-before affected areas of the banks to wave impact. Also, should the flow velocity increase, due to a greater flow rate, whilst the velocity restrictions of the river are kept as they are today, the velocity of ships relative to the water would likely increase (if the pilots do not lower the velocities themselves). This could mean that the ship-generated waves would form with higher amplitudes as the ship velocity relative to the water velocity is a prominent factor when discussing the magnitude of waves forming. Moreover, perhaps the flow restrictions which are applied to the river need to be changed in the future if increased annual mean flow rates occur.

It would be interesting if further work was performed along other sections of the river, where the properties are different (perhaps in a section where the river bends and is shallower, with lower maximum velocity allowed), so that a more thorough analysis could be made. Also, in order to eliminate the discussion regarding the value of the block coefficient, it might be favourable to study only a few ships of similar properties, as it would still be possible to acquire a large number of observations as many ships navigate the Göta River frequently. Some ships are even sister ships, like Clipper Sola and Clipper Sira (see passage number 14 and 16, respectively, in Appendix I). These two ships have identical dimensions and dead weight, and hence the block coefficient should be the same as well.

Another point of interest would be to do case studies of the areas which have a substantial amount of quick clay. This is of course only possible when the efforts to categorise the soils of the Göta River valley are completed. From a risk management point of view, it would be highly educational and extremely important to undertake such a study, seeing that there is a risk of landslides in the valley, possibly threatening infrastructure and property of large value, not to mention the water supply of the city of Gothenburg and the river ecology.

6 Conclusions

The formulas which were applied in order to theoretically estimate the ship-generated maximum wave height and drawdown provide results of varying accuracy when compared to the measurements. The calculated drawdown was poorly correlated and showed little, if any, pattern which might be linked to the observed drawdown. As for the maximum wave height, although a clear connection between theory and measurements was observed, the equations nearly always produced predictions which fell short of the real value. On the other hand, the results did not display a large variation, which speaks in favour of its applicability.

The poor correlation for the drawdown is most likely explained by the fact that there are no parameters in the formulas describing the effects of no-flow boundaries in a restricted water body. One factor which also affects the correlation is the fact that the ship block coefficient could not be determined satisfactorily. This is especially unfortunate for the calculated maximum wave height, as the calculation result exhibits considerable sensitivity towards the block coefficient. The use of an estimated block coefficient though, clearly results in maximum wave heights which are lower than the measured heights. The site-specific equations developed based on the measured data show a high level of agreement for upstream passages, but show poorer correlation when downstream passages are included. It is speculated that factors, such as differences in bed topography, influence the result to some degree.

The ship-generated waves, which were observed at Garn station, clearly induce bed shear stresses that frequently exceed the estimated bed sediment critical shear stress. The critical shear stress has been estimated by analysing calculated shear stresses and simultaneous turbidity readings, linking increases in the latter (which translate to an increase in the mass of SPM) to the former.

Furthermore, it is clear that the waves contribute to the transport of sediment in the river by eroding the river bed and banks, increasing the total mass of SPM which is transported with the river water. Given the fact that many ships travel along the whole river stretch, this means that every ship possibly erodes a stretch of 186 kilometres (299 miles) (up- and downstream the river).

An estimation of the effects of ship-generated waves indicated that about 40 000 tonnes of bed material is eroded every year, with a possible steep increase in the future due to extended utilization of the river by cargo and tanker vessels. Thus, the total annual eroded mass might even double. However, the calculations were based on the assumption that all sediment mobilized from the bed is transported away by the river without being re-deposited, which most likely results in a significant overestimation. In order to counter a possible increase in erosion, the vessel velocity restrictions could be lowered, as the ship-generated wave impact would most likely decrease in magnitude in response to this measure.

7 References

7.1 Literature

Bertram, V., 2000: *Practical Ship Hydrodynamics*. Elsevier, ISBN: 978-0-7506-4851-6, chapters 2-3.

Bogen, J. and Bønsnes, T.E., 2001: *The impact of erosion protection work on sediment transport in the River Gråelva, Norway.* Norwegian Water Resources and Energy Directorate. In: *Sediment Transfer through the Fluvial System*. Ed: Golosov, V., Belyaev, V. and Walling, D.E. (2004). International Association of Hydrological Sciences publication 288, ISBN 1-901502-67-8.

Bradbury, J., 2005: *Revised wave wake criteria for vessel operation on the lower Gordon River*. Department of Primary Industries, Water and Environment Resource Management and Conservation Division, Tasmania, 11th August 2005.

Campbell, C.G., Laycak, D.T., Hoppes, W., Tran, N.T. and Shi, F.G., 2004: *High concentration suspended sediment measurments using a continuous fiber optic in-stream transmissometer*. Lawrence Berkeley National Laboratory.
Available at: http://www.escholarship.org/uc/item/56d8b484. Downloaded 2010-06-10.

Enhage, L. and Wisaeus, D., 1975: *Fartygsgenererade Vågor – speciellt i kanaler* (Ship generated Waves – especially in channels). Chalmers University of Technology, Master Thesis.

French, R.H., 1994: *Open-Channel Hydraulics*. McGraw-Hill International Editions, Civil Engineering Series, chapter 4, ISBN-10: 0070221340, ISBN-13: 978-0070221345.

Golterman, H.L., Sly, P.G. and Thomas, R.L., 1983: *Study of the relationship between water quality and sediment transport – A contribution to the International Hydrological Programme*. UNESCO, Technical Papers in Hydrology 26, ISBN 92-3-102109-5.

Hamill, G.A., 1988: *The scouring action of the propeller jet produced by a slowly manoeuvring ship*. Bulletin Number 62, Permanent International Association of Navigation Congresses, Bulletin Number 62, pages 85–110. ISSN 03740001.

Hamill, G.A., Johnston, H.T. and Stewart, D.P., 1999: *Propeller Wash Scour near Quay Walls*. Journal of Waterway, Port, Coastal and Ocean Engineering, Volume 125, number 4, pages 170-175.

Hamill, G.A., McGarvey, J.A. and Hughes, D.A.B., 2004: *Determination of the efflux velocity from a ship's propeller*. Proceedings of the Institution of Civil Engineers, Maritime Engineering 157, issue MA2, paper 13026, pages 83-91.

Henn, R., Sharma, S.D. and Jiang, T., 2001: *Influence of Canal Topography on Ship Waves in Shallow Water*. 16th International Workshop on Water Waves and Floating Bodies. Available at http://www.iwwwfb.org/Workshops/16.htm.

Hultén, C., Edstam, T., Arvidsson, O. And Nilsson, G., 2006: *Geotekniska förutsättningar för ökad tappning från Vänern till Göta älv* (Geotechnical prerequsites for increased drainage from Lake Vänern to Göta River). Swedish Geotechnical Institute, Varia 565, ISSN-1100-6692, ISRN-SGI-VARIA--06/565--SE.

Institute of Shipping Analysis, 2006: *Scenario över Västsveriges betydelse som logistiknav i norra Europa 2020* (Scenario of western Sweden's significance as logistic hub in northern Europe 2020).

Jepsen, R., Roberts, J. And Gailani, J., 2004: *Erosion Measurements in Linear, Oscillatory, and Combined Oscillatory and Linear Flow Regimes*. Coastal Research and Education Foundation, Journal of Coastal Research, volume 20, number 4, pages 1096-1101. ISSN: 07490208.

Jiménez, G.F., 2009: *Turbidity Related to Suspended Particulate Matter in the River Göta Älv, Göteborg*. Chalmers University of Technology, Department of Civil and Environmental Engineering, Division of Water Environment Technology (pre-print paper).

Kriebel, D.L. and Seelig, W.N., 2005: *An empirical model for ship-generated waves*. Paper presented at the 7th International Conference on Mathematical and Numerical Aspects of Waves (WAVES'05).

Larson, M. and Hanson, H., 2006: *Sedimenttransport och erosion i Göta Älv: Inverkan av framtida klimatförändringar* (Sediment transport and erosion in Göta River: Influence of future climate change). Lund University, Faculty of Engineering, Division of Water Resources Engineering. Report courtesy of the authors.

Maa, J.P.-Y., Sanford, L. and Halka, J.P., 1998: *Sediment resuspension characteristics in Baltimore Harbor, Maryland*. Elsevier Science B.V., Marine Geology 146 (1998), pages 137-145.

Minella, J.P.G, Merten, G.H., Reichert, J.M. and Clarke, R.T., 2007: *Estimating suspended sediment concentrations from turbidity measurements and the calibration problem*. In: Hydrological Porcesses, Volume 22 Issue 12, pages 1819 – 1830. John Wiley and Sons.

Packman, J.J., Comings, K.J. and Booth, D.B., 1999: *Using turbidity to determine total suspended solids in urbanizing streams in the Puget Lowlands*. In: Confronting Uncertainty: Managing Change in Water Resources and the Environment, Canadian Water Resources Association annual meeting, Vancouver, pages 158–165.

Partheniades, E., 2009: *Cohesive Sediments in Open Channels - Erosion, Transport and Deposition*. Elsevier Inc. ISBN-13: 978-1-85617-556-2, chapter 2.

Sandford, L.P. and Maa, J.P.-Y., 2001: *A unified erosion formulation for fine sediments*. Elsevier, Marine Geology 179, pages 9-23.

Soulsby, R., 1997: *Dynamics of Marine Sands*. Thomas Telford, ISSN-10: 072772584X, ISSN-13: 978-0727725844.

Sundborg, Å. and Norrman, J., 1963: *Göta Älv, Hydrologi och morfologi med särskild hänsyn till erosionsprocesserna* (Göta River, Hydrology and morphology with special consideration of the erosion processes), Geological Survey of Sweden, Dissertations and papers in 4:0, number 43.

Swedish Commission on Climate and Vulnerability, 2007: *Sweden facing climate change – threats and opportunities*. Swedish Ministry of the Environment, the Commission on Climate and Vulnerability. Swedish Government Official Reports, SOU 2007:60, chapter 3.5.

Torsvik, T., Dysthe, K. and Pedersen, G., 2006: *Influence of variable Froude number on waves generated by ships in shallow water*. American Institute of Physics, Physics of Fluids vol. 18, issue 6, ISSN: 10706631, pages 062102-1 – 062102-11.

US Army Corps of Engineers, 1984: *Shore Protection Manual*. Department of the Army, US Army Corps of Engineers, chapter I, pages 16-17.

US Army Corps of Engineers, 2006: *Engineering and Design - Hydraulic Design of Deep Draft Navigation Projects*. Department of the Army, US Army Corps of Engineers, publication number EM 1110-2-1613, chapters 3-8.

Voulgaris, G., Wallbridge, S., Tomlinson, B.N. and Collins, M.B., 1995: *Laboratory investigations into wave period effects on sand bed erodibility, under the combined action of waves and currents*. Elsevier, Coastal Engineering volume 26, number 3-4, pages 117-134.

7.2 Other

Andersson, Å., 2010, Gothenburg Water. Personal communication 2010-06-04.

Dahlberg, B., 2009, Gothenburg Water, Division of Planning and Design, City of Gothenburg. Personal communication 2009-10-28.

Fink, J.C., 2005: *The effects of urbanization on Baird Creek, Green Bay, Wisconsin.* University of Wisconsin-Green Bay, chapter 4. Available at: http://www.uwgb.edu/watershed/fink/Fink_Thesis_TOC.pdf. Downloaded 2010-06-09.

Gothenburg Water, 2010: Continuous personal communication during June – October 2010.

Gyllenram, W., 2010: Hydraulic consultant at SMHI (Swedish Meteorological and Hydrological Institute). Personal communication.

Göransson, G., 2010: Employee of SGI.

Göta Älvs Vattenvårdsförbund, 2008: *Vattendragskontroll 2008* (Watercourse control 2008). Available at: http://www.gotaalvvvf.org/mainpage/Resultat/Arsrapport_A_Gota_2008.pdf. Downloaded 2010-03-05.

Larsson, R., 2005: *Kan Vänern ta sig ett nytt utlopp?* (Can Lake Vänern create a new flow path?). In: Vattenstänk Nr 5/2005 (in Swedish). Available at: http://www.sjv.se/download/18.394d9f45113e42376618000212/5+-+Oktober+2005.pdf. Downloaded 2010-06-07.

Öberg, M., 2010: GIS engineer at SGI, personal communication.

Ruling 1937-06-19, including addition 1955-03-25.

SMHI (Swedish Meteorological and Hydrological Institute), 2010a: *Stationslista nederbörd normalvärden* (Station list precipitation normal values). Available at: http://www.smhi.se/polopoly_fs/1.2874!rrm6190%5B1%5D.pdf. Downloaded 2010-04-04.

SMHI (Swedish Meteorological and Hydrological Institute), 2010b: *Normalvärden för nederbörd* (Normal values for precipitation). Available at: http://data.smhi.se/met/climate/time_series/month_year/normal_1961_1990/SMHI_month_year_normal_61_90_precipitation_mm.txt. Downloaded 2010-04-04.

SMHI (Swedish Meteorological and Hydrological Institute), 2010d: *Access of discharge and water level data*. Available at: http://wqweb.smhi.se/wqweb/send/stationRequest?language=en. Downloaded 2010-06-07 (at current date only compatible with internet Explorer).

Swedish Maritime Administration, 2010a: *Speed Restrictions Göta Älv*. Available at: http://www.sjofartsverket.se/en/About-us/Organization/Maritime-Traffic/Lake-Vanern-Maritime-Traffic-Area/Standards--Procedures/Speed-Restrictions-Gota-Alv/. Downloaded 2010-06-07.

Swedish Maritime Administration, 2010b: Historic data regarding pilot deployment for the year 2006. Personal communication.

Vänerkansliet, 2007: *Dricksvatten från Vänern* (Drinking water from Lake Vänern). Vänerkansliet, Länsstyrelsen Västra Götalands län. ISSN 1403-6134. Available at: http://www.lansstyrelsen.se/NR/rdonlyres/6D67A3C2-544E-4065-9355-F148A4AC7B65/0/infoblad_dricksvatten.pdf. Downloaded 2010-04-03.

Vattenfall, 2006a: Measurement data from Lilla Edet power station regarding flow rate and SWL. Personal communication.

Vattenfall (no date): *Göta Älv – En resa längs en av Sveriges storslagna älvar* (Göta River – A journey along one of Sweden's great rivers). Vattenfall advertisment sheet. Available at: http://www.vattenfall.se/sv/file/gota-alvsvpdf_11336351.pdf. Downloaded 2010-06-03.

Vattenfall, 2010: Personal communication with Driftcentralen Bispgården.

7.3 Figures

©2009 Google, Satellite photos from Google Earth.

©2010 Google, from: www.viss.lst.se. Available at: http://www.viss.lst.se/PublicMapResult.aspx?countyID=7&municipalityID=0&waterTypeID=35&FreeTextSearch=Göta%20Älv&SearchType=1. Downloaded 2010-06-01.

©Althage, 2010. Photos taken 2010 from various locations along Göta River.

©Geological Survey of Sweden, 2010a, translation by Althage, J., 2010. From www.sgu.se. Available at: http://www.sgu.se/sgu/sv/samhalle/risker/skred_s.htm. Downloaded 2010-06-01.

©Geological Survey of Sweden, 2010b, translation by Althage, J., 2010. From www.sgu.se.

© Göransson, 2010. Photo taken at Garn station.

©Lantmäteriet/Metria. From www.eniro.se. Downloaded 2010-06-10, 2010-07-30.

Geological Survey of Sweden, 1959: *Jordartskarta Götaälvdalen i tre blad, norra bladet* (Soil-type Map Göta River Valley in three papers, north paper). Ser. Ba Nr 20, Stockholm.

SMHI (Swedish Meteorological and Hydrological Institute), 2010c: *Nederbördsstationer* (Precipitation stations). Available at: http://www.smhi.se/polopoly_fs/1.3001!ndb%20stationer_jan2008.pdf. Downloaded 2010-04-04.

Appendix I – Summary of Ship Passages

#1 - Dornum 2010-06-28, 11:22

Draught: 4.5 m
Length overall:82 m
Maximum width: 12 m
Entrance length: ~12 m
Direction: Upstream
Constructed: 1993

SWL depth: 7.93 m
Dead weight: 2388 tonnes
Flow rate: ~ 550 m^3/s
Flow velocity: ~ 0.69 m/s
Velocity over bed: 3.55 m/s
Velocity relative to water: 4.24 m/s

Drawdown = 0.107 m
H_{max} = 0.165 m
Wave period (H_{max}) = 2.00 s
Wave length (H_{max}) = 6.25 m

Turbidity increase = 1.5 FNU
F_L = 0.1495
F_D = 0.4807

Block coefficient	**0.6**	**0.7**	**0.8**
Calculated H_{max} [m]	0.1930	0.1219	0.0729
Calculated drawdown [m]	0.1029	0.0949	0.0833
Modified Froude number	0.2549	0.2230	0.1952

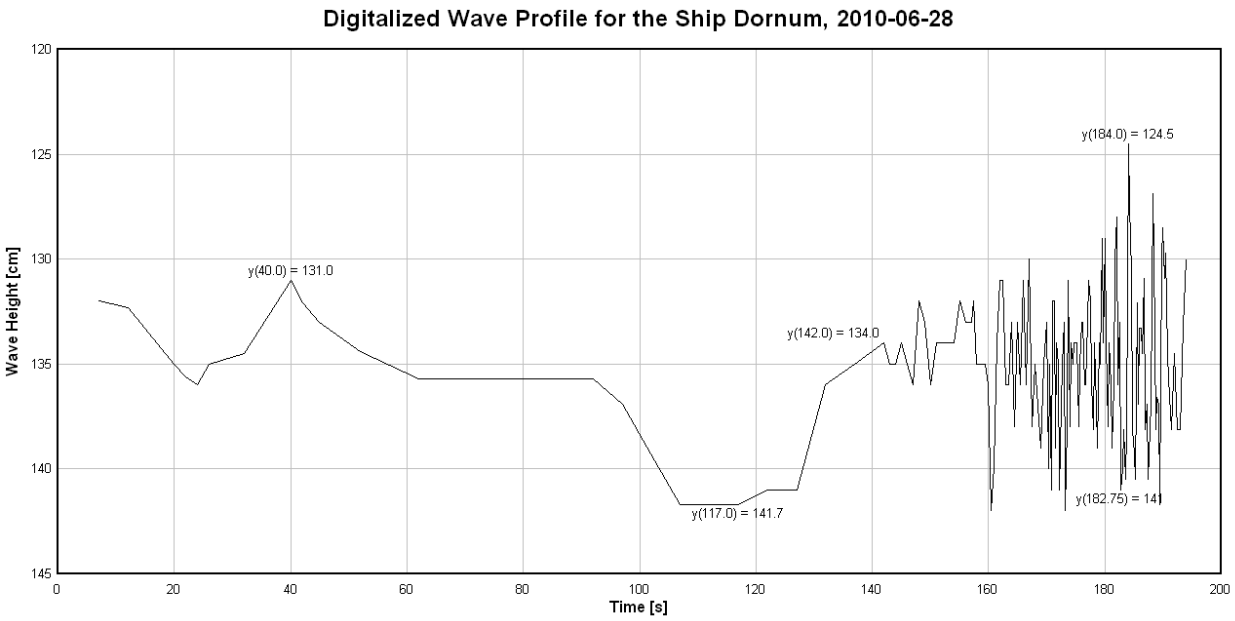
Digitalized Wave Profile for the Ship Dornum, 2010-06-28
Wave Height [cm]
Time [s]
y(40.0) = 131.0
y(117.0) = 141.7
y(142.0) = 134.0
y(184.0) = 124.5
y(182.75) = 141

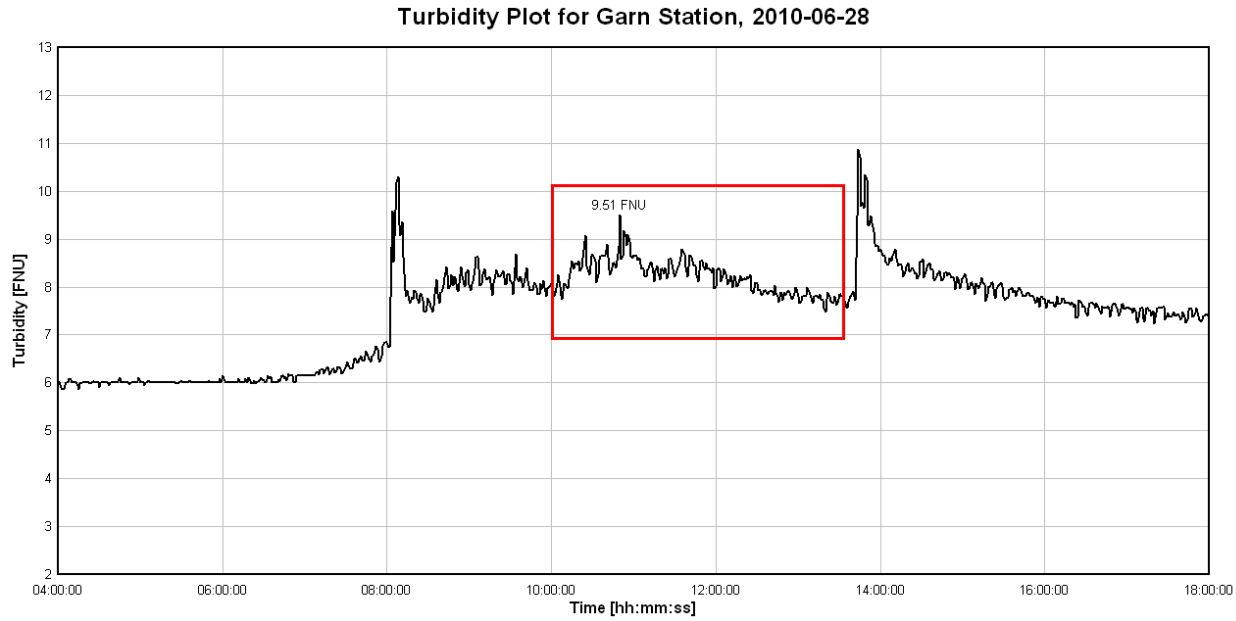
Turbidity Plot for Garn Station, 2010-06-28
Turbidity [FNU]
Time [hh:mm:ss]
9.51 FNU

#2 - Patria 2010-07-08, 15:12

Draught: 4.0 m
Length overall:83 m
Maximum width: 13 m
Entrance length: ~12 m
Direction: Upstream
Constructed: 1995

SWL depth: 7.74 m
Dead weight: 3519 tonnes
Flow rate: ~ 220 m^3/s
Flow velocity: ~ 0.28 m/s
Velocity over bed: 4.88 m/s
Velocity relative to water: 5.16 m/s

Drawdown = 0.441 m
H_{max} = 0.622 m
Wave period (H_{max}) = 2.40 s
Wave length (H_{max}) = 8.93 m

Turbidity increase = 6.2 FNU
F_L = 0.1808
F_D = 0.5922

Block coefficient	**0.6**	**0.7**	**0.8**
Calculated H_{max} [m]	0.4507	0.3080	0.2042
Calculated drawdown [m]	0.2470	0.2112	0.1728
Modified Froude number	0.2939	0.2603	0.2305

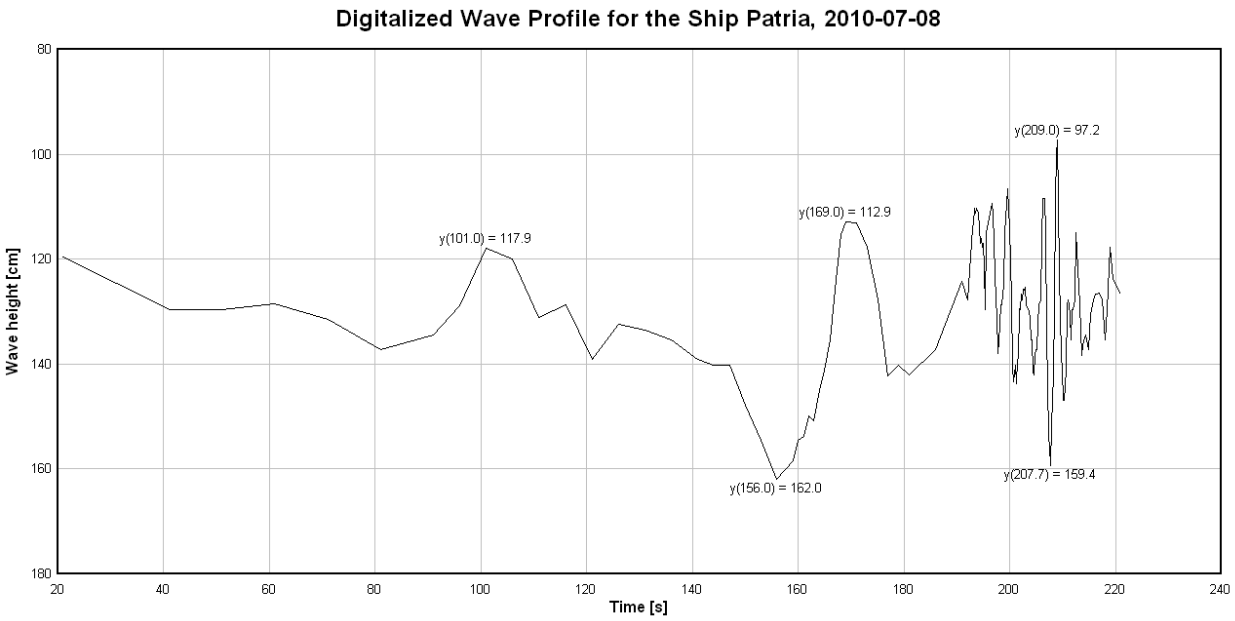
Digitalized Wave Profile for the Ship Patria, 2010-07-08
Wave height [cm]
Time [s]
y(101.0) = 117.9
y(156.0) = 162.0
y(169.0) = 112.9
y(209.0) = 97.2
y(207.7) = 159.4

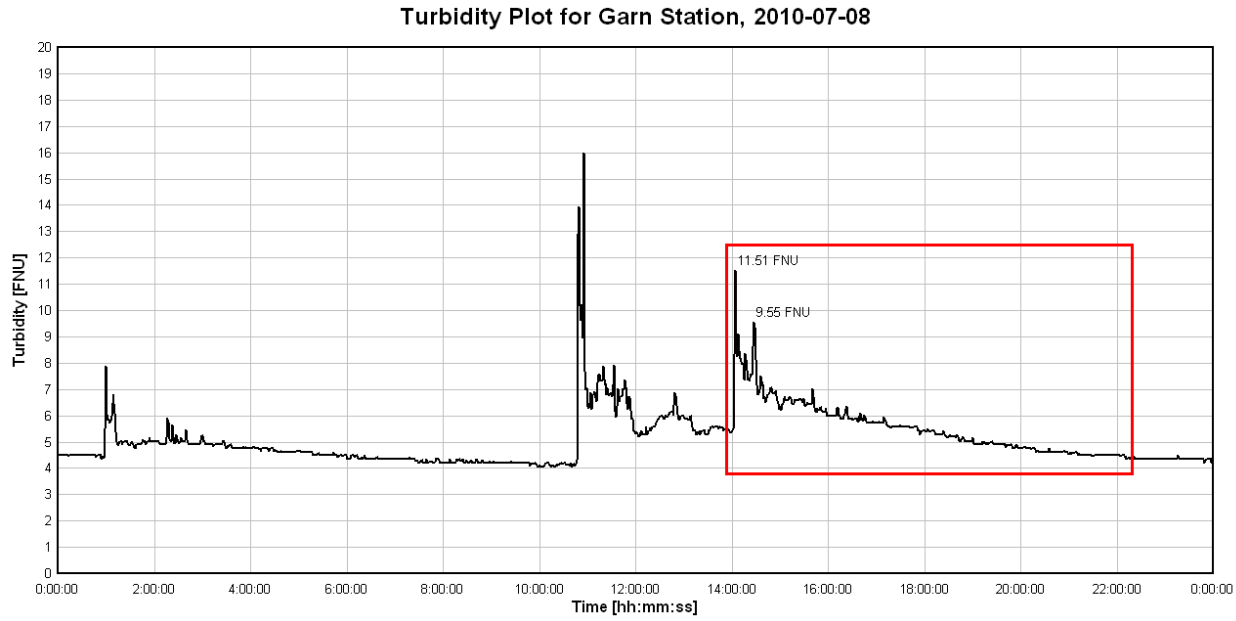
Turbidity Plot for Garn Station, 2010-07-08
Turbidity [FNU]
Time [hh:mm:ss]
11.51 FNU
9.55 FNU

#3 - Birthe Bres 2010-08-02, 12:13

Draught: 4.5 m
Length overall:88 m
Maximum width: 13 m
Entrance length: ~13 m
Direction: Upstream
Constructed: 2006

SWL depth: 7.92 m
Dead weight: 3750 tonnes
Flow rate: ~ 548 m^3/s
Flow velocity: ~ 0.69 m/s
Velocity over bed: 4.42 m/s
Velocity relative to water: 5.11 m/s

Drawdown = 0.571 m
H_{max} = 0.355 m
Wave period (H_{max}) = 3.00 s
Wave length (H_{max}) = 13.51 m

Turbidity increase = 16.9 FNU
F_L = 0.1739
F_D = 0.5797

Block coefficient	**0.6**	**0.7**	**0.8**
Calculated H_{max} [m]	0.4627	0.3047	0.1934
Calculated drawdown [m]	0.2405	0.1992	0.1594
Modified Froude number	0.2967	0.2596	0.2272

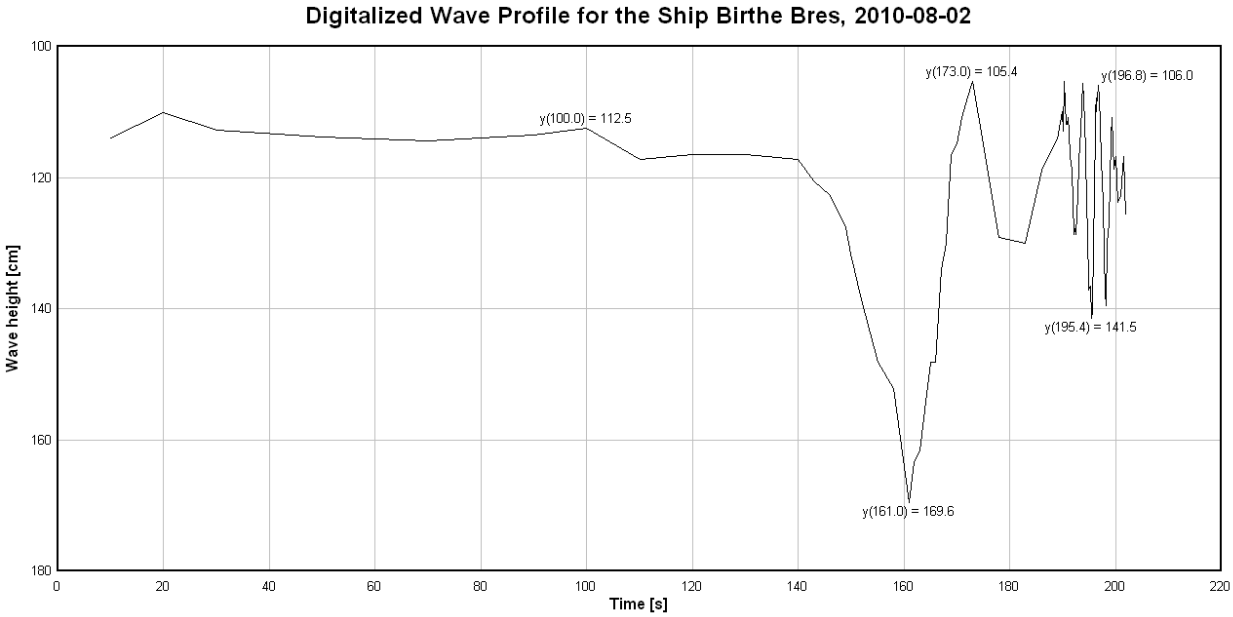
Digitalized Wave Profile for the Ship Birthe Bres, 2010-08-02
Wave height [cm]
Time [s]
y(100.0) = 112.5
y(161.0) = 169.6
y(173.0) = 105.4
y(195.4) = 141.5
y(196.8) = 106.0

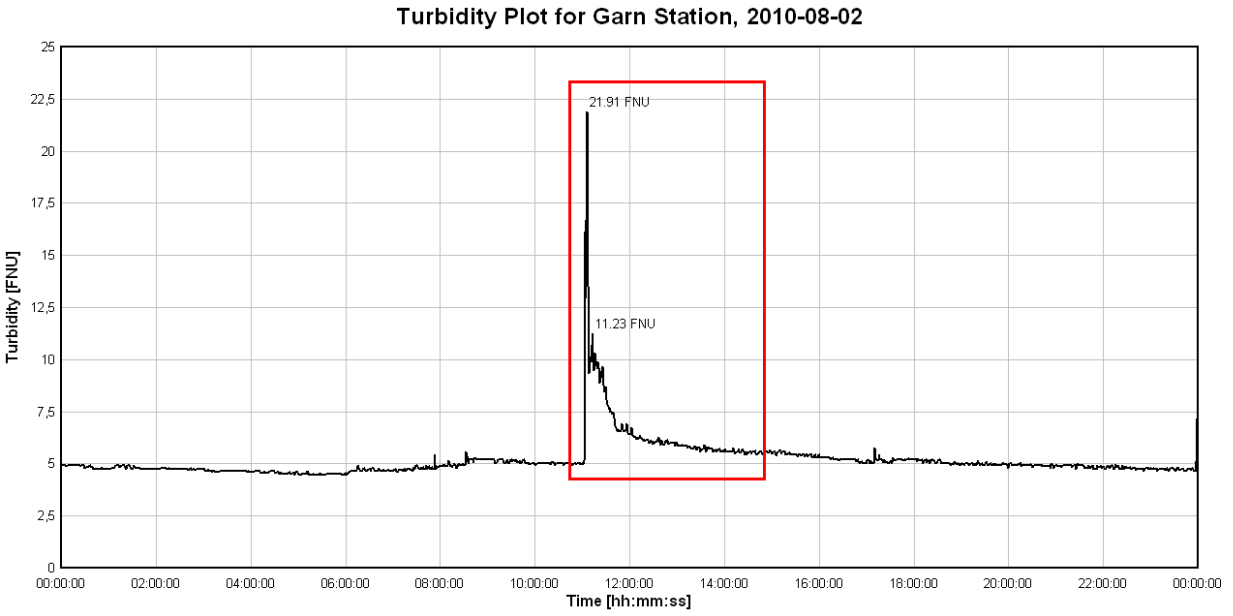
Turbidity Plot for Garn Station, 2010-08-02
Turbidity [FNU]
Time [hh:mm:ss]
21.91 FNU
11.23 FNU

#4 - Ann Rousing 2010-08-16, 12:35

Draught: 3.5 m
Length overall:85 m
Maximum width: 13 m
Entrance length: ~12 m
Direction: Upstream
Constructed: 1991

SWL depth: 8.01 m
Dead weight: 2752 tonnes
Flow rate: ~ 845 m^3/s
Flow velocity: ~ 1.05 m/s
Velocity over bed: 3.75 m/s
Velocity relative to water: 4.80 m/s

Drawdown = 0.120 m
H_{max} = 0.231 m
Wave period (H_{max}) = 2.40 s
Wave length (H_{max}) = 8.95 m

Turbidity increase = No clear increase
F_L = 0.1662
F_D = 0.5415

Block coefficient	**0.6**	**0.7**	**0.8**
Calculated H_{max} [m]	0.2374	0.1666	0.1134
Calculated drawdown [m]	0.1581	0.1508	0.1349
Modified Froude number	0.2507	0.2262	0.2041

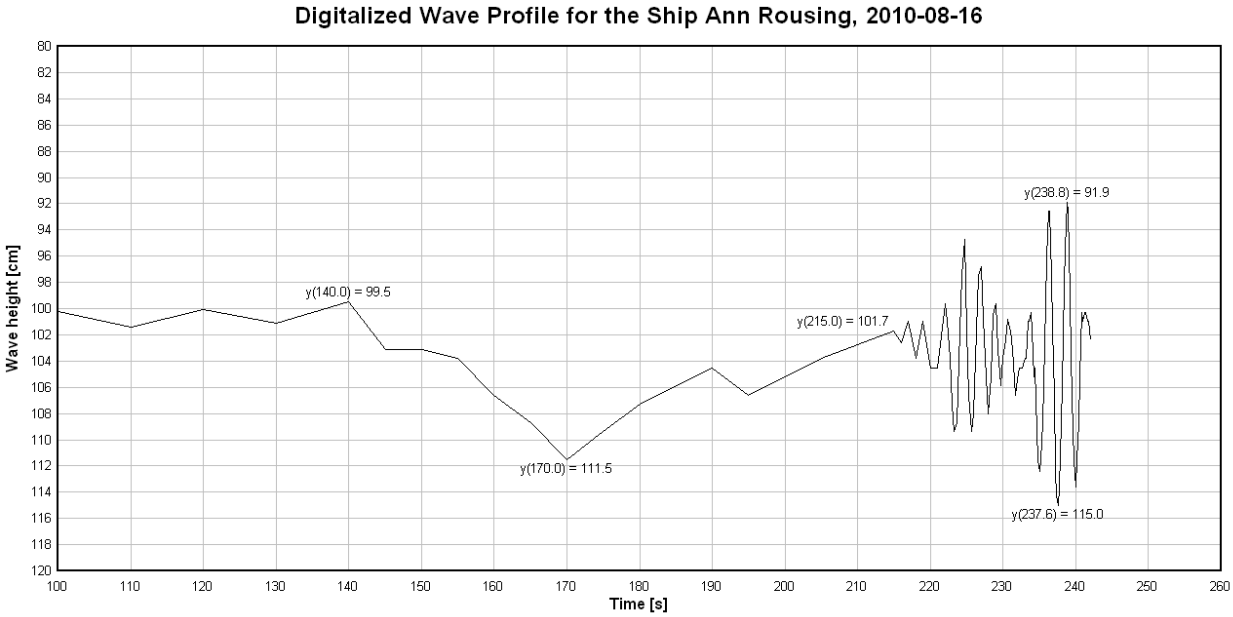
Digitalized Wave Profile for the Ship Ann Rousing, 2010-08-16
Wave height [cm]
Time [s]
y(140.0) = 99.5
y(170.0) = 111.5
y(215.0) = 101.7
y(238.8) = 91.9
y(237.6) = 115.0

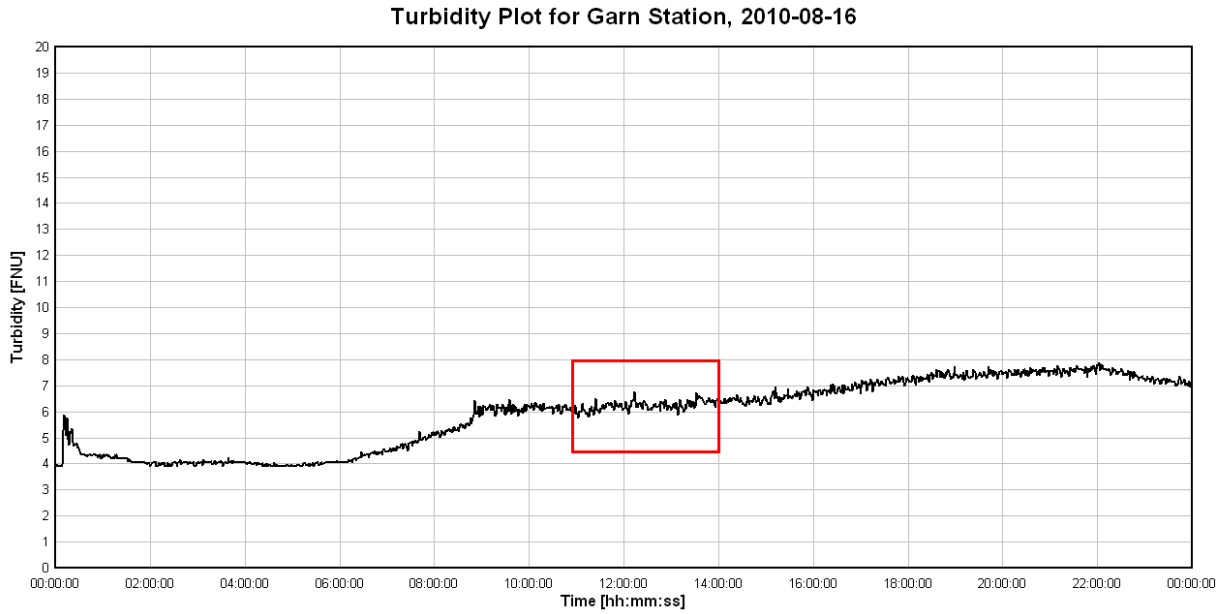
Turbidity Plot for Garn Station, 2010-08-16
Turbidity [FNU]
Time [hh:mm:ss]

#5 - Cedar 2010-08-18, 06:51

Draught: 4.2 m
Length overall:82 m
Maximum width: 11 m
Entrance length: ~11 m
Direction: Upstream
Constructed: 1981

SWL depth: 7.99 m
Dead weight: 1766 tonnes
Flow rate: ~ 547 m^3/s
Flow velocity: ~ 0.68 m/s
Velocity over bed: 3.29 m/s
Velocity relative to water: 3.97 m/s

Drawdown = 0.080 m
H_{max} = 0.102 m
Wave period (H_{max}) = 2.00 s
Wave length (H_{max}) = 6.25 m

Turbidity increase = No clear increase
F_L = 0.1400
F_D = 0.4484

Block coefficient	**0.6**	**0.7**	**0.8**
Calculated H_{max} [m]	0.1183	0.0746	0.0443
Calculated drawdown [m]	0.0795	0.0774	0.0710
Modified Froude number	0.2294	0.2028	0.1792

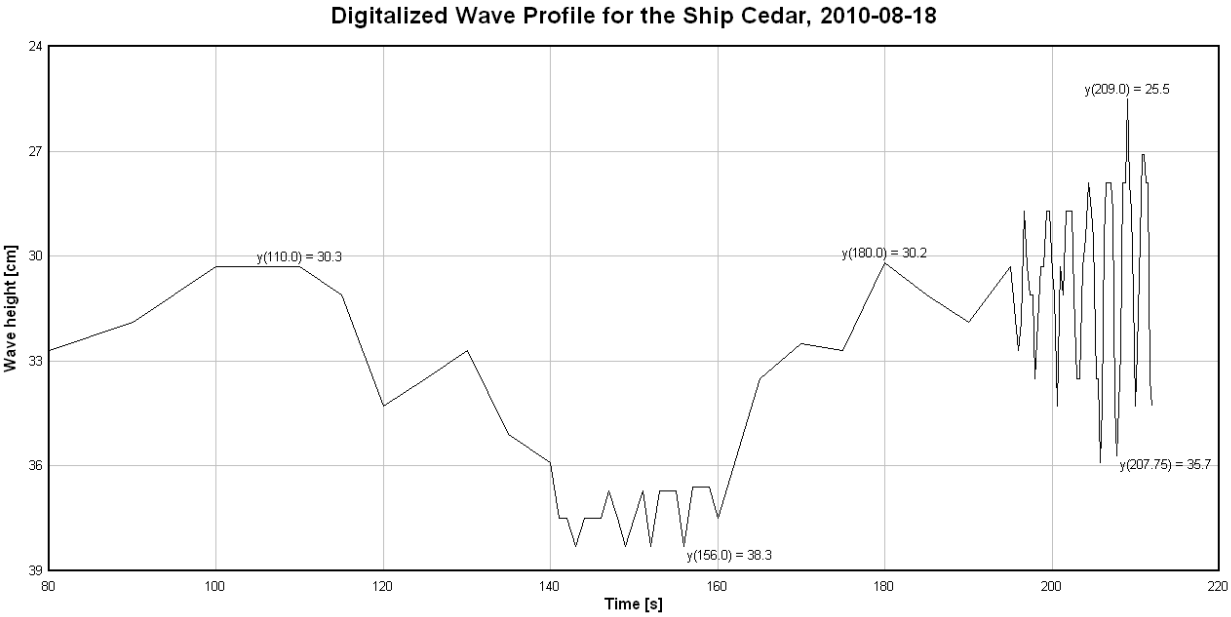
Digitalized Wave Profile for the Ship Cedar, 2010-08-18
Wave height [cm]
Time [s]
y(110.0) = 30.3
y(156.0) = 38.3
y(180.0) = 30.2
y(209.0) = 25.5
y(207.75) = 35.7

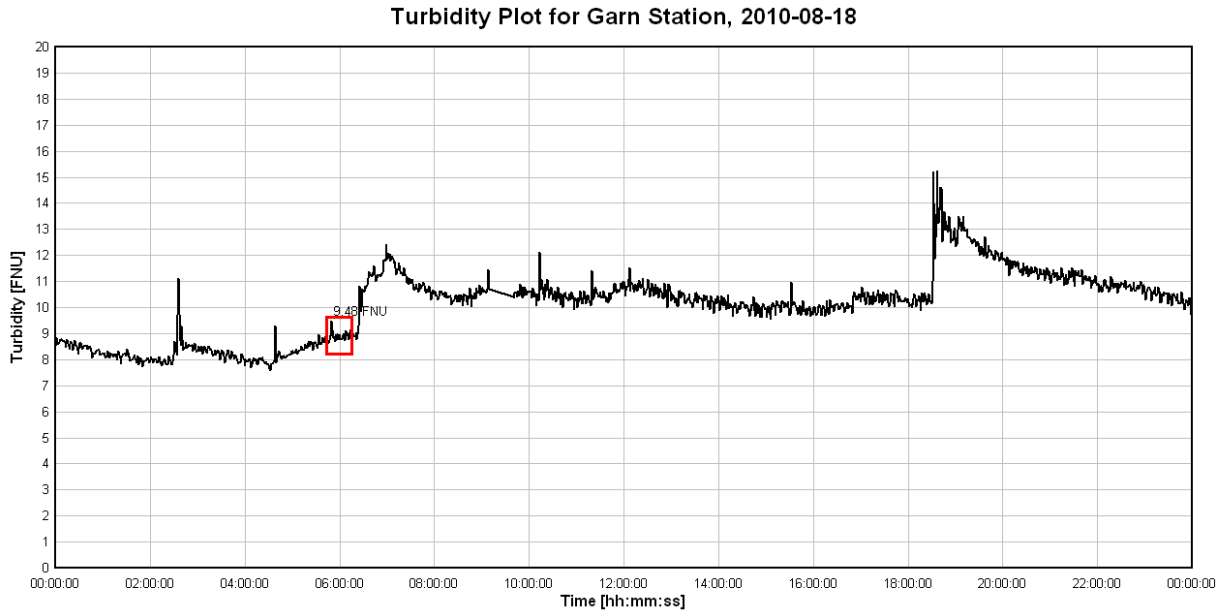
Turbidity Plot for Garn Station, 2010-08-18
Turbidity [FNU]
Time [hh:mm:ss]
9.48 FNU

#6 - Australis 2010-08-18, 07:27

Draught: 5.0 m
Length overall:83 m
Maximum width: 12.5 m
Entrance length: ~12 m
Direction: Upstream
Constructed: -

SWL depth: 8.07m
Dead weight: 2688 tonnes
Flow rate: ~ 580 m^3/s
Flow velocity: ~ 0.72 m/s
Velocity over bed: 3.75 m/s
Velocity relative to water: 4.47 m/s

Drawdown = 0.207 m
H_{max} = 0.291 m
Wave period (H_{max}) = 2.40 s
Wave length (H_{max}) = 8.95 m

Turbidity increase = 3.5 FNU
F_L = 0.1567
F_D =0.5024

Block coefficient	**0.6**	**0.7**	**0.8**
Calculated H_{max} [m]	0.2928	0.1825	0.1080
Calculated drawdown [m]	0.1200	0.1056	0.0896
Modified Froude number	0.2805	0.2425	0.2096

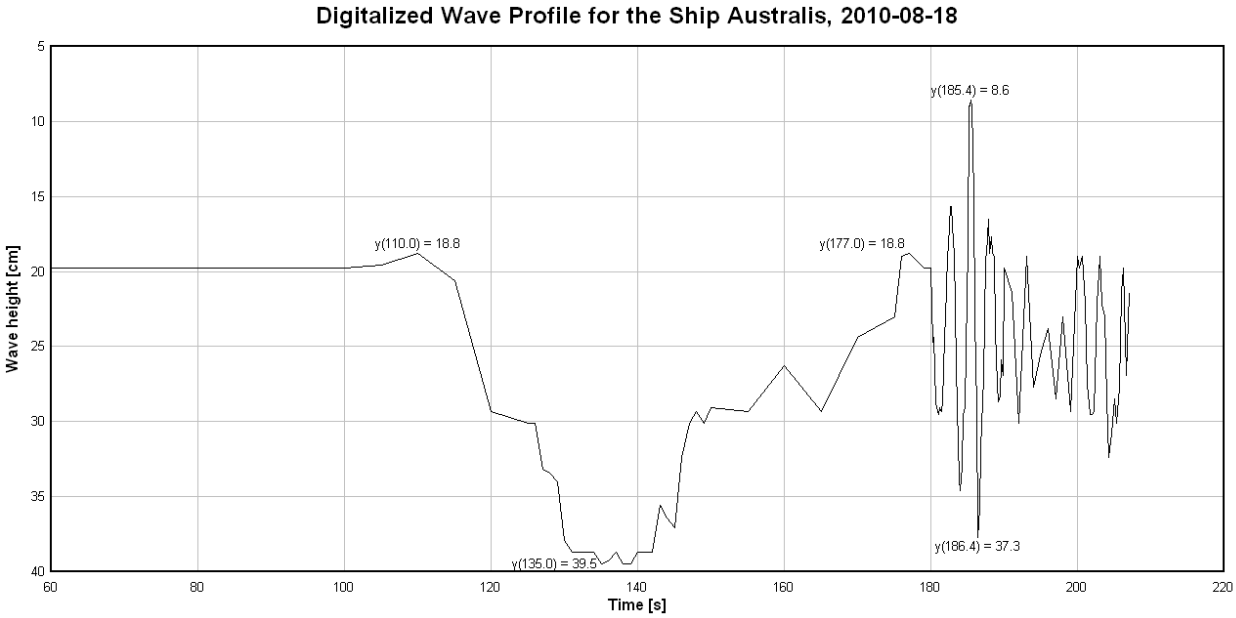
Digitalized Wave Profile for the Ship Australis, 2010-08-18
Wave height [cm]
Time [s]
y(110.0) = 18.8
y(135.0) = 39.5
y(177.0) = 18.8
y(185.4) = 8.6
y(186.4) = 37.3

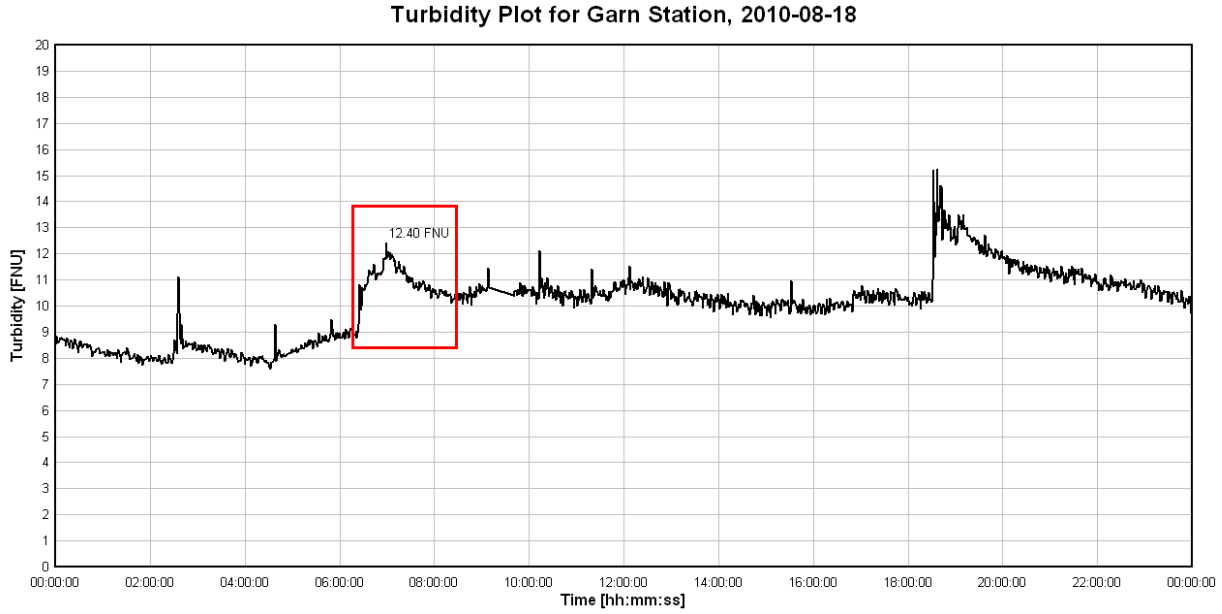
Turbidity Plot for Garn Station, 2010-08-18
Turbidity [FNU]
Time [hh:mm:ss]
12.40 FNU

#7 - Aspen 2010-08-18, 19:34

Draught: 4.8 m
Length overall: 83 m
Maximum width: 13 m
Entrance length: ~ 12 m
Direction: Upstream
Constructed: 2000

SWL depth: 8.22 m
Dead weight: 3037 tonnes
Flow rate: ~ 815 m^3/s
Flow velocity: ~ 0.99 m/s
Velocity over bed: 4.06 m/s
Velocity relative to water: 5.05 m/s

Drawdown = 0.223 m
H_{max} = 0.435 m
Wave period (H_{max}) = 2.80 s
Wave length (H_{max}) = 12.02 m

Turbidity increase = 5.0 FNU
F_L = 0.1770
F_D = 0.5624

Block coefficient	**0.6**	**0.7**	**0.8**
Calculated H_{max} [m]	0.4890	0.3205	0.2026
Calculated drawdown [m]	0.1913	0.1621	0.1326
Modified Froude number	0.3064	0.2671	0.2329

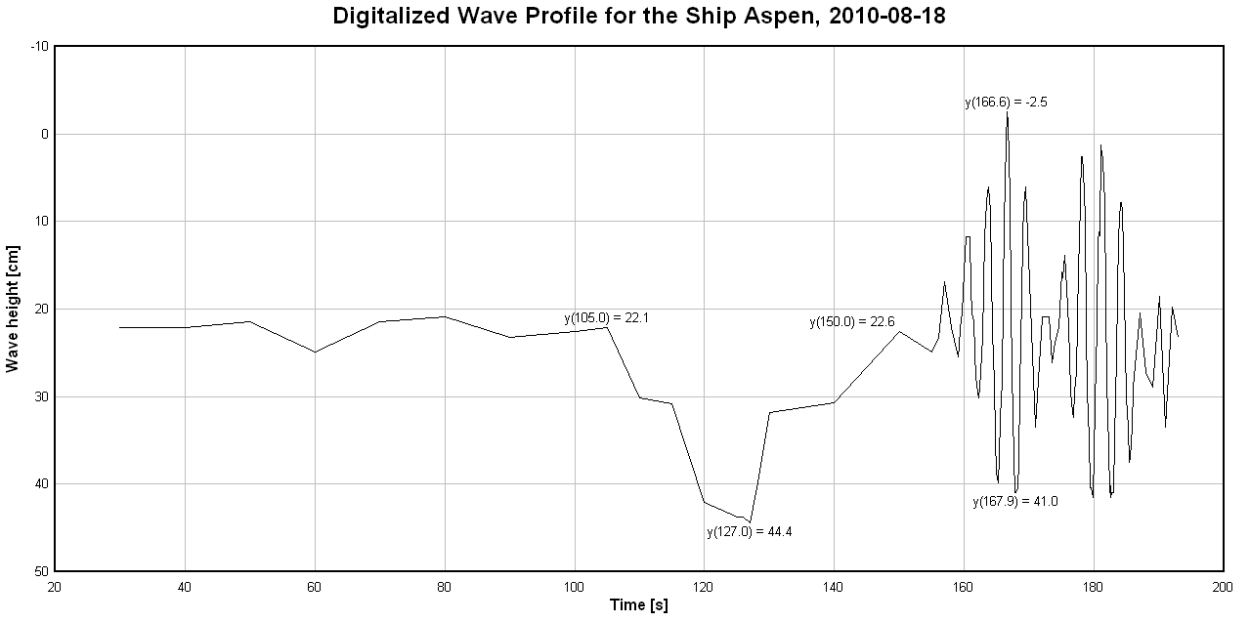
Digitalized Wave Profile for the Ship Aspen, 2010-08-18
Wave height [cm]
Time [s]
y(105.0) = 22.1
y(127.0) = 44.4
y(150.0) = 22.6
y(166.6) = -2.5
y(167.9) = 41.0

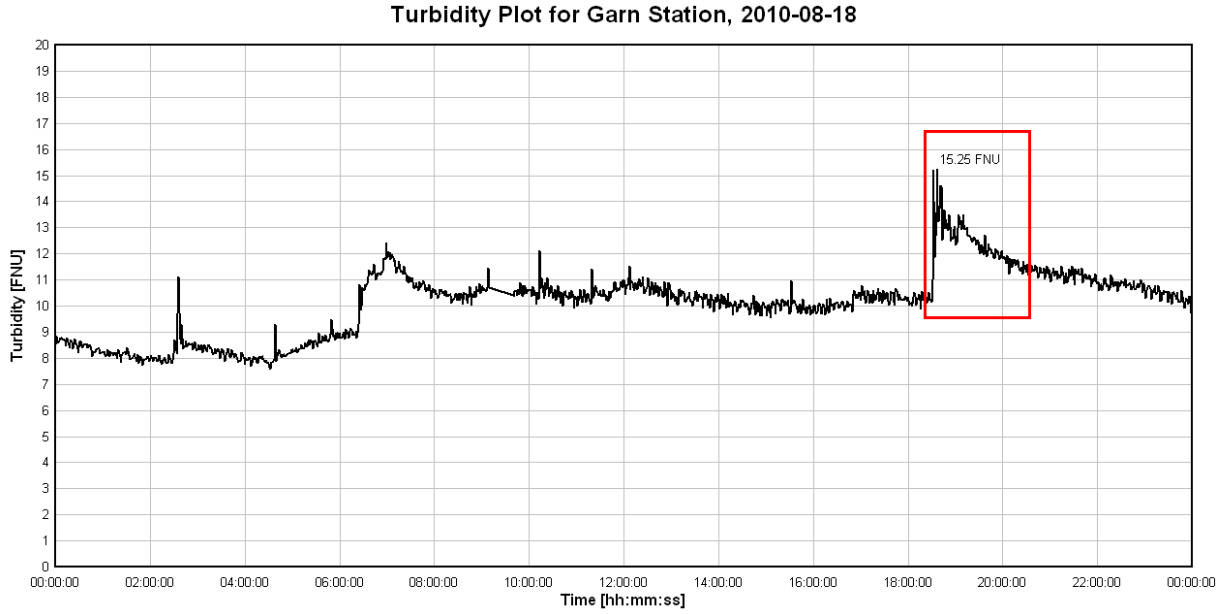
Turbidity Plot for Garn Station, 2010-08-18
Turbidity [FNU]
Time [hh:mm:ss]
15.25 FNU

#8 - Uno 2010-08-18, 20:06

Draught: 3.2 m
Length overall: 79 m
Maximum width: 11 m
Entrance length: ~ 11 m
Direction: Upstream
Constructed: 1986

SWL depth: 8.22 m
Dead weight: 2111 tonnes
Flow rate: ~ 815 m^3/s
Flow velocity: ~ 0.99 m/s
Velocity over bed: 3.96 m/s
Velocity relative to water: 4.95 m/s

Drawdown = 0.051 m
H_{max} = 0.132 m
Wave period (H_{max}) = 2.50 s
Wave length (H_{max}) = 8.96 m

Turbidity increase = 1.1 FNU (unsecure correlation)
F_L = 0.1778
F_D = 0.5512

Block coefficient	**0.6**	**0.7**	**0.8**
Calculated H_{max} [m]	0.2655	0.1948	0.1399
Calculated drawdown [m]	0.1658	0.1634	0.1500
Modified Froude number	0.2564	0.2340	0.2135

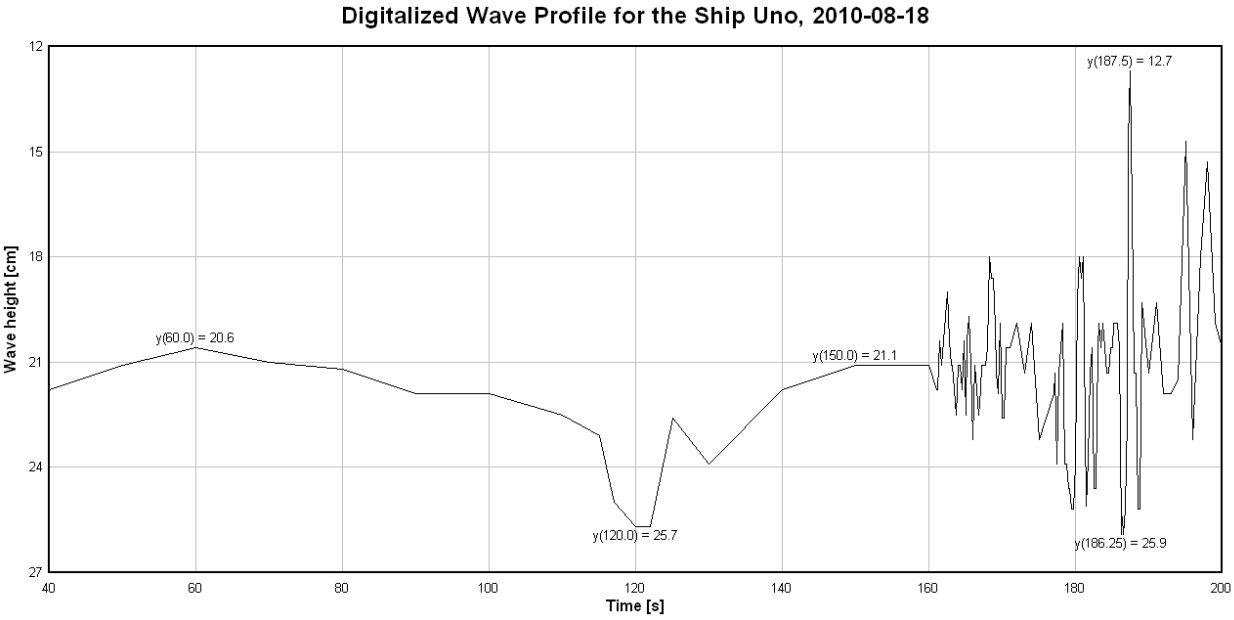
Digitalized Wave Profile for the Ship Uno, 2010-08-18
Wave height [cm]
Time [s]
y(60.0) = 20.6
y(120.0) = 25.7
y(150.0) = 21.1
y(187.5) = 12.7
y(186.25) = 25.9

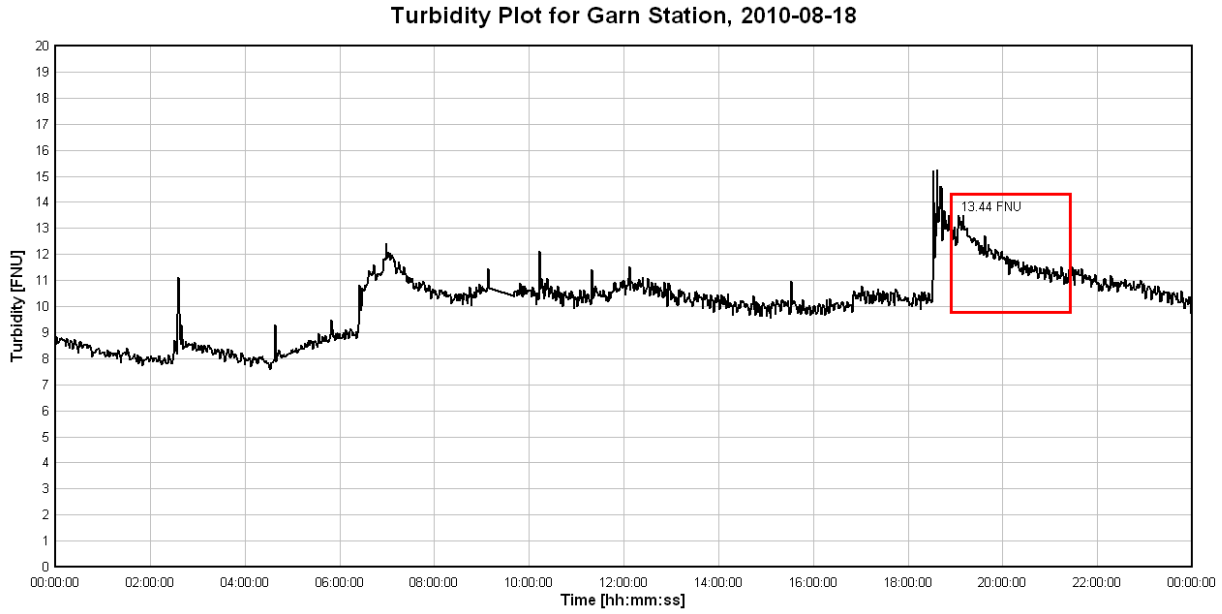
Turbidity Plot for Garn Station, 2010-08-18
Turbidity [FNU]
Time [hh:mm:ss]
13.44 FNU

#9 - Ann Rousing 2010-08-19, 09:34

Draught: 4.4 m
Length overall:85 m
Maximum width: 13 m
Entrance length: ~12 m
Direction: Downstream
Constructed: 1991

SWL depth: 8.26 m
Dead weight: 2752 tonnes
Flow rate: ~ 845 m^3/s
Flow velocity: ~ 1.02 m/s
Velocity over bed: 5.65 m/s
Velocity relative to water: 4.63 m/s

Drawdown = 0.231 m
H_{max} = 0.577 m
Wave period (H_{max}) = 1.75
Wave length (H_{max}) = 4.78 m

Turbidity increase = 2.3 FNU
F_L = 0.1603
F_D = 0.5143

Block coefficient	**0.6**	**0.7**	**0.8**
Calculated H_{max} [m]	0.2635	0.1733	0.1093
Calculated drawdown [m]	0.1385	0.1262	0.1094
Modified Froude number	0.2645	0.2334	0.2060

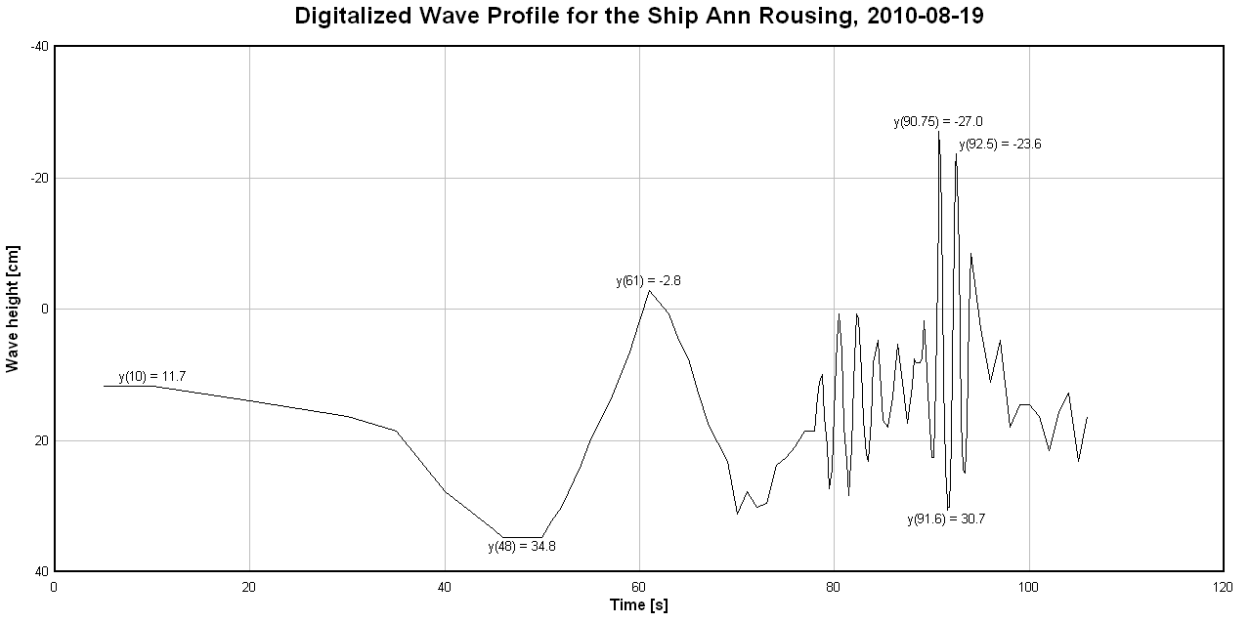
Digitalized Wave Profile for the Ship Ann Rousing, 2010-08-19
Wave height [cm]
Time [s]
y(10) = 11.7
y(48) = 34.8
y(61) = -2.8
y(90.75) = -27.0
y(92.5) = -23.6
y(91.6) = 30.7

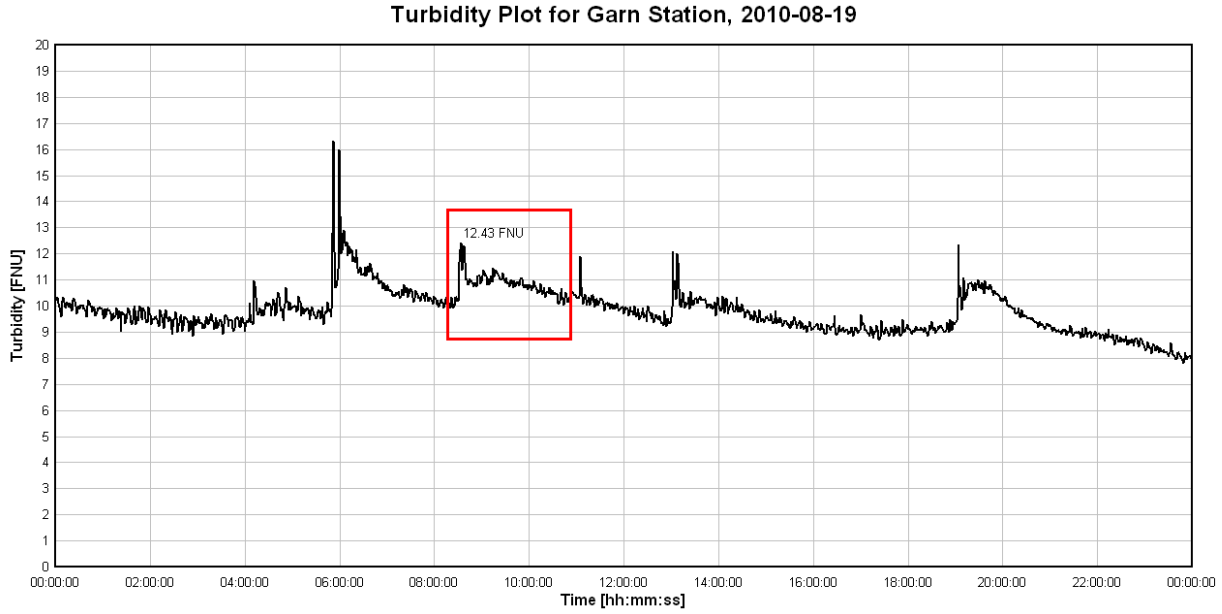
Turbidity Plot for Garn Station, 2010-08-19
Turbidity [FNU]
Time [hh:mm:ss]
12.43 FNU

#10 - RMS Lagona 2010-08-19, 10:17

Draught: 3.8 m
Length overall:88 m
Maximum width: 12 m
Entrance length: ~13 m
Direction: Downstream
Constructed: 2000

SWL depth: 8.22 m
Dead weight: 2688 tonnes
Flow rate: ~ 850 m^3/s
Flow velocity: ~ 1.03 m/s
Velocity over bed: 5.50 m/s
Velocity relative to water: 4.47 m/s

Drawdown = 0.223 m
Real H_{max} = 0.385 m
Wave period (H_{max}) = 1.80 s
Wave length (H_{max}) = 5.06 m

Turbidity increase = No clear increase
F_L = 0.1521
F_D = 0.4978

Block coefficient	**0.6**	**0.7**	**0.8**
Calculated H_{max} [m]	0.1667	0.1123	0.0726
Calculated drawdown [m]	0.1177	0.1140	0.1037
Modified Froude number	0.2349	0.2108	0.1891

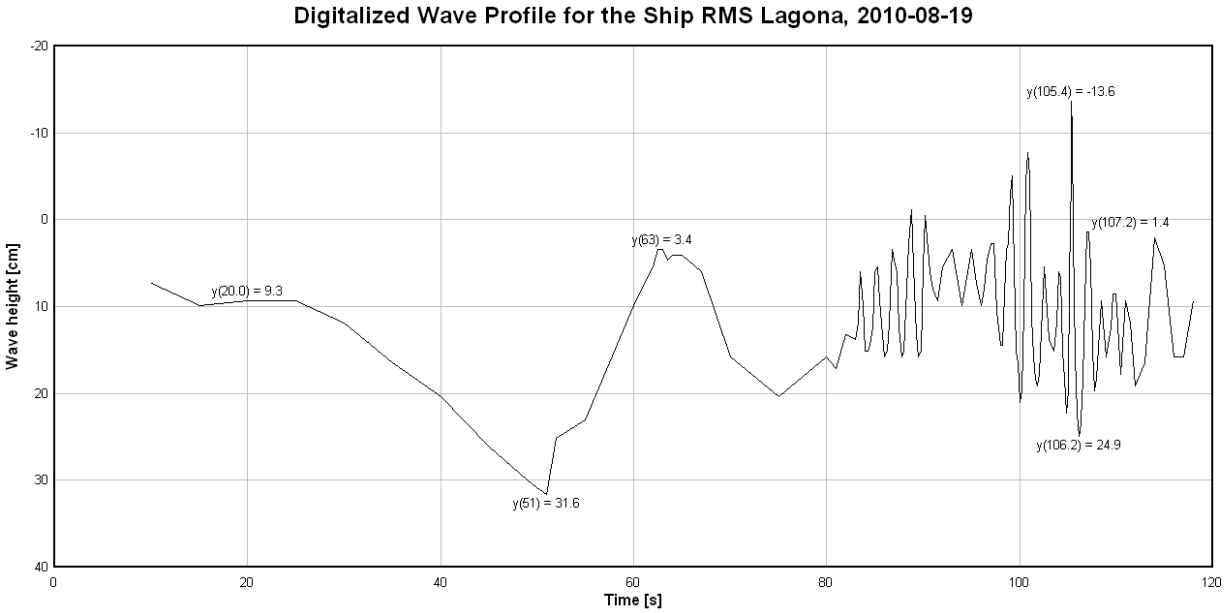
Digitalized Wave Profile for the Ship RMS Lagona, 2010-08-19
Wave height [cm]
Time [s]
y(20.0) = 9.3
y(51) = 31.6
y(63) = 3.4
y(105.4) = -13.6
y(106.2) = 24.9
y(107.2) = 1.4

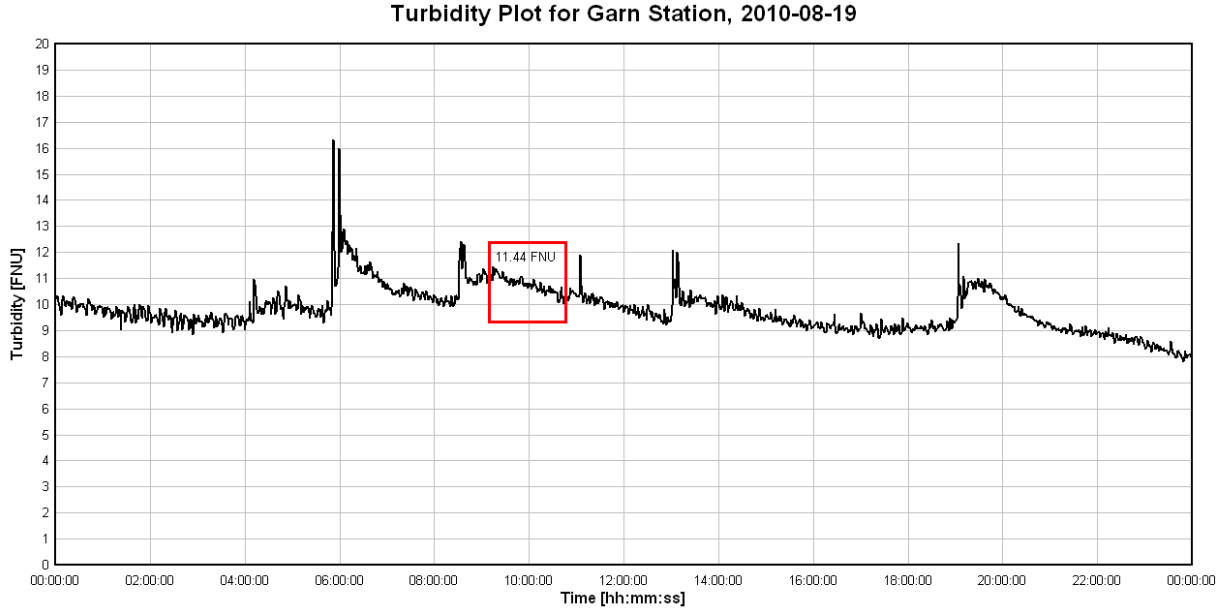
Turbidity Plot for Garn Station, 2010-08-19
Turbidity [FNU]
Time [hh:mm:ss]
11.44 FNU

#11 - Australis 2010-08-19, 11:46

Draught: 4.5 m
Length overall:83 m
Maximum width: 12.5 m
Entrance length: ~12 m
Direction: Downstream
Constructed: -

SWL depth: 8.31 m
Dead weight: 2688 tonnes
Flow rate: ~ 860 m^3/s
Flow velocity: ~ 1.03 m/s
Velocity over bed: 5.55 m/s
Velocity relative to water: 4.52 m/s

Drawdown = 0.170 m
H_{max} = 0.195 m
Wave period (H_{max}) = 1.375 s
Wave length (H_{max}) = 2.97 m

Turbidity increase = No clear increase
F_L = 0.1584
F_D = 0.5006

Block coefficient	**0.6**	**0.7**	**0.8**
Calculated H_{max} [m]	0.2459	0.1603	0.1000
Calculated drawdown [m]	0.1213	0.1118	0.0979
Modified Froude number	0.2635	0.2320	0.2043

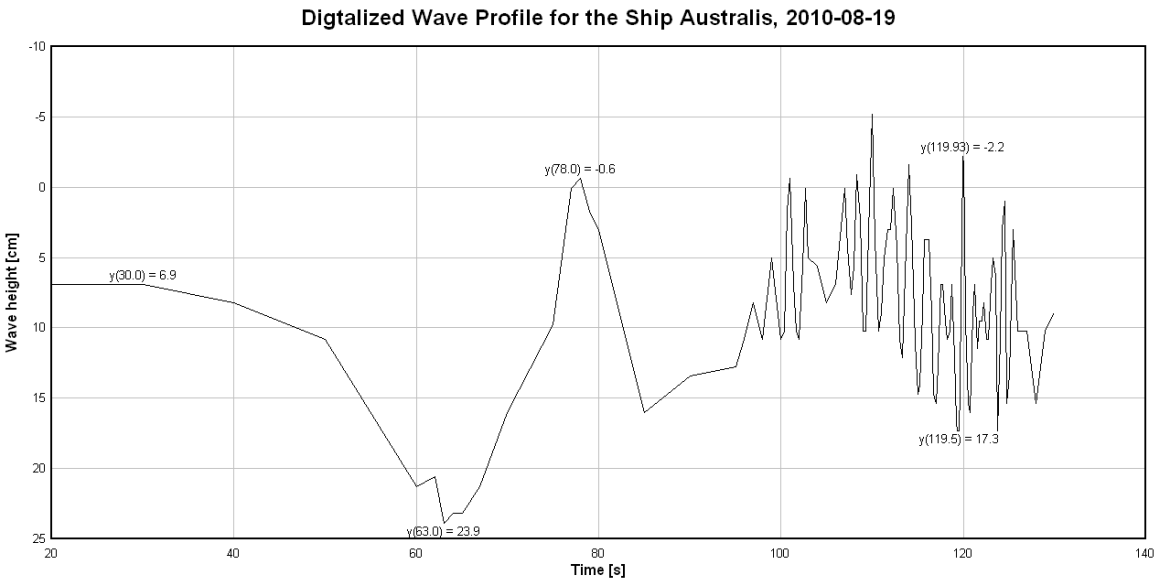
Digtalized Wave Profile for the Ship Australis, 2010-08-19
Wave height [cm]
Time [s]
y(30.0) = 6.9
y(63.0) = 23.9
y(78.0) = -0.6
y(119.5) = 17.3
y(119.93) = -2.2

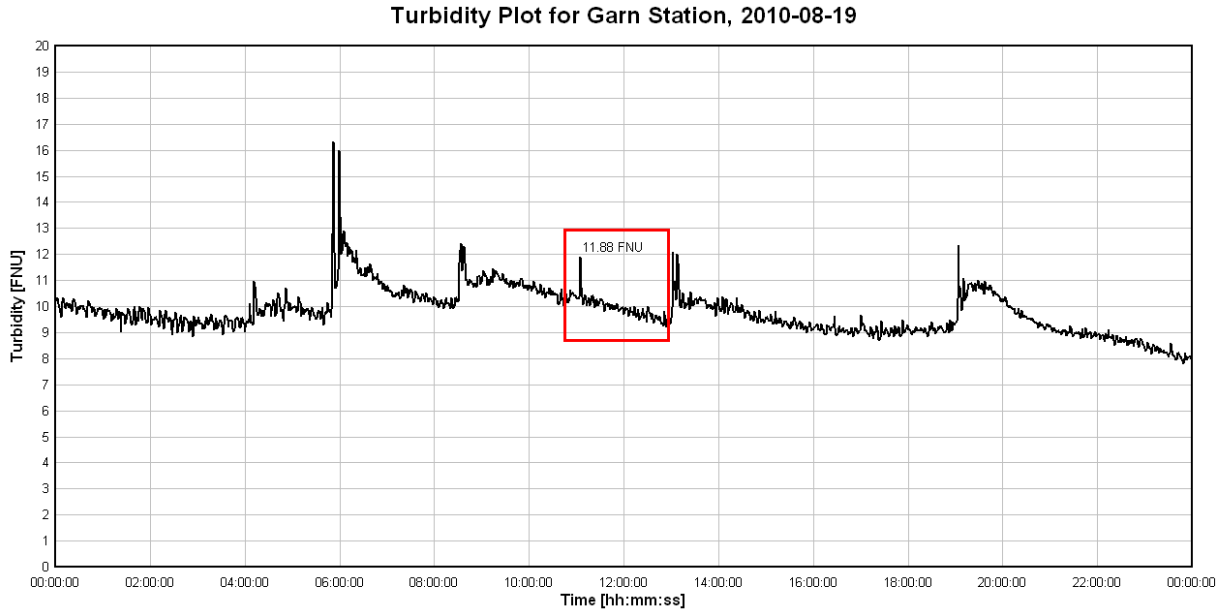
Turbidity Plot for Garn Station, 2010-08-19
Turbidity [FNU]
Time [hh:mm:ss]
11.88 FNU

#12 - Swe-Bulk 2010-08-20, 09:23

Draught: 4.0 m
Length overall:87 m
Maximum width: 13 m
Entrance length: ~13 m
Direction: Upstream
Constructed: 1991

SWL depth: 8.35 m
Dead weight: 3269 tonnes
Flow rate: ~ 800 m^3/s
Flow velocity: ~ 0.96 m/s
Velocity over bed: 4.57 m/s
Velocity relative to water: 5.53 m/s

Drawdown = 0.095 m
H_{max} = 0.435 m
Wave period (H_{max}) = 2.90 s
Wave length (H_{max}) = 12.84 m

Turbidity increase = 2.1 FNU
F_L = 0.1893
F_D = 0.6110

Block coefficient	**0.6**	**0.7**	**0.8**
Calculated H_{max} [m]	0.5406	0.3810	0.2619
Calculated drawdown [m]	0.2988	0.2599	0.2149
Modified Froude number	0.2970	0.2653	0.2371

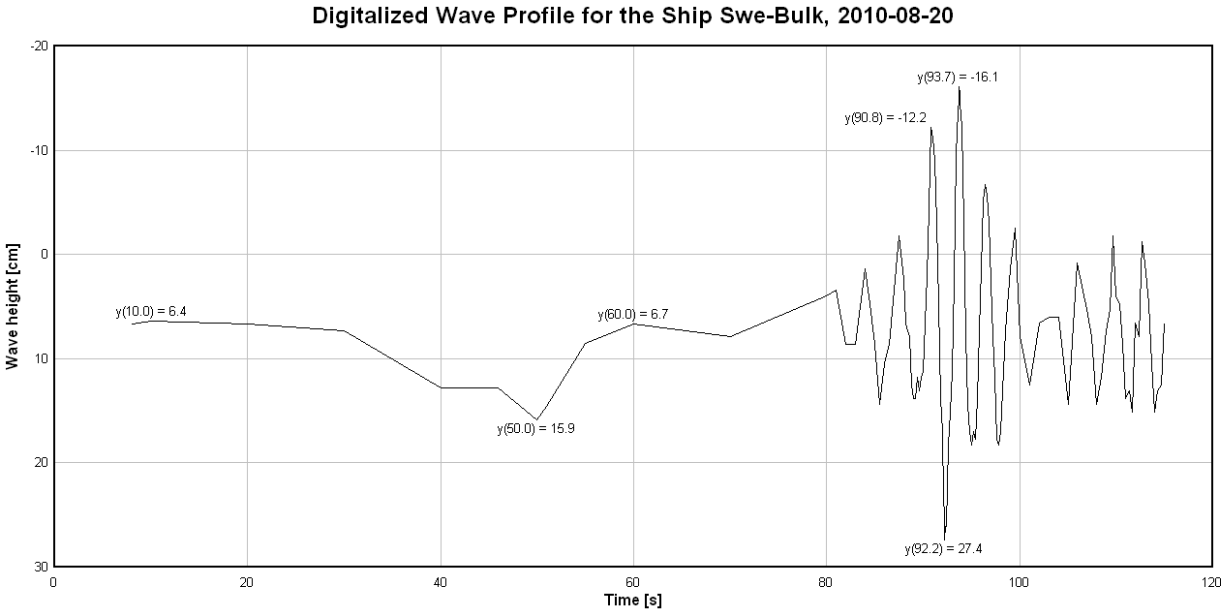
Digitalized Wave Profile for the Ship Swe-Bulk, 2010-08-20
Wave height [cm]
Time [s]
y(10.0) = 6.4
y(50.0) = 15.9
y(60.0) = 6.7
y(90.8) = -12.2
y(93.7) = -16.1
y(92.2) = 27.4

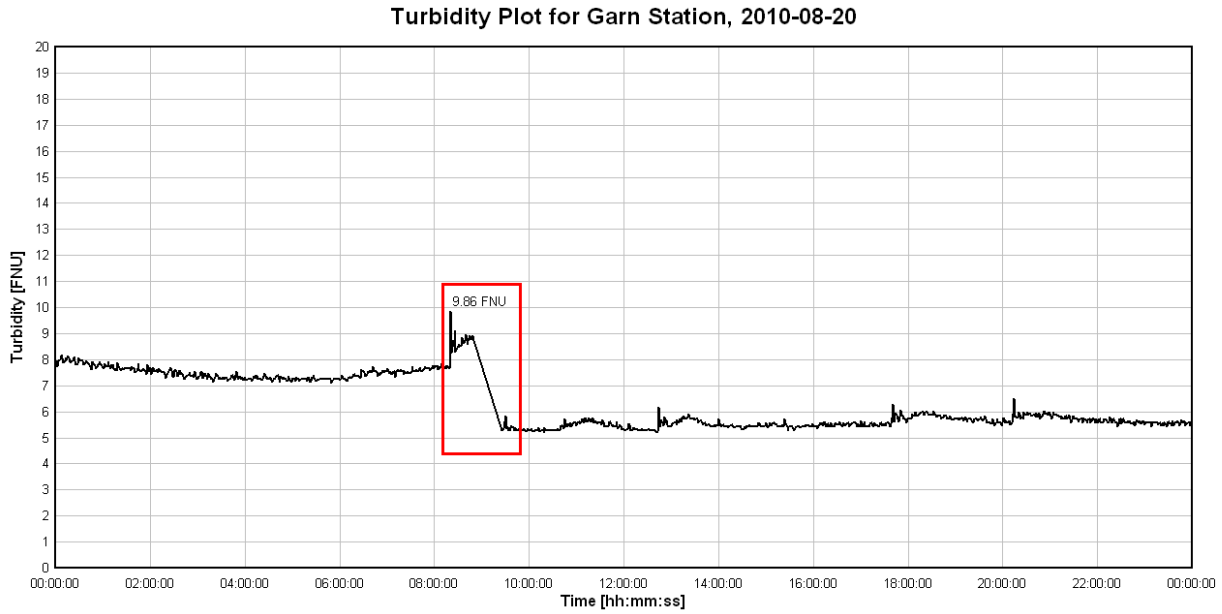
Turbidity Plot for Garn Station, 2010-08-20
Turbidity [FNU]
Time [hh:mm:ss]
9.86 FNU

#13 - Uno 2010-08-20, 11:43

Draught: 3.9 m
Length overall:79 m
Maximum width: 11 m
Entrance length: ~11 m
Direction: Downstream
Constructed: 1986

SWL depth: 8.32 m
Dead weight: 2111 tonnes
Flow rate: ~ 820 m^3/s
Flow velocity: ~ 0.99 m/s
Velocity over bed: 5.65 m/s
Velocity relative to water: 4.66 m/s

Drawdown = 0.115 m
H_{max} = 0.423 m
Wave period (H_{max}) = 1.75 s
Wave length (H_{max}) = 4.78 m

Turbidity increase = No clear increase
F_L = 0.1674
F_D = 0.5158

Block coefficient	**0.6**	**0.7**	**0.8**
Calculated H_{max} [m]	0.2466	0.1701	0.1136
Calculated drawdown [m]	0.1312	0.1253	0.1126
Modified Froude number	0.2601	0.2329	0.2086

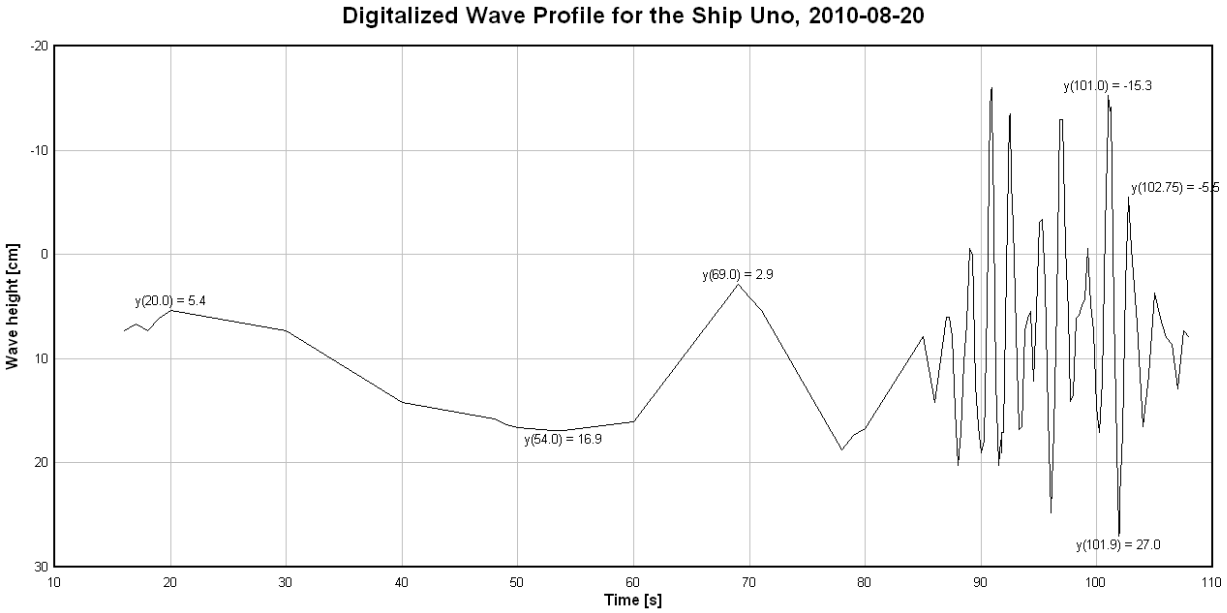
Digitalized Wave Profile for the Ship Uno, 2010-08-20
Wave height [cm]
Time [s]
y(20.0) = 5.4
y(54.0) = 16.9
y(69.0) = 2.9
y(101.0) = -15.3
y(102.75) = -5.5
y(101.9) = 27.0

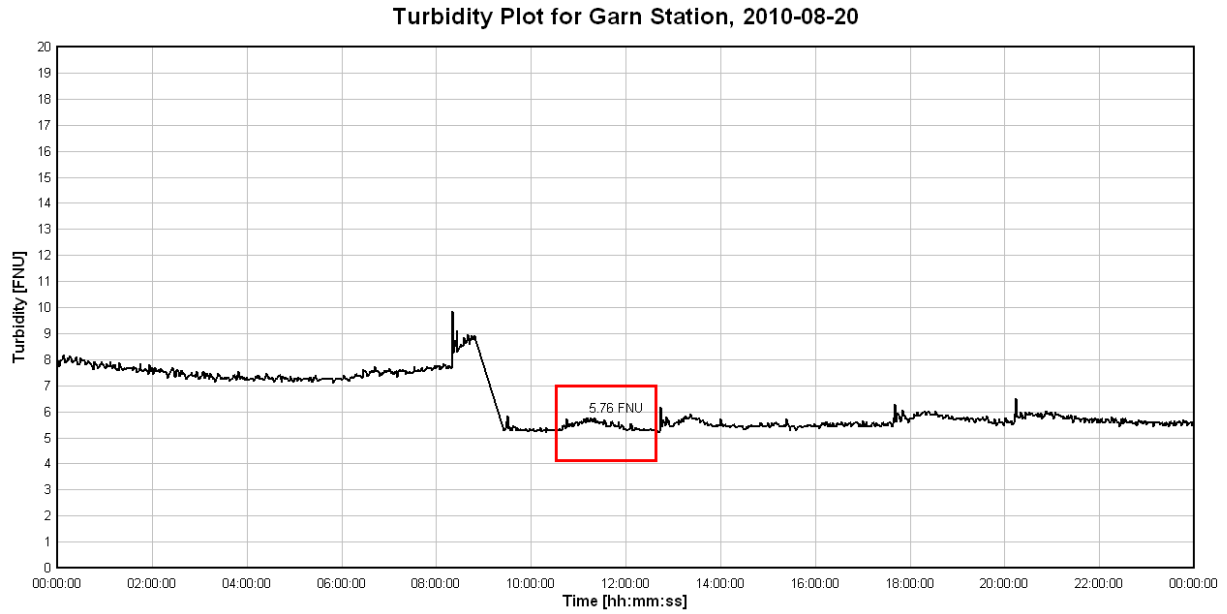
Turbidity Plot for Garn Station, 2010-08-20
Turbidity [FNU]
Time [hh:mm:ss]
5.76 FNU

#14 - Clipper Sola 2010-08-22, 08:48

Draught: 5.4 m
Length overall:89 m
Maximum width: 13 m
Entrance length: ~13 m
Direction: Upstream
Constructed: 2007

SWL depth: 8.13 m
Dead weight: 4000 tonnes
Flow rate: ~ 542 m^3/s
Flow velocity: ~ 0.67 m/s
Velocity over bed: 4.21 m/s
Velocity relative to water: 4.88 m/s

Drawdown = 0.350 m
H_{max} = 0.334 m
Wave period (H_{max}) = 2.60 s
Wave length (H_{max}) = 10.45 m

Turbidity increase = 5.3 FNU
F_L = 0.1652
F_D = 0.5464

Block coefficient	**0.6**	**0.7**	**0.8**
Calculated H_{max} [m]	0.4758	0.2941	0.1731
Calculated drawdown [m]	0.1830	0.1481	0.1175
Modified Froude number	0.3083	0.2638	0.2257

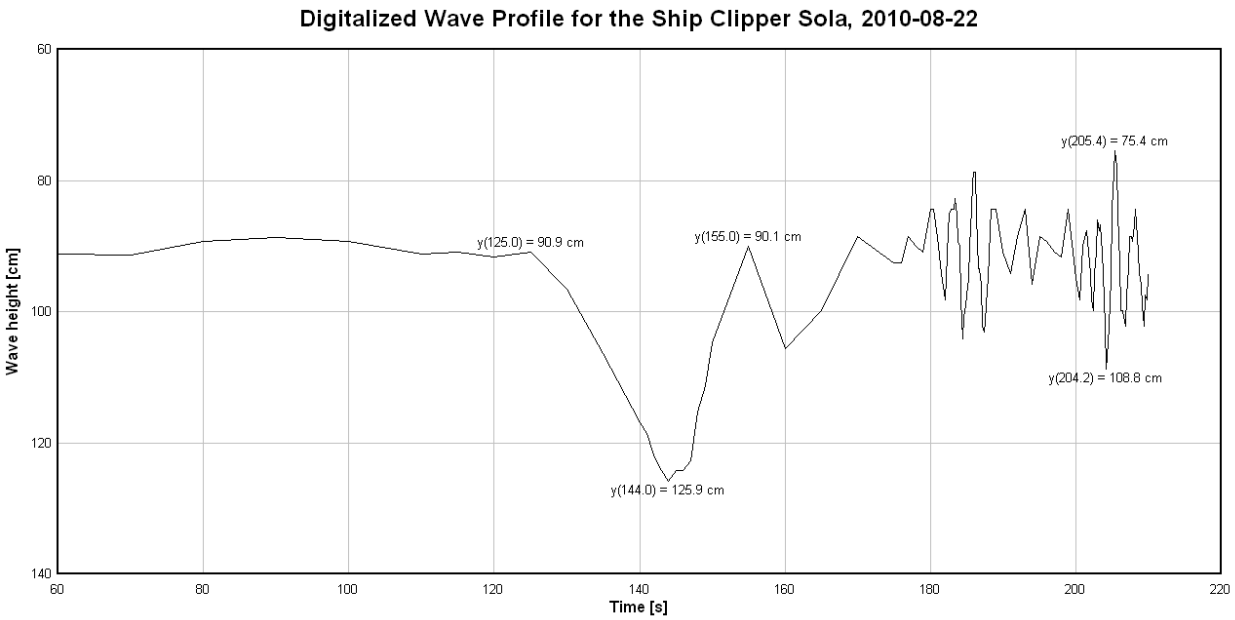
Digitalized Wave Profile for the Ship Clipper Sola, 2010-08-22
Wave height [cm]
Time [s]
y(125.0) = 90.9 cm
y(144.0) = 125.9 cm
y(155.0) = 90.1 cm
y(205.4) = 75.4 cm
y(204.2) = 108.8 cm

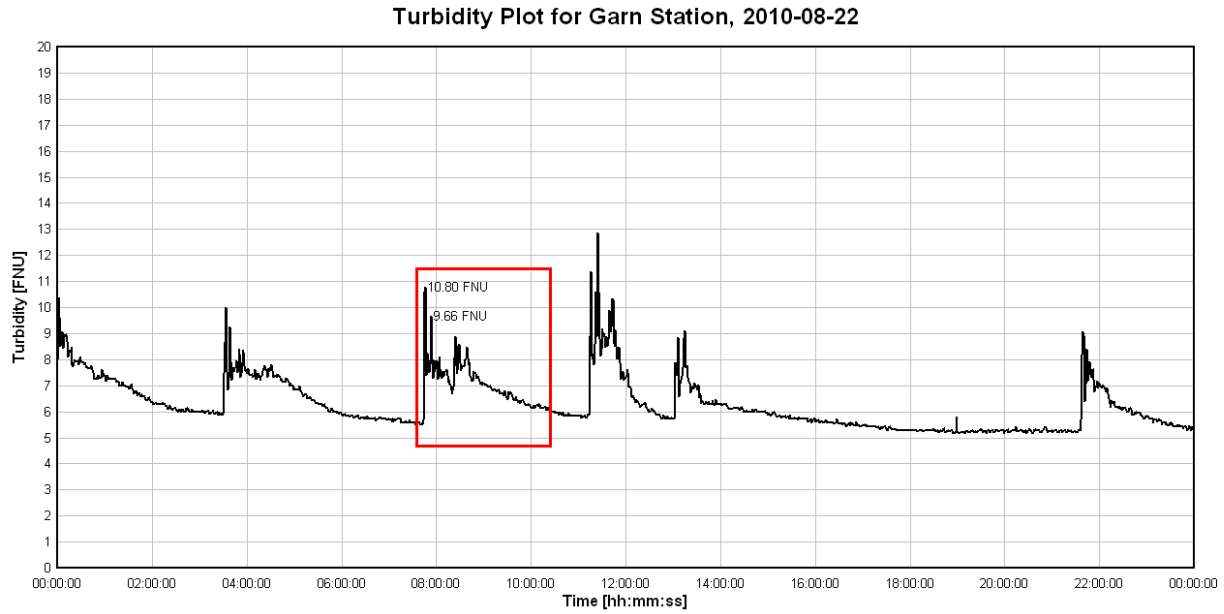
Turbidity Plot for Garn Station, 2010-08-22
Turbidity [FNU]
Time [hh:mm:ss]
10.80 FNU
9.66 FNU

#15 - Naven 2010-08-22, 09:26

Draught: 5.4 m
Length overall:89 m
Maximum width: 13 m
Entrance length: ~13 m
Direction: Upstream
Constructed: 1991

SWL depth: 8.13 m
Dead weight: 4191 tonnes
Flow rate: ~ 543 m^3/s
Flow velocity: ~ 0.67 m/s
Velocity over bed: 3.86 m/s
Velocity relative to water: 4.53 m/s

Drawdown = 0.232 m
H_{max} = 0.371 m
Wave period (H_{max}) = 1.70 s
Wave length (H_{max}) = 4.51 m

Turbidity increase = 2.2 FNU
F_L = 0.1533
F_D = 0.5072

Block coefficient	**0.6**	**0.7**	**0.8**
Calculated H_{max} [m]	0.3276	0.1982	0.1132
Calculated drawdown [m]	0.1364	0.1152	0.0947
Modified Froude number	0.2862	0.2449	0.2095

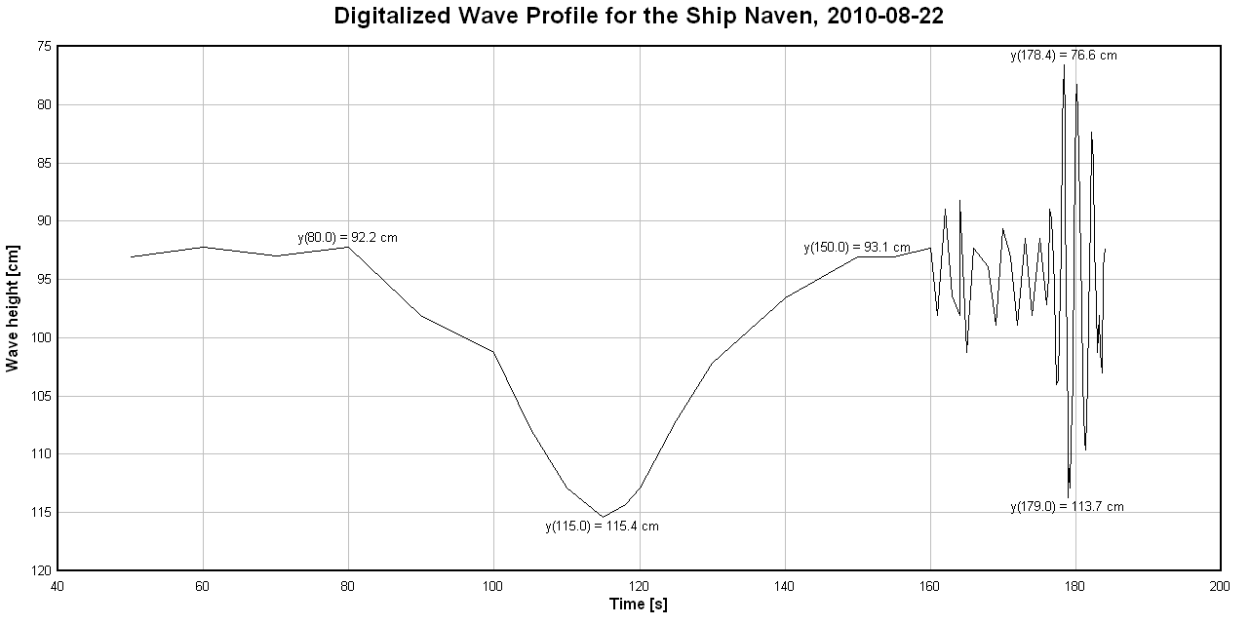
Digitalized Wave Profile for the Ship Naven, 2010-08-22
Wave height [cm]
Time [s]
y(80.0) = 92.2 cm
y(115.0) = 115.4 cm
y(150.0) = 93.1 cm
y(178.4) = 76.6 cm
y(179.0) = 113.7 cm

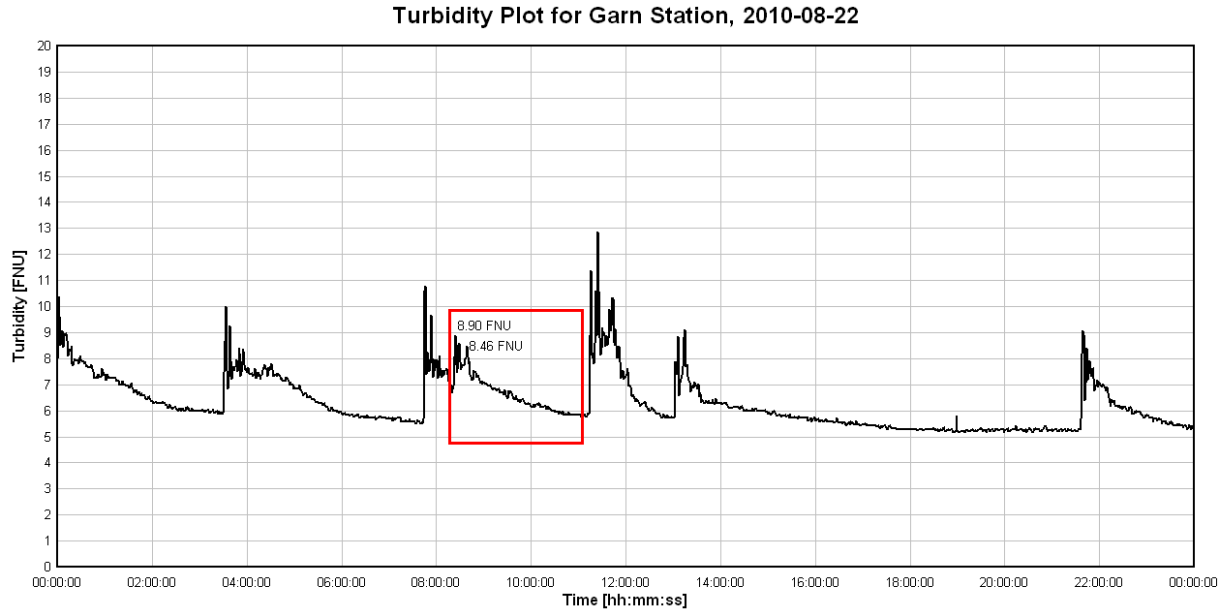
Turbidity Plot for Garn Station, 2010-08-22
Turbidity [FNU]
Time [hh:mm:ss]
8.90 FNU
8.46 FNU

#16 - Clipper Sira 2010-09-13, 08:55

Draught: 5.4 m
Length overall:89 m
Maximum width: 13 m
Entrance length: ~13 m
Direction: Upstream
Constructed: 2006

SWL depth: 8.02 m
Dead weight: 4000 tonnes
Flow rate: ~ 700 m^3/s
Flow velocity: ~ 0.87 m/s
Velocity over bed: 3.96 m/s
Velocity relative to water: 4.83 m/s

Drawdown = 0.478 m
H_{max} = 0.232 m
Wave period (H_{max}) = 2.75 s
Wave length (H_{max}) = 11.59 m

Turbidity increase = 7.2 FNU
F_L = 0.1635
F_D = 0.5445

Block coefficient	**0.6**	**0.7**	**0.8**
Calculated H_{max} [m]	0.4638	0.2845	0.1659
Calculated drawdown [m]	0.1817	0.1461	0.1154
Modified Froude number	0.3078	0.2628	0.2243

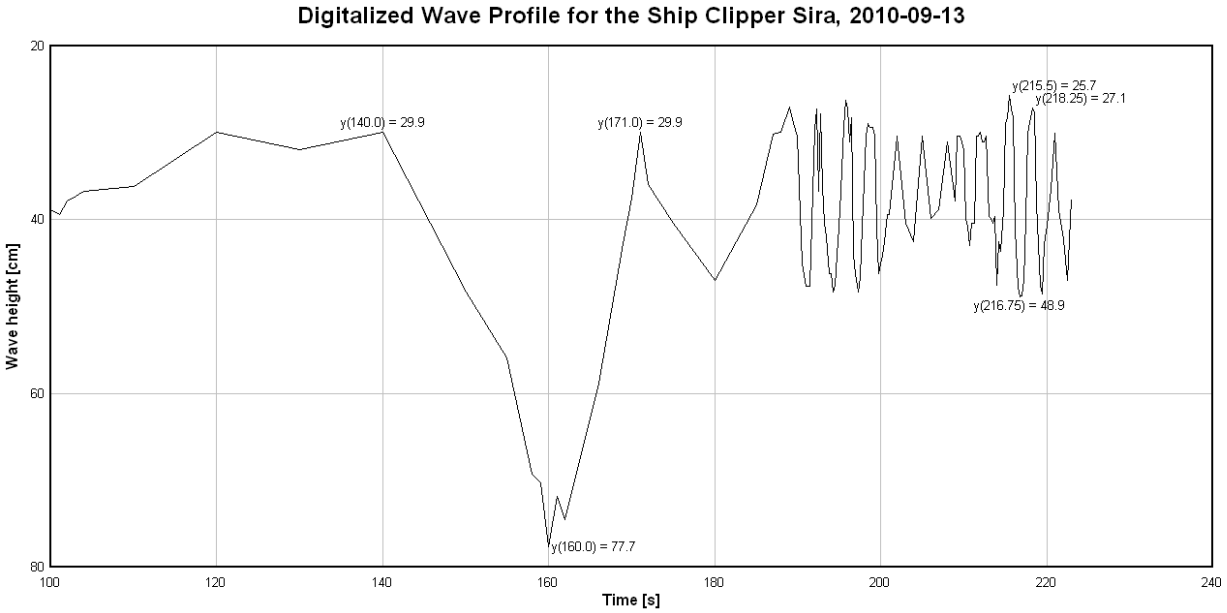
Digitalized Wave Profile for the Ship Clipper Sira, 2010-09-13
Wave height [cm]
Time [s]
y(140.0) = 29.9
y(171.0) = 29.9
y(160.0) = 77.7
y(215.5) = 25.7
y(218.25) = 27.1
y(216.75) = 48.9

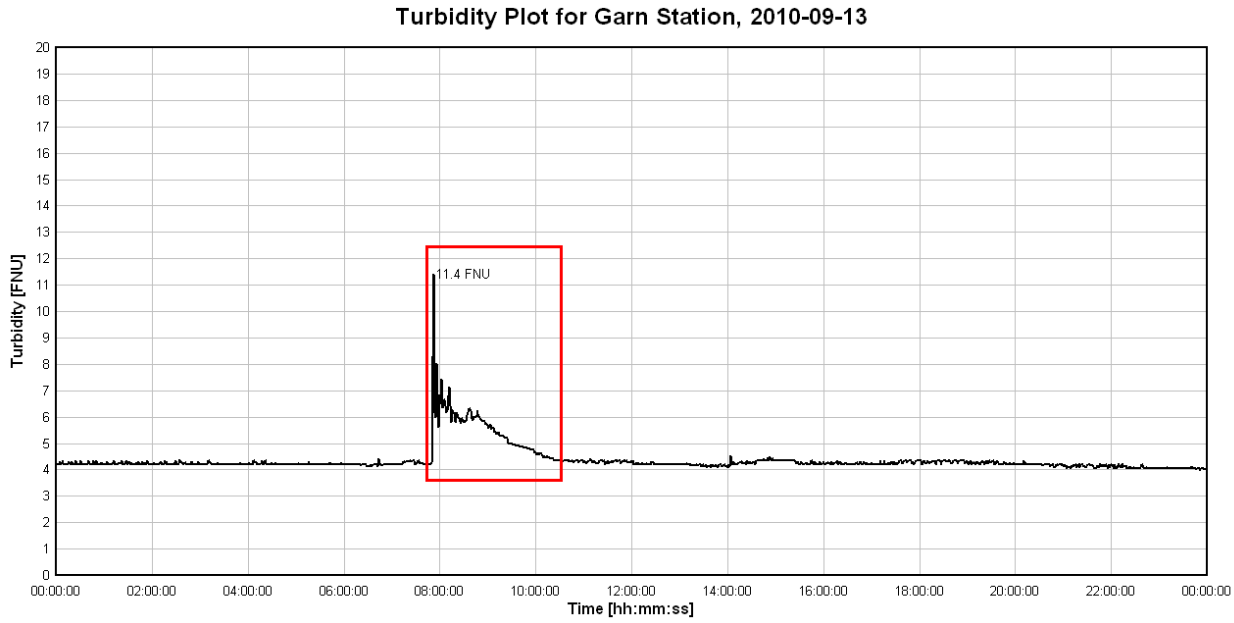
Turbidity Plot for Garn Station, 2010-09-13
Turbidity [FNU]
Time [hh:mm:ss]
11.4 FNU

#17 - Anmar-S 2010-09-21, 11:02

Draught: 3.90 m
Length overall:82 m
Maximum width: 12 m
Entrance length: ~11 m
Direction: Upstream
Constructed: 1993

SWL depth: 8.12 m
Dead weight: 1590 tonnes
Flow rate: ~ 710 m^3/s
Flow velocity: ~ 0.87 m/s
Velocity over bed: 3.90 m/s
Velocity relative to water: 4.77 m/s

Drawdown = 0.098 m
H_{max} = 0.168 m
Wave period (H_{max}) = 2.50 s
Wave length (H_{max}) = 9.70 m

Turbidity increase = No clear increase
F_L = 0.1682
F_D = 0.5344

Block coefficient	**0.6**	**0.7**	**0.8**
Calculated H_{max} [m]	0.2746	0.1884	0.1251
Calculated drawdown [m]	0.1550	0.1440	0.1263
Modified Froude number	0.2642	0.2360	0.2108

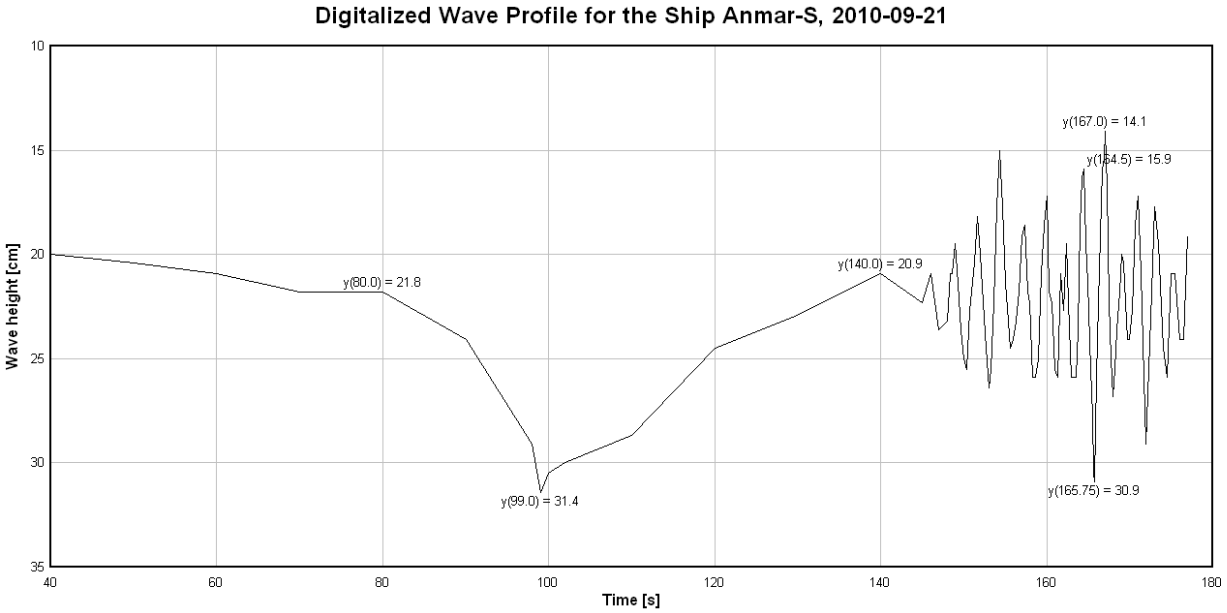
Digitalized Wave Profile for the Ship Anmar-S, 2010-09-21
Wave height [cm]
Time [s]
y(80.0) = 21.8
y(99.0) = 31.4
y(140.0) = 20.9
y(167.0) = 14.1
y(164.5) = 15.9
y(165.75) = 30.9

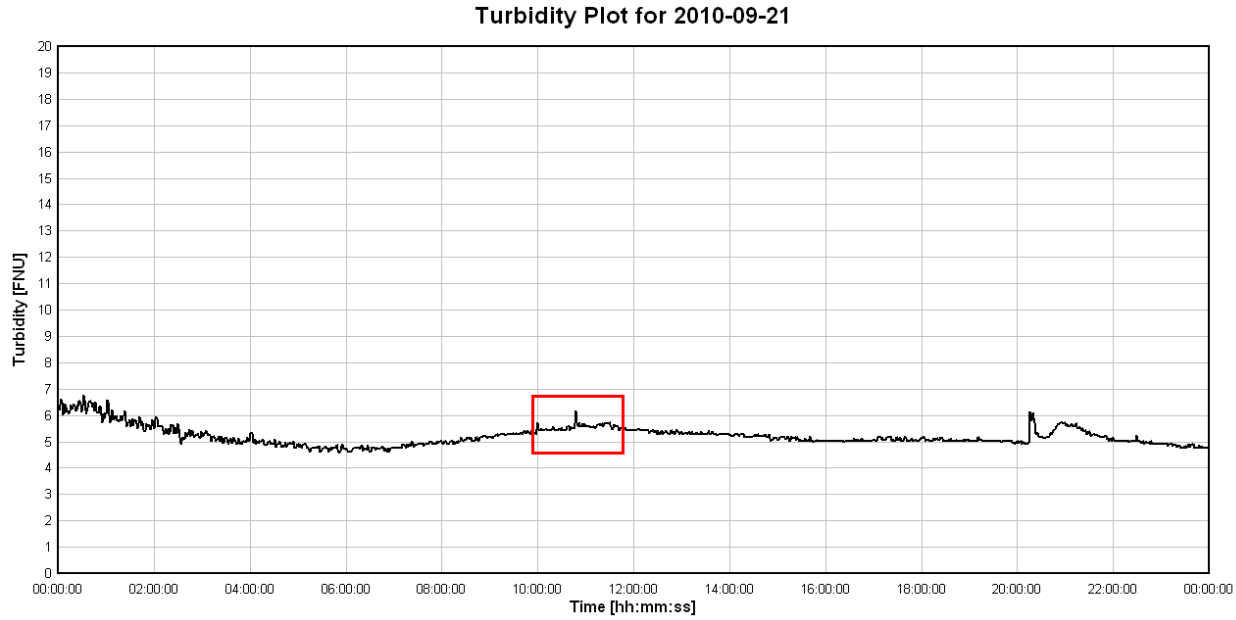
Turbidity Plot for 2010-09-21
Turbidity [FNU]
Time [hh:mm:ss]